Durham E-Theses

Some problems of flash tubs operation

Doe, P.J.

How to cite:

Doe, P.J. (1975) *Some problems of flash tubs operation,* Durham theses, Durham University. Available at Durham E-Theses Online: http://etheses.dur.ac.uk/8592/

Use policy

SOME PROBLEMS OF FLASH TUBE OPERATION

by

P.J. Doe B.Sc.

A thesis submitted to the University of Durham

for the Degree of Master of Science.

July 1975

CONTENTS

ABSTRACT

A review has been made of the development of the neon flash
tube, from its introduction by Conversi in 1955, up to the present day.

Particular attention is paid to the problems which arose
from attempts to use flash tube arrays on accelerator experiments,
namely the long sensitive and recovery times of the tubes, and the
loss of efficiency at high event rates, caused by internal clearing
fields.

The problems arising from attempts to describe analytically
the flash tube discharge mechanism are also discussed.

An investigation of the decay mechanism of the internal
clearing fields has been made, which indicated that the effect may be
overcome by decreasing the surface resistance of the outer wall of the
flash tube.

A description of a gamma ray detector, utilising flash tubes
as the detecting elements, interspersed with lead absorber, is
included. The energy and spatial resolutions are found to compare
favourably with those of more complex and expensive detectors. The
problems arising from the use of this detector in the e^+ test beam at
the Daresbury Laboratory are discussed.

CHAPTER 1

THE DEVELOPMENT AND USES OF FLASH TUBES

1.1 Introduction

The flash tube was introduced by Conversi and Gozzini (1), and since then has changed very little. The flash tube is a triggerable device, in the same class of detectors as the spark chamber, requiring an auxiliary detector to register the passage of an ionising particle, after which the flash tube can be triggered. A typical flash tube consists of a sealed soda glass tube, 0.5 - 2cm. in diameter, up to several metres in length, filled with a 70% neon, 30% helium mixture, at a pressure of 200 torr to 3 atmospheres, depending on the diameter of the tube.

1.2 A Typical Detector

A typical detector consists of a number of flash tubes placed adjacent to each other in a plane, sandwiched between two metal electrodes. Each tube is either painted, or sleeved in thin P.V.C. tubing to prevent photons from one discharging tube causing an adjacent tube to ignite. It is usual for the detector to consist of many such planes, the tube axis being orthogonal in alternate

planes, to provide X, Y coordinates of the particle. Triggering counters, usually of plastic scintillator, are placed either side of the final electrodes, to detect the passage of an ionising particle through the array. A coincidence from the triggering counters fires a spark gap or hydrogen thyratron, by means of which an impulsive electric field is applied across the tubes.

A typical field is of the order of 5 KV/cm and 5 microsec. duration. Under this electric field the ionisation left in the path of the particle will avalanche, causing the tube to discharge by a combination of Townsend and Streamer mechanisms. Under typical H.T. pulse conditions the discharge will propagate down the length of the tube causing the whole tube to light up, indicating the passage of an ionising particle through the tube.

1.3 Readout Mechanism

The most common forms of readout for flash tubes utilise either photographic methods or external probes.

The light output of a flash tube lies in the yellow-red region of the spectrum, and given that the tube is operating under optimum conditions the variation of intensity is about 5% (2). The arrangement for photographic readout is very similar to that used in optical spark chambers, using mirrors to equalise the path lengths and reduce the angle subtended at the camera. The flash tube does not suffer from the depth of focus problems of the spark chamber, since the discharge fills the whole length of the tube.

The external probe method, developed by Ayre and Thompson (3), utilises the capacitative coupling between the plasma of the discharging gas, and a small electrically conducting probe, placed

FIGURE 1 EFFICIENCY VERSUS APPLIED FIELD

□ Gardener et al.
○ Coxell and Wolfendale
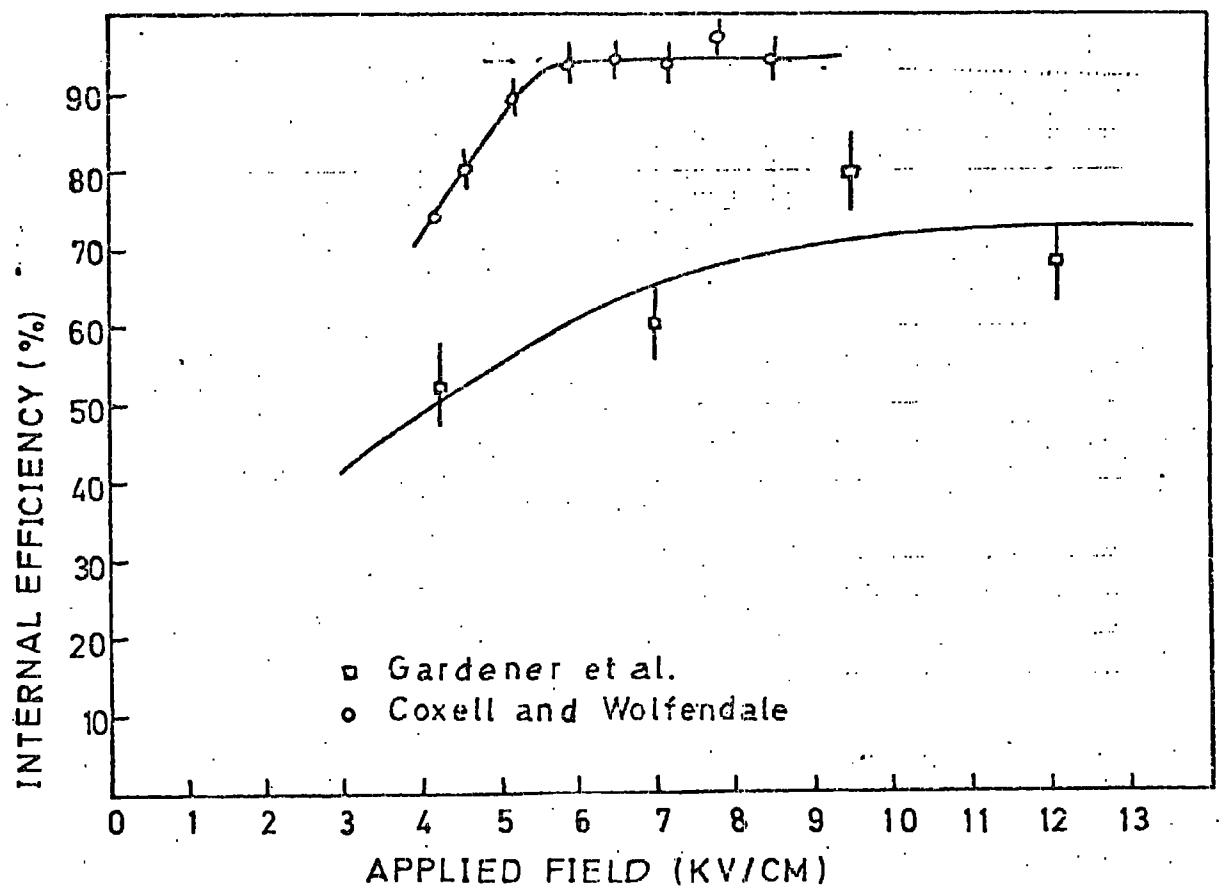
FIGURE 2 EFFICIENCY VERSUS APPLIED FIELD

(1)   (2)   (3)

RC=40 micro. sec. (1)
RC=4 micro. sec. (2)
RC=0.4 micro. sec.(3)
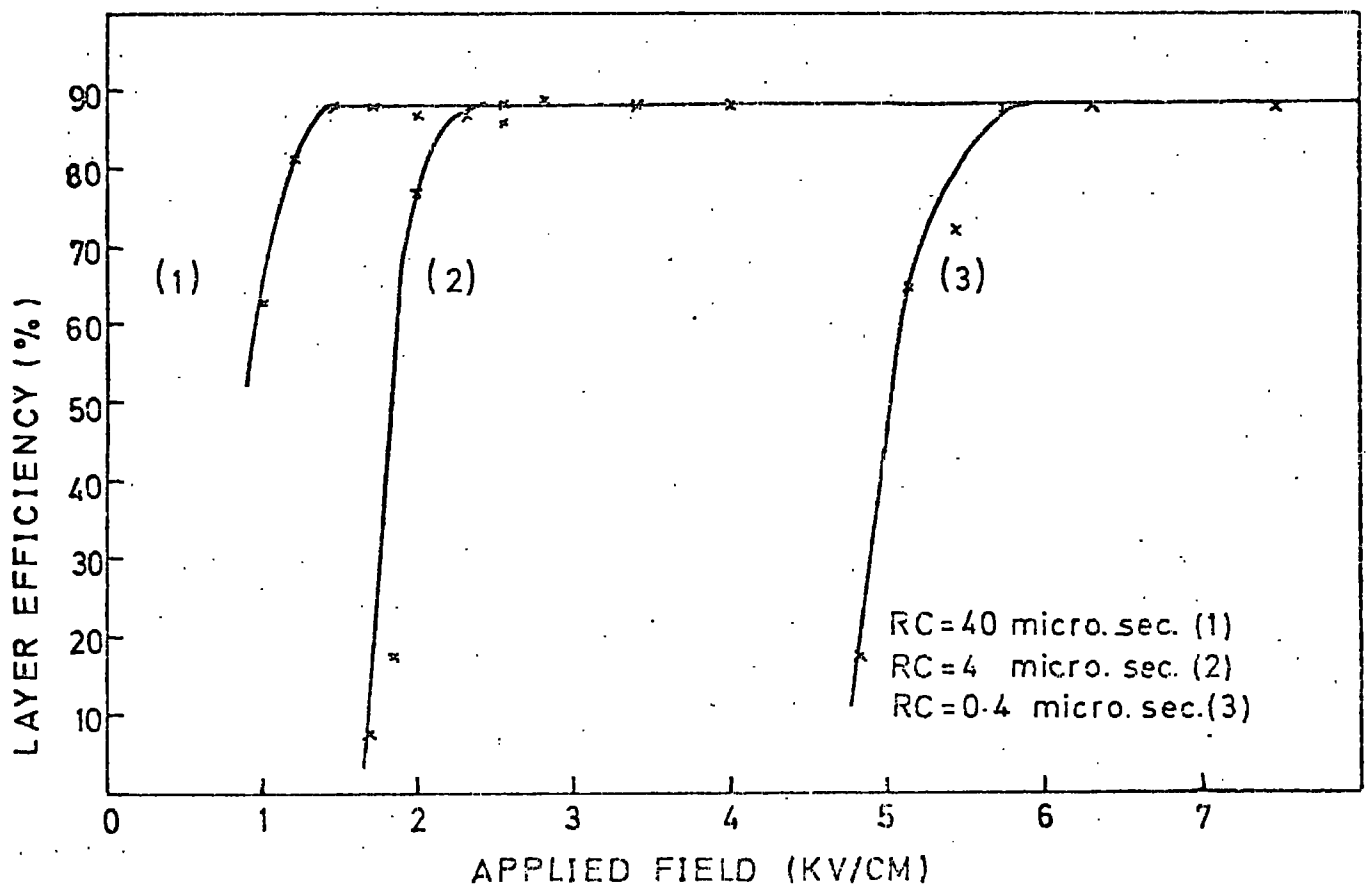
FIGURE 3 EFFICIENCY VERSUS RISE TIME
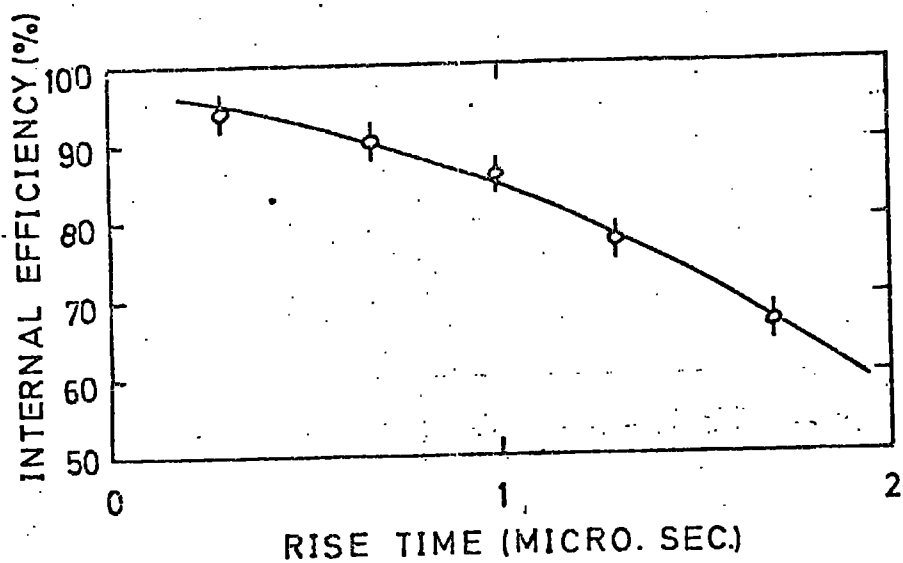
Coxell and Wolfendale.

FIGURE 4 EFFICIENCY VERSUS DELAY
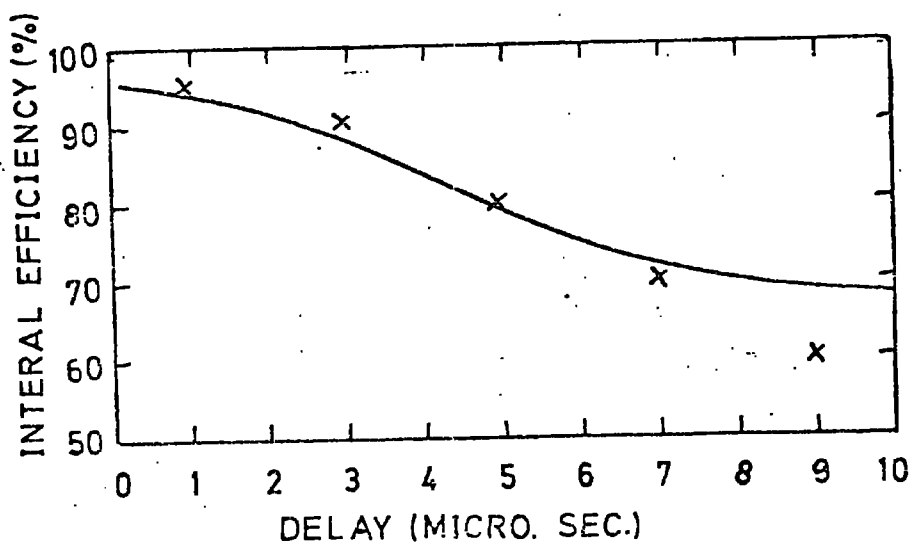
Conversi et al.

x Experiment —— Theory

against the window at the end of the flash tube. The probe is connected to ground by a resistor, and depending on the value of this resistor, signals of 1 to several hundred volts can be obtained. Thus CAMAC compatible signals can easily be obtained (4), enabling large amounts of data to be handled conveniently by on-line computer techniques.

Photomultipliers have also been used to output data from flash tubes. The magnitude of the output from the photomultiplier is related to the number of tubes igniting. This method has applications in extensive air shower studies (9), where the number of tubes igniting is proportional to the energy deposited in the array.

1.4 Basic Characteristics of Flash Tubes

Figures (1) to (4) show the effect on the efficiency of varying the magnitude, length, risetime and delay of the high voltage pulse applied to tubes of 1.6 cm internal diameter filled with 70% Ne, 30% He. The efficiency shown in each case is the "internal efficiency"; this is the probability of a tube lighting up if a particle has passed through its gaseous volume, and is almost 100% under optimum operating conditions. Another expression of the efficiency used is the "layer efficiency"; this is always less than the internal efficiency and is related to it by the ratio of the internal and external diameters of the tubes.

As expected, fig.(1) shows the efficiency to rise with rising field strength. Fig.(2) shows the effect of pulse length. Two types of pulse are usually used, a square pulse from a delay line or an exponentially decaying pulse, formed by discharging a capacitor through a resistor. Holroyd (5) found that for short pulses (approx.

0.4 microsec) large fields had to be applied to obtain even a faint discharge, however for larger pulses (approx. 4.0 microsec) the tubes performed correctly. Figure (3) shows the effect of the pulse risetime. A slowly rising pulse will sweep charge to the walls of the tube without initiating a discharge. Risetimes of up to 200 nsec. are usually acceptable, depending on the width of the tube. Figure (4) shows the effect of varying the delay between the passage of the particle and the application of the high voltage pulse. It can be seen that for long delays the charges are lost from the gas, either to the walls, or by recombination, thus lowering the efficiency of the tube.

Two other important properties of flash tubes are the sensitive time and the recovery time. These determine the rate at which flash tubes can operate.

The sensitive time is defined as the time after the passage of an ionising particle for the detecting efficiency to fall to 50%. The sensitive time of standard tubes is about 100 microsec. Reduction of this time requires removal of the free electrons in the gas. This can be achieved by addition of electronegative gases (4) such as O_2, CO_2, SF_6 etc. to absorb the free electrons. Alternatively a small alternating field (± 10 V, 50 Hz) (4) will remove free electrons in a few nsec. By these means the sensitive time has been reduced to about 1.0 microsec. (see figure (5))

The recovery time is defined as the time after the passage of an ionising particle for the reignition probability to fall to 50%. The recovery time of a standard flash tube is rarely better than 300 msec; since the time required by one electron to diffuse to the walls of the tube is only a few milliseconds, a secondary electron production process is indicated. This will be discussed later. The

FIGURE 5 EFFICIENCY VERSUS TIME DELAY FOR SEVERAL SINUSOIDAL CLEARING FIELDS

DELAY (MICRO. SEC.)
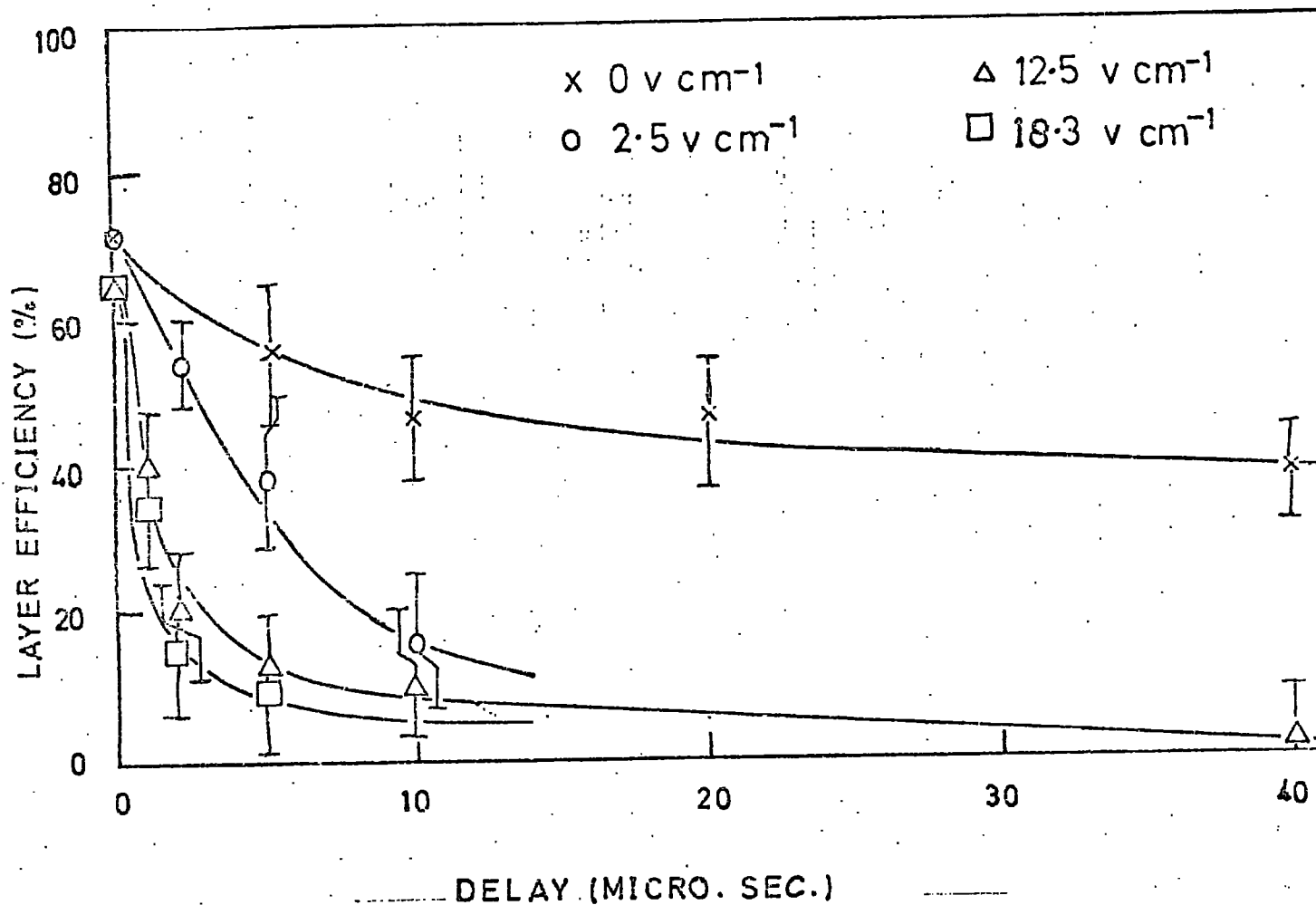
Chaney et al.

FIGURE 6   REIGNITION PROBILITY VERSUS TIME INTERVAL FOR Ne + CH$_4$
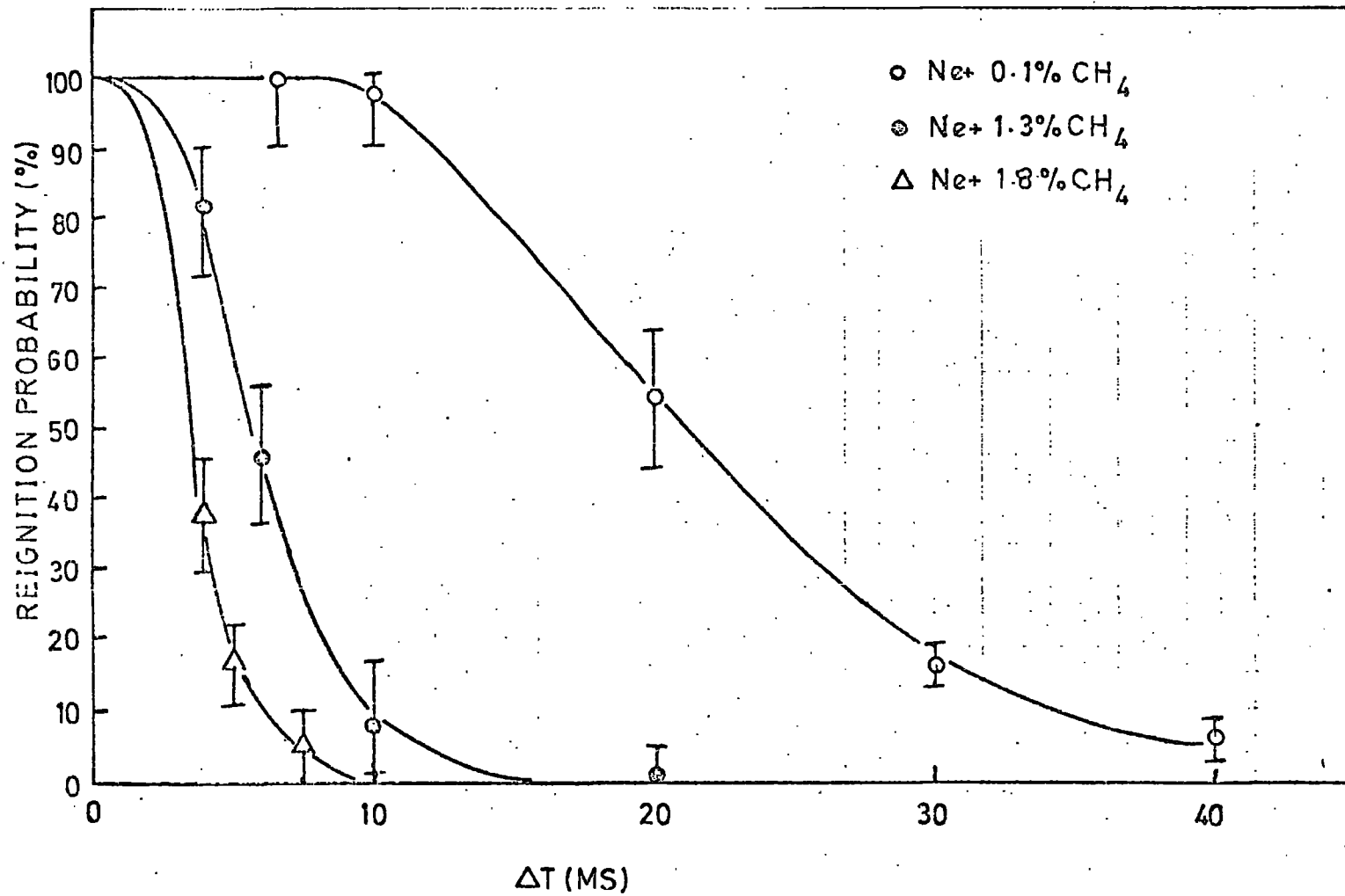
Chaney et al

recovery time has recently been reduced by the addition of small
quantities of molecular gas (4), such as CH_4, to about 0.6 msec.
(see figure (6)).

1.5 Use of Flash Tubes in Cosmic Ray Experiments

There are many features about flash tubes which suit them
to studies of cosmic rays, the most important being:

1) Flash tubes are simple, relatively robust, are reliable
over long periods of time, do not require constant attention, operate
satisfactorily over a wide range of temperatures and pressures, and
do not require a constant supply of gas. They are apparently
unaffected by magnetic fields, although no positive data is available
to confirm this.

2) The tubes are relatively inexpensive, the cost per tube
being independent of length. Large arrays can be constructed and their
geometry altered to suit various requirements.

3) A wide range of readout is available, including a simple,
inexpensive digitization system allowing on-line operation and
electronic decision making.

4) The tubes operate efficiently under a wide range of pulse
parameters (ie. low fields, relatively slow risetimes, long pulse
lengths), electrical interference with other apparatus can be kept to
a minimum under these conditions.

5) Good multitrack efficiency, since each flash tube is a
separate unit, unaffected by the presence of neighbouring flash tubes.
Reasonable spatial resolution depending on the tube width. 3-D track
reconstruction and the ability to offer a degree of energy resolution.

Cosmic ray experiments using flash tubes can be broadly divided into two sections:

A) Those using flash tubes primarily as track defining devices, eg.:

Magnetic Spectrometers: An example of this is the MARS experiment (6), which momentum analyses particles of energy up to 5.8 TeV/c, using a 300 ton magnet, with an integral Bdl of 8 x 10^6 gauss/cm. The readout system is of the electronic probe type.

Neutrino Studies: The Case-Witts-Irvine experiment (7) is the largest of this type, containing 50,000 2 M x 1.9 cm. tubes, situated 2 miles underground. A similar experiment was carried out at the Kolar gold mines in India (8).

Extensive Air Showers (EAS): The flash tube's high multitrack efficiency, and ability to cover large areas, make it very suitable to EAS studies. The largest detector of EAS is at Kiel (9), the main hodoscope being 31 M^2, containing 180,000 flash tubes, each 1 cm in diameter with an approximately spherical inner volume, filled with neon at 600 torr. The events are recorded photographically.

B) Experiments in which one or more of the flash tube parameters are varied to provide information about particular properties (ie. charge, mass) of a particle, eg.:

Search for Heavy Primary Cosmic Rays: A balloon borne experiment (10) has utilised the fact that ionisation densities produced by relativistic particles passing through a gas is proportional to Z^2. As the delay in the application of the high voltage pulse is increased, then only particles with an increasingly higher

atomic number will be detected with 100% efficiency.

Quark Searches: Ashton et al. (11) use the same concept to
search for fractionally charged quarks. Quarks should have a smaller
detecting efficiency owing to their fractional charge, thus for long
delays a single quark track will cause less tubes to ignite along its
length than a unitarily charged particle.

Energy Loss Measurements: Diggerty et al. (12) have shown
that energy loss by particles of equal momenta depends on the mass of
the particle. Studies of protons and muons in the range 0.1 to 10
GeV/c with a delay of 50 to 80 microsec applied to the flash tubes,
have produced distinct curves for protons and muons, thus allowing
discrimination between particles of equal momenta.

1.6 Use of Flash Tubes on Accelerator Experiments

It is with the application of flash tubes to accelerator
experiments that their major disadvantages become apparent, namely
the long sensitive and recovery times. The spark chamber, which made
its appearance shortly after the flash tube, was found to have better
sensitive and recovery times and was generally accepted for
accelerator experiments, despite its greater cost, complexity and
less versatility. The advent of the MWPC and other wire chambers
placed flash tubes further into the background as a suitable detector
for beamline experiments.

Work by Holroyd (5) and Chaney (4) has reduced the
sensitive and recovery times sufficiently for flash tubes to be
considered suitable for operation in the high background and rates
found on accelerators.

1.6.1 Reduction of Sensitive Time

The sensitive time may be reduced from 100 microsec. to a few microsec. by the addition of electronegative gases such as O_2, CO_2, CCl_4, SO_2 or SF_6. SF_6 has the highest capture cross section for thermal electrons, and the addition of as little as $1 \times 10^{-4}\%$ will reduce the sensitive time to 2 microsec. (13).

Another method is to apply an alternating square wave electric field across the tube to sweep out the free electrons (4). The frequency of the applied field must be high enough to change polarity before the charges deposited on the walls have time to move round the wall, and thereby back off the applied field (as happened with attempts to use a D.C. clearing field (5)).

Applied fields as small as 10 V/cm. reduce the sensitive time to approximately 2 microsec. Of the two methods described, the second is preferable since it allows a wider range of operating conditions, whereas the sealed "doped" tubes will only provide one value of sensitive time.

1.6.2 Reduction of Recovery Time.

It would be thought that the recovery time could be reduced by the same method as the sensitive time, however, experiments have shown (4) that the recovery time (of the order of 1 sec. or more in normal Ne-He tubes) was reduced by a factor of only 2, by the application of a 200 V/cm. clearing field. This is in disagreement with the theory (14) which predicts that all charge should be removed by the clearing field in approximately 50 microsec. This indicates that a secondary electron production is taking place.

As yet no complete explanation of this effect has been

found, but experiments indicate (5) that the induced clearing fields caused by charges deposited on the glass are of sufficient strength to cause localised Townsend avalanches, producing photons and electrons. These photons, incident on the glass, produce more secondary electrons, which in turn avalanche. This process will continue until. the induced fields have decayed to a value which will not support a Townsend avalanche. Another possible explanation of the long recovery time could be de-excitation of metastable atoms, however the lifetime of metastables in neon (15) is two orders of magnitude too small, and could not be entirely responsible for the long recovery times observed.

Chaney (4) found that by the addition of 2% CH_4 to the gas, the recovery time was reduced to 0.6 msec. Other molecular gases (H_2, CO_2, O_2, C_2H_6, C_4H_{10}) also reduced the recovery time, but CH_4 was chosen because of its availability and cheapness. The addition of up to 2% CH_4 had no ill effects on the other properties of the flash tube.

No satisfactory explanation has yet been found for the way in which the molecular gases reduce the recovery time, but it is thought that because of its broad absorption spectrum, the molecular gases are able to absorb the photons responsible for production of the secondary electrons.

No value for the lifetime of CH_4 in flash tubes has yet been found. It is expected that the CH_4 molecule will eventually be broken down by the action of the discharge, necessitating the refilling of the tubes. However, tubes pulsed 10^6 times showed no increase in recovery time.

1.6.3 Rate Effects

Although the sensitive and recovery times have been reduced to acceptable values, a further problem arises when flash tubes are operated at high rates.

The problem is seen as a dropping off of efficiency as the rate is increased. This is due to the high electric fields produced by charges being deposited on the walls of the tube. Unless these charges can be removed (by conduction over the surface of the tube) before the next discharge, then the field will continue to increase until an equilibrium is reached. The buildup of these fields can be reduced by:

1) Reducing the H.T. pulse length, thereby sweeping less charge to the walls.

2) Increasing the surface conductivity of the glass, thereby allowing the charges to decay away more rapidly.

3) Reducing the H.T. pulse height. (Since the effective field is less than the applied field due to the reverse direction of the induced field, any reduction of the H.T. pulse will probably result in loss of efficiency.)

4) Reducing to a minimum the delay between the passage of the particle and the application of the high voltage pulse, so that there is less chance of the ionisation due to the particle being swept away by the induced fields. (Probably very difficult, since, in the extreme case of high rate, the the induced field is of a sufficient magnitude to sweep out the majority of free charges in less than 200 nsec., and the tubes will not flash at all.(5))

These induced charges also manifest themselves in the form of weaker discharges (caused by the backing off of the H.T. pulse),

and by an increase in the rate of spurious flashing (caused by localised Townsend discharges initiated by the large fields).

The problem of the induced fields will be further discussed in chapter 3.

1.7 Some Flash Tube Arrays used on Accelerators

Work has been caried out by Breare et al. (*16*) using conventional flash tubes, made of Jena 16B low resistance glass, 0.5 cm in internal diameter, 50 cm long, filled with Ne (70%), He (30%) + 2% CH_4. These tubes were arranged in 12 planes or modules, each module containing 64 tubes, arranged in two orthogonal sets of 32, to provide X and Y coordinates. Sheets of lead, up to 1.8 radiation lengths thick were placed between each module to generate showers in the array when it was placed in a monochromatic positron beam, of energy 0.5 to 3.5 GeV/c. Using this setup, a mean spatial resolution of ± 3.8 mm., and energy resolution of 43% was achieved. The problems arising from this experiment will be discussed in detail in chapter 5.

The effect of induced fields at high rates was also observed; it was found that at 30 events/sec. the efficiency dropped to 40%, however, the chamber did not have the optimum H.T. parameters for operating at these high rates.

Conversi et al. (*17*) have conducted a number of experiments using plastic flash tubes. The advantages of using plastic instead of glass are that the lower surface resistances available help remove induced clearing fields, and that the low Z for plastic materials helps reduce coulomb scattering, allowing work with lower energy particles.

The problems arising from using plastics are that because of its relatively porous nature, a sealed tube cannot be used, also outgassing would poison the gas of a sealed tube causing the characteristics of each tube to differ widely. Thus the tubes require a constant gas flow through them.

Conversi found no variation in the sensitive time of his tubes when the rate was changed from 0.2 to 2.0 events/sec., and cites this as evidence that no clearing fields were being built up. No reduction in sensitive time was observed when a 50 Hz clearing field was applied, however, the sensitive time was increased as the gas flow was increased. This seems to indicate that in plastic flash tubes electrons caused by the ionising particle are lost to impurities emanating from the walls rather than by diffusion to the walls as in glass flash tubes.

An array of plastic flash tubes has been designed to fit around one of the intersections of the 1.5 GeV/c electron-positron storage ring at Frascati. As yet no results of these tests are known, although further work is at present being conducted by Conversi at CERN.

1.3 Conclusion

It is seen that flash tubes have enjoyed considerable sucess in their use in cosmic ray studies, and the problems arising from their application to accelerator experiments have been well defined, and in many cases solutions found by previous workers. A deeper understanding of the mechanisms of these problems and their solutions will be achieved by fitting a quantitative description to them. Attempts to do this are covered in the next chapter.

References

1   The "Hodoscope Chamber" a new instrument for nuclear research:
M. Conversi et al.   Nuovo Cimento 2 (1955), 189-191

2   Flash tube hodoscope chambers: M. Conversi and G. Brosco.
Ann. Rev. Nucl. Sc. 23 (1973), 75-123

3   Digitisation of neon flash tubes: C.A. Ayre and M.G.
Thompson.   Nucl.Inst. Meth. 69 (1969), 106-108

4   J.E. Chaney,   Ph.D. Thesis, 1974, Durham University.

5   F.W. Holroyd,   Ph.D. Thesis, 1971, Durham University.

6   The Durham Magnetic Automated Research Spectrograph,
(M.A.R.S.):   C.A. Ayre, Ph.D. Thesis, 1971,
Durham University.

7   Case-Wits-Irvine Conversi hodoscope, efficiency and high
voltage pulsing system: M.F. Crouch, Internal report,
Case Western Reserve University, 1968.

8   M.G.K. Menon et al.   Proc. Roy. Soc. A301, 137, (1967)

9   Aufbau Eines Hodoskops Fur Luftschauermessungen.
Experimentell-physikalische Diplomarbeit de Mathematisch-
Naturwissenschaftlichen Fakultät de Christian-Albrechts-
Universität nu Kiel, (1965).

10   Neon flash tube arrays as trajectory defining elements for
heavy nuclei. Proc. 12th Int. Conf. on Cosmic Rays,
Hobart 4 (1971) 1543-48

11   F. Ashton et al. (1971)   J. Physics, A4, 395

12   Neon flash tubes as energy loss measuring devices.
I.S. Diggory et al. Proc. 12th Int. Conf. on Cosmic Rays
Hobart 4 (1971) 1533-7

13   A flash tube chamber suitable for use at high repetition rates. J.E. Chaney et al. Nucl. Inst. Meth. <u>124</u> (1975), 61-71.

14   A.V. Phelps, J.L. Pack, Phys. Rev. <u>121</u> (1961) 798.

15   A.V. Phelps, Phys Rev. <u>114</u> (1959), 1011.

16   A digitised neon flash tube chamber suitable for γ ray detection. J.E. Chaney et al. Nucl. Inst. Meth. <u>125</u> (1975), 189-196.

17   Plastic chambers: M. Conversi et al. Conf. on Inst. for High Energy Physics, Frascati, 1973, 184-192.

CHAPTER 2

THE DISCHARGE MECHANISMS

2.1 The Discharge

In this chapter a qualitative description of the flash tube discharge mechanisms will be given, followed by an account of attempts to fit a quantitative description to the discharge.

The basic discharge process is well understood, however in practice there arise many problems, as discussed in chapter 1, which make the task of a complete quantitative description very complex. As yet no analytical theory exists which completely describes the discharge mechanism.

2.1.1 The Probability of a Discharge Occuring

For a discharge to occur when the high voltage pulse is applied it is neccesary for free electrons to exist in the gas.

When a particle passes through a gas it will deposit some of its energy in the gas. Taking a typical gas density of 1 mg/cm^3, and an energy loss by the particle in the gas of 2 MeV/gm.cm^2, then the particle will deposit approximately 2 KeV in traversing a flash tube.

The energy will be distributed in the gas in various ways,

but the majority will be in the form of electronic excitation,
including metastable production, and in ionisation. Excited atoms
produce resonant and non-resonant photons. Resonant photons can be
neglected since these proceed slowly through the gas (approximately
10^{-2} cm/sec.) being absorbed and re-emitted, and since the high
voltage pulse is applied for approximately 10^{-5} sec. these can have
little effect on the discharge.

Non-resonant photons proceed straight to the walls, where
they are absorbed and may produce photoelectrons. These photoelectrons
will be seen to be important to the propagation of the discharge
down the tube.

Metastable atoms decay with the emission of resonant photons,
however, in the presence of very small quantities of argon the
metastables are de-excited by ionising the argon atom (Penning
effect), producing a free electron.

Of the ionised components produced, the positive ions will
play no part since they move so slowly, unless they are within a few
angstroms distance of the wall, where they may produce secondary
electrons by virtue of their potential energy (1).

Assuming it requires 36.3 eV to produce an ion pair in
neon, and that for muons in the momentum range 1.5 GeV/c to 1000
GeV/c, the mean energy loss is 1220 eV/cm., then it can be expected
that approximately 33.6 ion pairs/cm/atmosphere will be produced in
neon by a cosmic ray muon (2).

During the time between the production of the primary
electrons and the application of the high voltage pulse, there are
a number of ways in which an electron may be lost from the gas, the
most important being:

1) Movement to the walls either by diffusion or by drift under the effect of an electric field.

2) Attachment to electronegative impurities, eg. oxygen molecules. These impurities may have been deliberately added to reduce the sensitive and recovery times.

Of those electrons remaining in the gas, only those which are a sufficient distance from the walls to allow the formation of a Townsend avalanche, will take part in the discharge.

2.2 The Discharge

There are two mechanisms involved in the flash tube discharge, the Townsend mechanism and streamer formation. The extent to which each mechanism contributes to the breakdown depends principally on the gas pressure, the magnitude of the applied field and the diameter of the tube. The Townsend mechanism predominates in low pressure tubes (1 atm. and less) and will occur at field strengths as low as 1 KV/cm. Streamer breakdown requires much higher fields, in order to produce the large quantities of charge necessary for their formation. In practice, when a tube discharges, it does so, usually, by both Townsend avalanche and streamer formation.

2.2.1 Discharge by Townsend Mechanism.

The Townsend mechanism requires only one electron to be present in the gas, at a distance $\geqslant$ the formative distance from the wall, to initiate an avalanche. The formative distance will depend on the gas pressure and composition and on the magnitude of the applied field. It has been found (3) that for tubes of 1.6 cm.

FIGURE 7
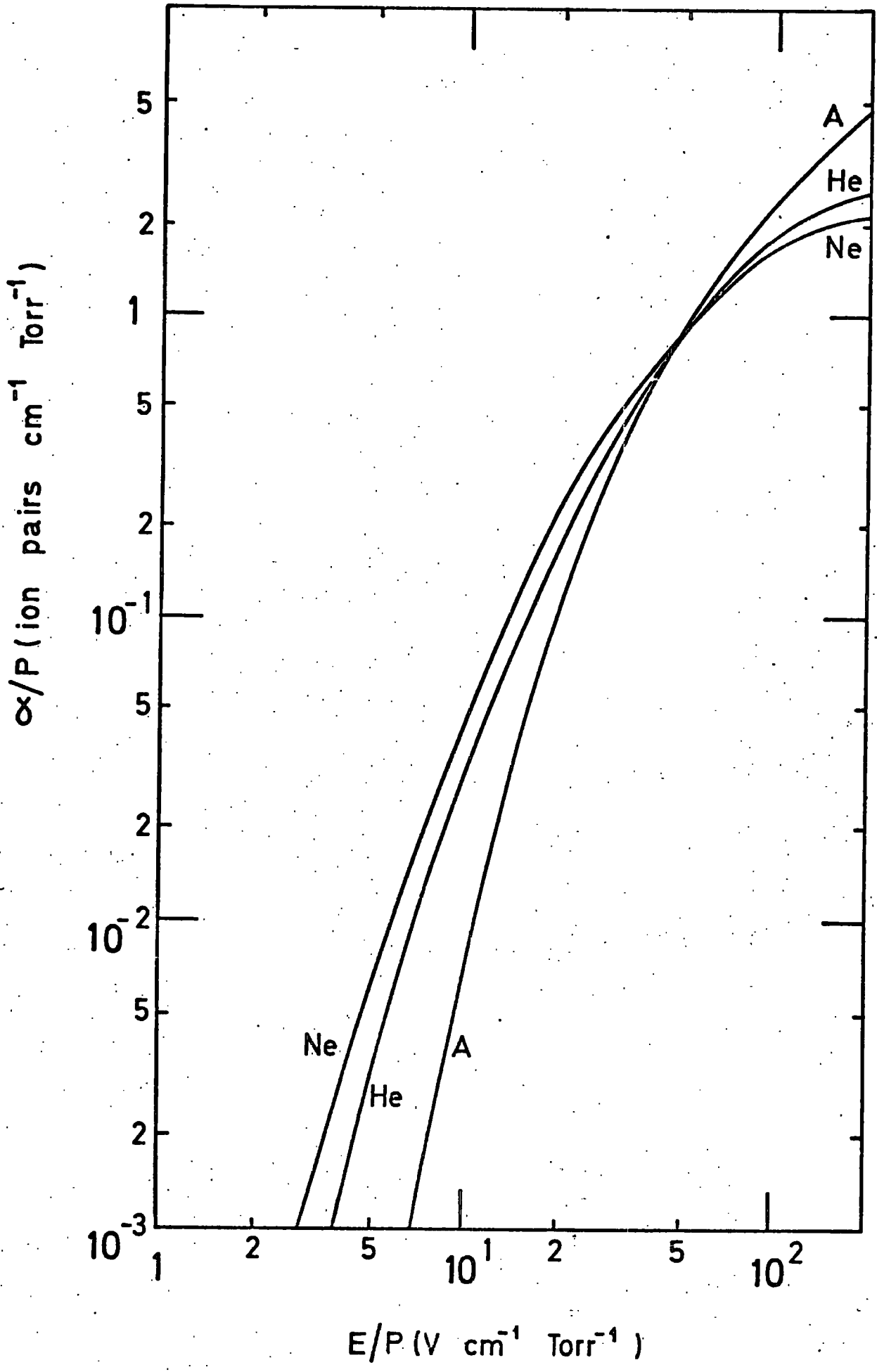
internal diameter, filled with 98% Ne and 2% He at 600 torr, using a
4 KV/cm. field, that a formative distance of 0.75 cm. gave a good
fit of the experimental points to the theory.

With the application of the electric field, the electron
is accelerated to the positive electrode. In doing so it gains energy,
which is then lost by collisions with gas atoms. The energy imparted
to the atom may be sufficient to ionise it and produce further
electrons. By this method the avalanche grows, the number of electrons
produced in a distance x, being given by the Townsend equation

$$n = n_o \exp(\alpha x)$$

where n_o = number of initial electrons
α = Townsend's 1st ionisation coefficient.

It can be seen from figure (4) that the higher the applied
field the more rapidly the avalanche builds up.

The discharge will cross the tube in times of typically
50 nsec. Once the electrons reach the wall they are effectively lost
from the gas, and the discharge will cease, unless the initial
avalanche produces secondary avalanches. This is most likely to be
caused by photons from the ionisation process striking the glass walls
and causing photoemission. The photoelectric yield of glass is 0.01
(4), and assuming that the number of photons produced in the initial
avalanche must be at least the number of ion pairs produced, then
there should be a copious supply of secondary electrons to maintain
the discharge. Figure (8) illustrates this process, and it is by
this process that the discharge propagates down the length of the

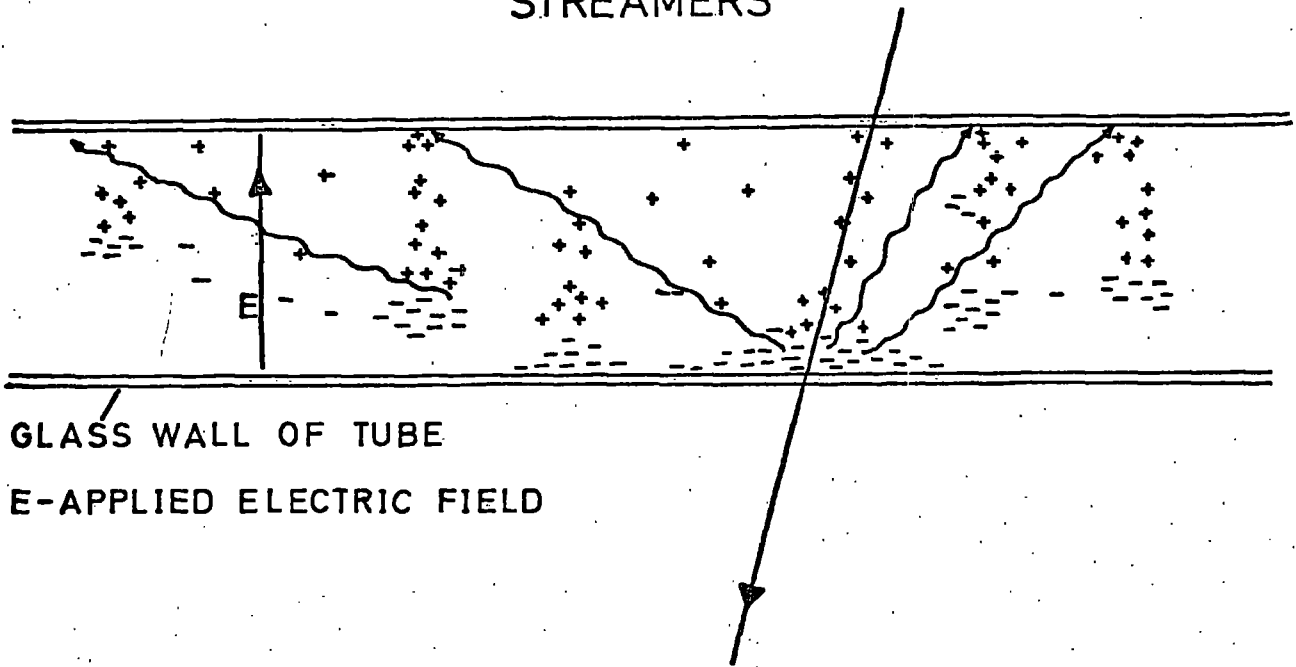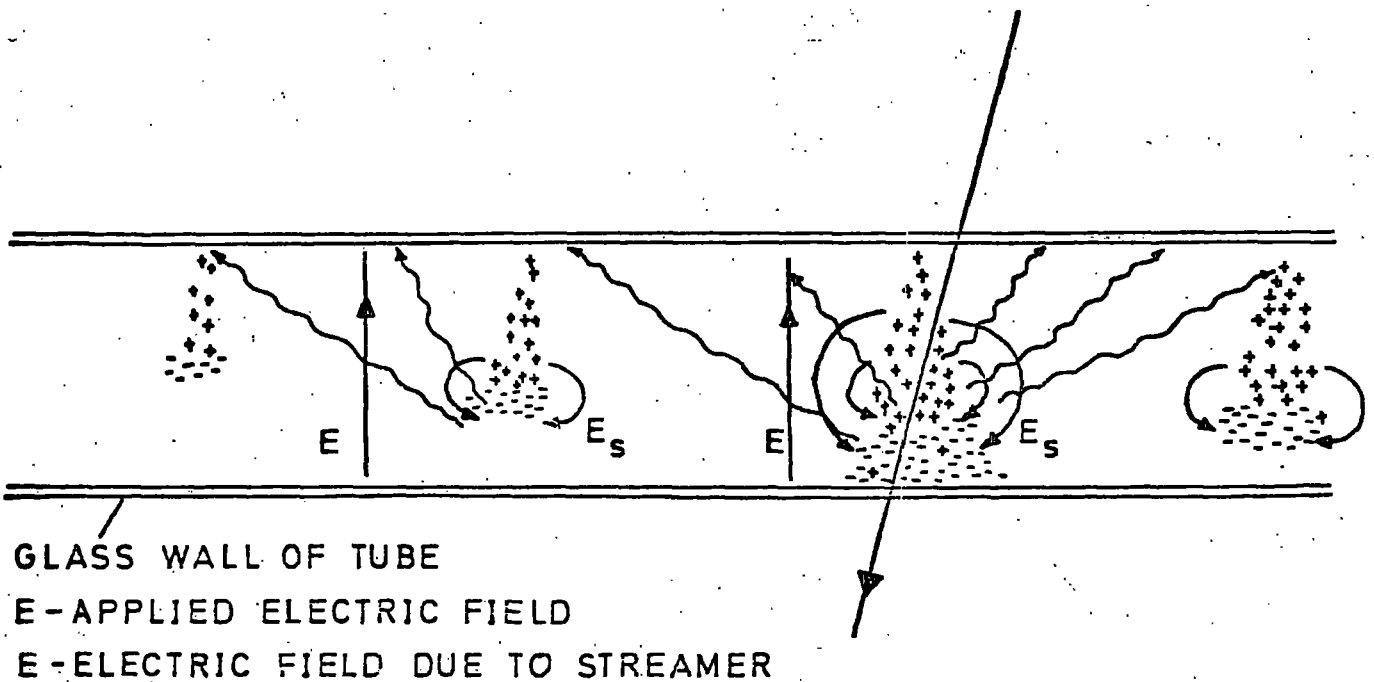FIGURE 8 DISCHARGE WITHOUT PRODUCTION OF STREAMERS

GLASS WALL OF TUBE

E-APPLIED ELECTRIC FIELD

FIGURE 9 DISCHARGE WITH PRODUCTION OF STREAMERS

GLASS WALL OF TUBE

E-APPLIED ELECTRIC FIELD

E-ELECTRIC FIELD DUE TO STREAMER

tube. The rate of propagation has been measured as 6.7×10^8 cm/sec.
(5) in tubes filled with Ne-He at 3 atm.


2.2.2 Discharge with Streamer Production.

The formation of streamers requires very high electric
fields. These fields are produced by separation of the two charge
components, accentuating the field at the head and tail of the
avalanche. The Raether criterion for streamer formation requires that
the radial field produced by charge separation should be of
approximately the same magnitude as the applied field, and for this
to be so requires the production of approximately 10^8 electrons in
the initial avalanche. To produce this number from a single electron
in a 1 cm. internal diameter tube filled at 600 torr, requires an
external field of 5.5 KV/cm. However, this is an over-estimation;
since an ionising particle produces approximately 30 electrons, the
avalanche will be initiated by more than one electron. This has been
borne out by experiment (6). Another mechanism producing secondary
electrons and thereby lowering the field necessary for the production
of streamers, in the Penning effect, whereby neon atoms can be
ionised by excited helium atoms.

Figure (9) shows a schematic diagram for streamer
production. As with the Townsend mechanism, the discharge is
propagated along the tube by photo-production of secondary electrons.
The speed of propagation has been measured for 1.6 cm. internal
diameter tubes filled with Ne-He at 600 torr, and found to be
3.6×10^8 cm/sec. (5).

When viewed from the side a tube undergoing a Townsend
discharge will be filled completely with a diffuse glow, the

FIGURE 10   DURATION OF DISCHARGE
AS A FUNCTION OF FLASH TUBE LENGTH
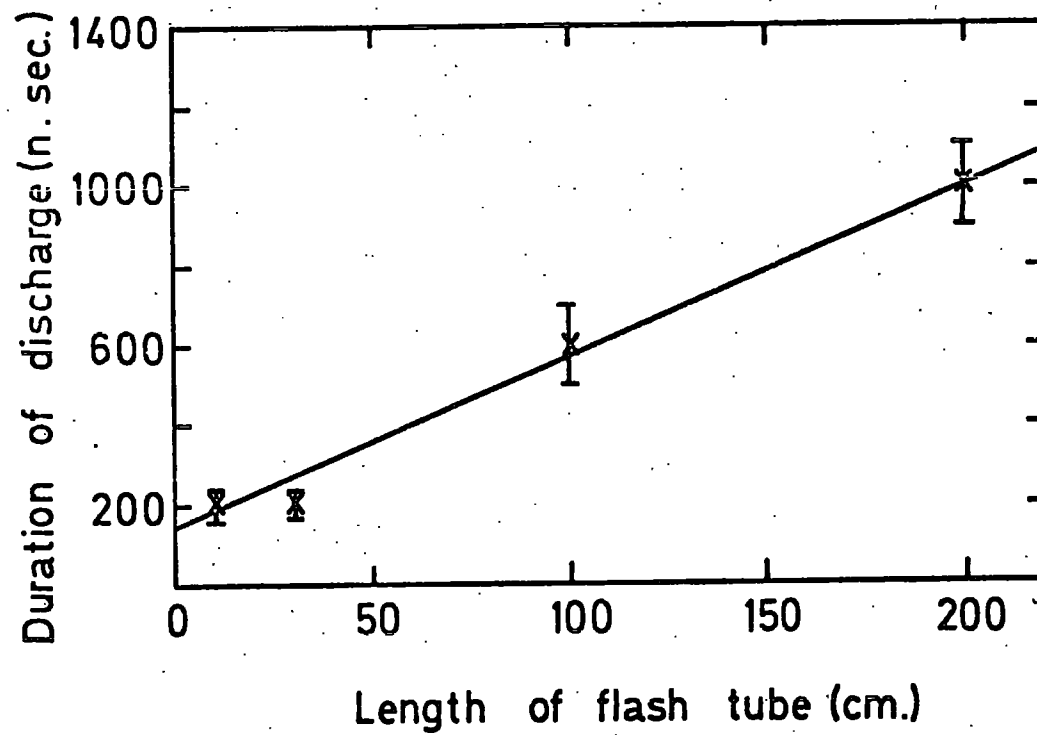
individual avalanches being indistinguishable. However, in a tube which is discharging with the production of streamers, individual streamers are clearly visible. The distinct spacing is caused by the distortion of the electric field in the region of a particular streamer preventing the production of a streamer close by. Hampson and Rastin (6) have found the average spacing to be 0.45 cm., which is in agreement with theory.

2.3 Termination of Discharge

The discharge will terminate when the amount of charge deposited on the walls is sufficient to produce a reverse field which lowers the effective field to a point where discharges can no longer be maintained.

In order to back off a 10 KV field applied to a flash tube of 5 pF capacitance, approximately 4×10^{11} electrons must be deposited on the walls of the tube. This estimate is confirmed by the observation that some 10^{12} photons are produced in a discharge (7). Bearing in mind that the number of photons produced is in excess of the number of ion pairs produced (8), then the agreement is good.

Studies of the light outputs from flash tubes have shown that the duration of the discharge is proportional to the length of the tube, and lasts for about the same amount of time it takes for the discharge to propagate down the length of the tube, even though the H.T. pulse is applied for much longer. This indicates that the discharge is self quenching. Figures (10) and (11) illustrate these effects.

FIGURE 11   H.T. pulse and light pulse
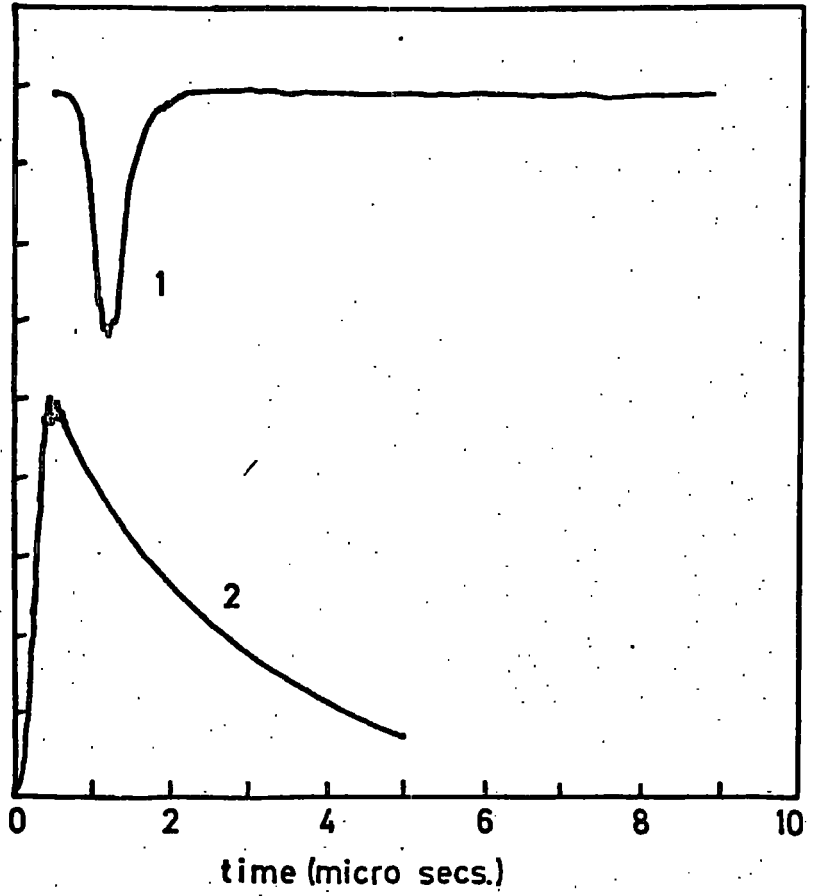
1 light pulse

2 H.T. pulse

2.4 Quantitative Description of Discharge Mechanism

The first successful attempt to fit a quantitative description to the discharge mechanism was developed in 1959 by Lloyd (9), who obtained efficiency-delay curves, considering thermal diffusion as the only means of removal of the primary electrons. Further work carried out at Nottingham (6), Rome (10) and Durham (11), extended the theory to include the many other factors which influence the characteristics of the tubes. The following is a review of their work, and the problems which remain to be solved.

2.4.1 Formation and Loss of Primary Electrons

As shown earlier, a minimum ionising particle will produce approximately 33.6 ion pairs/cm/atm. along its path. Then, for a particle passing a distance x from the centre of a tube, radius r, filled with gas at pressure P, the number of primary electrons produced is given by:

$$n(x) = 2Pm_0\sqrt{r^2-x^2}$$

where $m_0 = 33.6 \text{ cm}^{-1} \text{ atm.}^{-1}$

After a time t, some of these primary electrons will be lost from the gas through the following processes:

1) Attachment to electronegative impurities.

2) Recombination with positive ions.

3) Diffusion to the walls of the tube.

4) Drift to the walls of the tube under the effect of an electric field.

Process 2 can be neglected since m_0 and the recombination probability are small.

Process 4 becomes increasingly significant as the rate of flashing of the tubes is increased. However, an exact analytical treatment is extremely difficult, and as yet, only a Monte Carlo simulation has been used with any success to tackle this problem. Process 4 has been neglected in the present treatment, which assumes only processes 1 and 3.

Process 1 is of great significance, for only 0.1% contamination with oxygen will reduce the number of primary electrons by more than 50% within 20 microsec.

The probability of attachment to electronegative impurities after time t can be written;

$$P(t) = \frac{n(t,x)}{n(0,x)} = \exp(-bcut/\lambda_0) \tag{1}$$

where c = % of impurities

b = probability of attachment

u = mean velocity

λ_0 = mean free path

Process 3 can be accounted for by Lloyd's diffusion theory, and equation (1) can be rewritten as:

$$P(t,x) = \left[\exp(-bcut/\lambda_0)\right]\left[\sum_{\beta} \frac{\exp(-\beta^2 Dt/r^2)\int J_0(\beta^2/r)dy}{\beta J_1(\beta)\sqrt{r^2-x^2}}\right] \tag{2}$$

where D = electron diffusion coefficient

J_0 and J_1 = Bessel functions of order 0 and 1

β = roots of equation $J_0(x) = 0$

To a first approximation only the first term of Lloyd's expression may be considered, and using the relation:

$$D = \lambda u/3$$

equation (2) can be rewritten as:

$$P(t,x) = \exp\left\{-\left[3bc/\lambda\lambda_0 + (\beta_1/r)^2\right]Dt\right\} \qquad (3)$$

The use of the diffusion coefficient for thermal electrons for D, is not strictly correct, since the initial velocity of the primary electrons will be higher than thermal velocities, and therefore will suffer more initial collisions, resulting in a shorter sensitive time. Lloyd has estimated the correction to be small, and in the present treatment the effect will be neglected.

2.4.2 The Discharge

As described previously, streamer production requires the enhancement of the applied electric field by the presence of large numbers of secondary charges produced in the Townsend avalanche. The number of charges must exceed e^{20} (12) and the avalanche must advance over a distance d, given by:
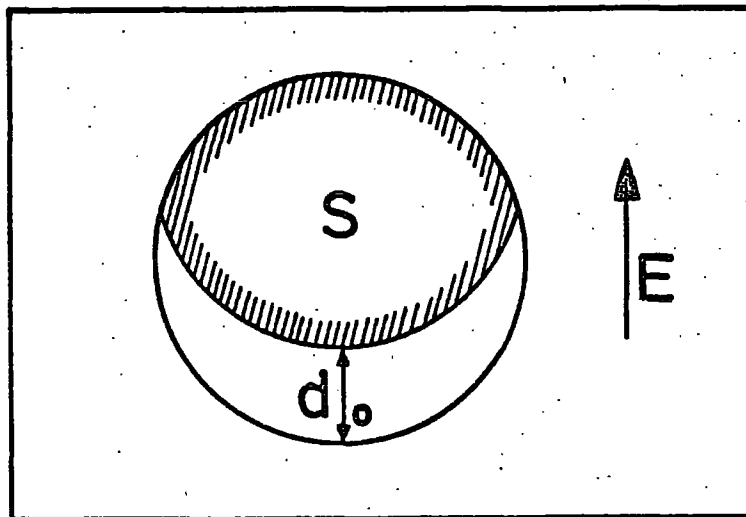
$$d = 20/\alpha$$

FIGURE 12   FORMATIVE DISTANCE FOR
STREAMER PRODUCTION

d is the formative distance for an avalanche to produce a streamer, and therefore only electrons shown in the region S in figure (12) can take part in the discharge. The calculation of the number of electrons present in S is complex (10), since initially the electrons lie along the path of the ionising particle. However, for longer time delays, the distribution becomes more uniform, and the number of electrons, f, present in S can be written as:

$$f = S/\pi r^2 = 1-(2\phi+\sin 2\phi)/\pi \tag{4}$$

where $\phi = \arcsin(d_o/2r)$

Hampson and Rastin (6) found that in high pressure tubes, the probability of a primary electron initiating an avalanche large enough to create a streamer, was small. The streamers are formed some time after the initial avalanche, when secondary electrons (caused by photo-production in the glass) initiate further avalanches and raise the number of free charges to the level required for streamer production.

2.4.3 Efficiency and Sensitive Time

The probability of the tube flashing, and therefore its efficiency, depends on the number of primary electrons, $n(x)$, the probability of these electrons being lost from the gas, $P(t,x)$ and the probability of the remaining electrons being a formative distance from the walls when the high voltage pulse is applied, f.

Assuming for simplicity a Poisson distribution (it is actually Landau), this can be expressed as:

$$\eta(x,t) = 1-\exp\left[-n(x).P(t,x).f\right] \tag{5}$$

then the efficiency-delay curve is given by:

$$\eta(t) = \int_{0}^{r}\eta(x)\,dx \tag{6}$$

Using the relation:

$$n(x) = 2Pm_0\sqrt{r^2-x^2}$$

and the equations (3) and (5), the sensitive time may be written as:

$$t_s = \frac{\ln\left[(2rPm_0f/\ln2)\sqrt{1-(x/r)^2}\right]}{\left[3bc/\lambda\lambda_0 + \beta_1/r^2\right]D} \tag{7}$$

The dependence of t_s on x can be removed by taking its average value over x.

$$t_s = \frac{\ln(2ArPm_0f/\ln2)}{\left[3bc/\lambda\lambda_0 + (\beta_1/r)^2\right]D} \tag{8}$$

where A is a geometrical factor, which, assuming

$$2rPm_0f/\ln2 \gg 1$$

can be evaluated by computing the average of

$$\ln(2rPm_0 f\sqrt{1-(x/r)^2}/\ln 2)$$

and is found to be 0.75

The theoretical curves obtained using these equations do not always give a good fit to the experimental data, the predicted sensitive time being almost double that observed (10). Possible reasons for this discrepancy are:

1) The finite rise time of the H.T. pulse sweeps electrons out of the gas without initiating a discharge, effectively lowering the value of f.

2) The presence of small quantities of electronegative impurities reducing f.

3) The presence of induced electric fields sweeping electrons from the gas, also reducing f.

The degree to which each of these factors influence η and t_s are unknown, and to describe them analytically would greatly complicate the theory. Since f is subject to so many variables it is more convenient to obtain a value experimentally and insert it into the equations.

2.4.4 Recovery Time

Assuming that each streamer contains 5×10^8 electrons, and that there are 2.5 streamers per cm. (section 2.2.2), then immediately after the discharge, there should be approximately 10^9 electrons/cc. in the gas.

The mechanisms for removal of charge from the gas are the same as those listed in 2.4.1. However, since the charge density is

now very great, the recombination of positive ions and electrons can no longer be neglected. Brosco (10) has derived a theoretical expression for the recovery time, considering diffusion and recombination as the mechanisms of electron and positive ion loss, which is shown below:

$$\frac{\partial}{\partial t}\int_0^x P_\pm' \cdot x \cdot dx = xD_\pm \frac{\partial}{\partial x} P_\pm - \delta \int_0^x P_\pm P_\mp x \cdot dx + 4\pi P_\pm eK_\pm \int_0^x \left[P_\pm - P_\mp \right] x \cdot dx \qquad (9)$$

where $P_+(x,t)$, $P_-(x,t)$ are the charge densities at time t, distance x from the tube axis.

D_+, D_- are the diffusion coefficients for the positive and negative charges.

δ is the electron-ion recombination coefficient.

K_+, K_- are the ion and electron mobilities.

The first two terms describe electron-ion diffusion and recombination. The last term describes the effect of the radial field caused by ambipolar diffusion, which counteracts the diffusion of electrons to the walls.

Using the above equations it has been shown (10) that ambipolar diffusion occurs for a time T_1, given by:

$$T_1 = \frac{r^2}{6D_+} \cdot \ln \frac{1 + dD_+/r}{1 + 6D_+/\delta \rho_0 r^2} \qquad (10)$$

where $d = (4e^2/KT)$

$\rho_0 = \rho_+(0) = \rho_-(0)$ charge density at zero time.

Also an additional time T_2 must elapse before the reignition probability in a gas of volume V_1 falls below 10%, and is given by:

$$T_2 = \frac{r^2}{6D_-} \ln \frac{6Vf}{dr^2 \ln(10/9)} \qquad (11)$$

It is found that $T_2 \ll T_1$ and for most cases the recovery time can be considered as that given by equation (10). For noble gases the agreement between experiment and theory is quite good.

If electronegative impurities are present in sufficient quantities to dominate the processes responsible for electron disappearance, then the recovery time is given by:

$$T_r = \ln(\rho_0 V \lambda_0 f/bcu) \qquad (12)$$

where the symbols have the same meaning as previously assigned to them. However, this equation gives values of T_r considerably smaller than those found experimentally, and as yet it is not understood why.

2.4.5 Induced Clearing Fields

Holroyd (11) has used a Monte Carlo method to investigate the effects of electron drift caused by the electric fields of charges adhering to the tube walls. Considering only the formative distance, drift and diffusion, efficiency-delay curves were obtained for various values of formative distance and drift velocity. From these results, and experimental data, a value for the amount of

charge deposited on the walls was ascertained.

The Monte Carlo approach is a simple one, and such a treatment could include all the major effects influencing the performance of flash tubes, provided the probability of their occurrance is known. This approach may be the only practical way of fitting quantitative descriptions to the observed behaviour.

2.5 Conclusion

There does not exist an analytical description which will successfully describe all major mechanisms involved in the discharge of a flash tube, although individual effects under a narrow range of conditions can be predicted quite well by theory. It is probable that a complete quantitative description of the discharge is only possible using a Monte Carlo approach similar to that used by Holroyd.

The problem of the induced clearing field is the most difficult to describe analytically, probably because little is known definately about its formation and decay. The work that has been done on this problem is described in the two following chapters.

References

1   J.E. Chaney, Ph.D. Thesis, 1974, Durham University.

2   The ionisation loss of relativistic μ mesons in Neon.
Eyeions et al. Proc. Phys. Soc. A68 739, 1955.

3   F.W. Holroyd, Ph.D. Thesis, 1971, Durham University.

4   W.L. Harries and A. Von Engel, 1954, Proc. R. Soc. A22
490-508.

5   Particle location along the length of a neon flash tube.
C.A. Ayre et al. Nucl. Inst. Meth. 103 (1972), 49-52.

6   An investigation into the flash tube discharge mechanism.
Hampson and Rastin. Nucl. Inst. Meth. 96 (1971), 197-203

7   Optical measurements on neon flash tubes. Coxell et al.
Suppl. Nuovo Cimento 21 (1961), 28-38.

8   S. Corrigan and A. Von Engel, 1958. Proc. Phys. Soc. 72
786-790.

9   On the efficiency of the neon flash tube. J.L. Lloyd.
Proc. Phys. Soc. 75 (1960), 387-394.

10   G. Brosco, Ph.D. Thesis, 1972, University of Rome.

11   A computer simulated model for diffusion and drift of
electrons in flash tubes. Holroyd et al.
Nucl. Inst. Meth. 100 (1972) 277-280.

12   Electron avalanches and breakdown in gases: H. Reather
1964, Butterworth Press.

13   High Pressure Neon Flash Tubes. H. Coxell, A.W. Wolfendale.
Proc. Phys. Soc. 75 (1960) 373-386.

CHAPTER 3

INDUCED CLEARING FIELDS

3.1 Observation of Induced Clearing Fields

The effect of induced clearing fields was first reported by Pickersgill (1), who observed that the efficiency-delay curves differed according to the length of the high voltage pulse used. It was suggested that polarisation was taking place in the glass, effectively backing off the applied H.T. pulse, thus lowering the efficiency.

Clearing field effects were also observed by Crouch (2), who noted that the magnitude of the effect depended not only on pulse length, but also on rate, temperature, humidity and pulse shape, a bipolar pulse considerably reducing the effect of the fields, as did high temperatures and humidities. The evidence indicated that the effect was due to charges deposited on the walls of the tube, producing electric fields, which required times of up to minutes to decay, depending on the parameters mentioned above.

The question as to whether the clearing fields are caused by polarisation in the glass, or by charge deposited on the glass surface was resolved by Hampson and Rastin (3), who observed that clearing fields were only built up in tubes which had discharged, and

that tubes which had been subject to the same high voltage pulses,
but had not discharged, showed no clearing field effects. This
associated the clearing fields with the production of large quantities
of free charge. Further evidence was provided by the fact that the
magnitude of the clearing field effect depended upon the resistance
of the glass tube, supporting the theory that the fields decay by
conduction of the induced charges, either across the glass surface,
or through its volume.

Whilst studying these fields, Holroyd (4) noticed the
presence of a long term clearing field, taking several days to decay
away. No satisfactory explanation has been found for this long term
effect, but it was suggested that it may be caused by polarisation of
the glass, or by electrons trapped in the glass surface.

3.2 Formation of Induced Clearing Fields

Extensive investigations of induced clearing fields have
been made by Holroyd (4), who, by extending the work of Crouch and
Hampson and Rastin, was able to make quantitative conclusions
concerning the nature of the clearing fields. Unless otherwise stated,
all results quoted in this chapter were obtained by her, using
1 metre tubes, internal diameter 1.6 cm., filled with 98% Ne, 2% He
at 60 cm.Hg.

3.2.1 Short Term Clearing Field

The short term clearing field is caused by charges
resulting from the discharge being deposited onto the walls of the
tube. This produces an electric field across the tube, which reduces
the efficiency by sweeping out the primary electrons, and "backing

FIGURE 13   efficiency versus delay for various pulse lengths
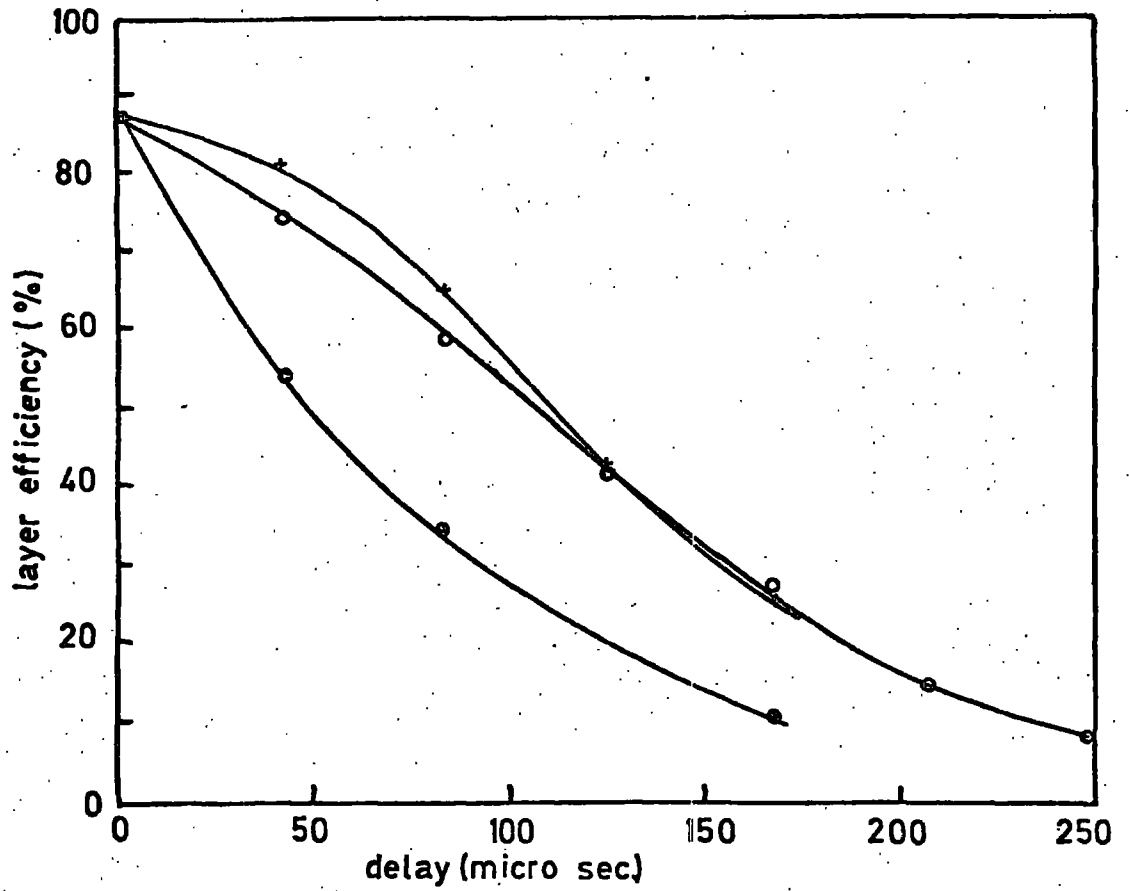
pulse lengths

+ =   0·4 micro secs. R.C.

o =   4·0 micro secs. R.C.

● =   40·0 micro secs. R.C.

off" the applied high voltage.

The electrons from the discharge will be removed completely from the gas in times of 100 to 200 nsec., adhering to the tube wall nearest the positive electrode. The more massive positive ions move relatively slowly, and depending on the length of the high voltage pulse, a proportion of them will be swept to the wall nearest the negative electrode, to which they will adhere. Those positive ions remaining in the gas after the removal of the applied high voltage pulse, will then drift under the influence of the attractive force due to the electrons, and the repulsion due to the ions, to the wall, where they will quickly recombine with the electrons there.

The amount of positive charge deposited on the walls will depend principally on the length and magnitude of the high voltage pulse. The variation of efficiency as a function of delay, for various pulse lengths, is shown in figure (13). If according to Lloyd's theoretical treatment, diffusion was the only mechanism for the removal of the primary electrons, then the efficiency should not change with pulse length. However the decrease in efficiency indicates the presence of another mechanism (the induced field) which removes the primary electrons more rapidly than by simple diffusion.

Comparing these experimental efficiency curves with those showing efficiency as a function of delay for various drift velocities, obtained theoretically from a Monte Carlo simulation using diffusion and drift (see chapter 2), it can be seen that the magnitude of the observed clearing fields decreases with increasing delay, as is to be expected.

Figure (15) shows the variation of clearing field with efficiency for different high voltage pulse lengths. This was obtained

by first comparing the experimental efficiencies at a certain delay
with the theoretical plot of efficiency versus drift velocity, for
the same delay, thus giving a relationship between delay and drift
velocity. Using the data of Pack and Phelps (5), the field necessary,
and therefore the number of charges required, to produce this drift
velocity can be found.

The data of Pack and Phelps refers to pure neon, and the
above treatment assumes the relationship between field and drift
velocity is not significantly different in pure neon, and the 98% Ne,
2% He mixture used in the tubes.

A method of finding the drift velocity independently of
the data of Pack and Phelps was devised by Stubbs (6). Using
experimental efficiency delay curves obtained for 3 different values
of applied alternating field strength, a theoretical fit was made to
one of these curves using a Monte Carlo technique, which assumed an
alternating drift velocity. From the drift velocity which gave the
best fit, values were obtained for the drift velocity associated
with the other two fields. Using these two derived velocities good
fits were made to the other two efficiency-delay curves, indicating
the validity of the method. Thus the value of the drift velocity
for a particular field may be found, avoiding the assumptions about
the gas mixture made in using Pack and Phelps' data.

The maximum induced field was obtained using a pulse
length of 40 microsec., beyond which the field did not increase
significantly. This must represent the time required to sweep out
the largest number of positive ions to the walls. This is consistant
with the value of 80 microsec. given by the data of Pack and Phelps
for the drift velocity of positive ions in a field of 4 KV/cm.

The short term induced field is found to be independant of
the magnitude of the applied field. This result is surprising, since
the amount of charge produced increases as the intensity of the
applied field increases, and therefore larger fields can be expected.
Also the drift velocity of the positive ions increases, depositing
a greater proportion of charge on the walls in a given time. No
satisfactory explanation for this result has yet been found.

3.2.2 Decay of Short Term Clearing Fields.

The induced clearing field will decay by conduction of
the electrons over the surface, or through the volume of the glass,
thus recombining with the positive ions trapped in the glass surface.
The time constant, τ, of the decay will be determined by the
resistance of the glass and the capacity of the tube. Holroyd found
the capacitance of the tubes to be 4.25 pF, and the volume resistance
of the soda glass was measured as $5.3 \times 10^{13} \Omega$. The surface resistance
of chemically clean glass was found to be $5 \times 10^{13} \Omega$, although values
as low as $10^{8} \Omega$ were recorded, depending on the amount the glass
surface was contaminated. Assuming that the inner surface of the flash
tube was relatively clean, due to its method of manufacture, a value
of 2.7 seconds was calculated for τ.

A glass with a lower resistance, which still maintains
good mechanical properties is "Jena 16B", this has a resistance of
approximately $6 \times 10^{10} \Omega$ at $21^{\circ}C$ (7) and is now used for tubes which
are operated at a high rate (9).

The induced clearing field will decay according to :

$$V = V_{o} \exp(-t/\tau)$$

where V = field at time t

V_o = field at time t = 0

τ = decay costant = RC

The magnitude of the clearing field is proportional to the amount of charge deposited on the tube walls, this can be written as:

$$\frac{dn}{dt} = \frac{s-n}{\tau}$$

where s = rate of deposition of charge

n = number of electrons

τ = decay constant

Using these two relationships, Holroyd (4) derived an analytical expression for the quantity of charge deposited, and therefore the strength of the clearing field. It can be seen below, that the expression predicts correctly that the strength of the clearing field is proportional to the length of the high voltage pulse.

$$V \propto RCV_o\eta\, (\tau /t)(1-\exp(-t/\tau))$$

where V = clearing field

RC = decay constant of high voltage pulse

V_o = initial field

η = efficiency

τ = decay constant of charge

t = time interval between flashes

FIGURE 14

R.C. constant of high voltage pulse (micro.sec.)

FIGURE 15

Efficiency
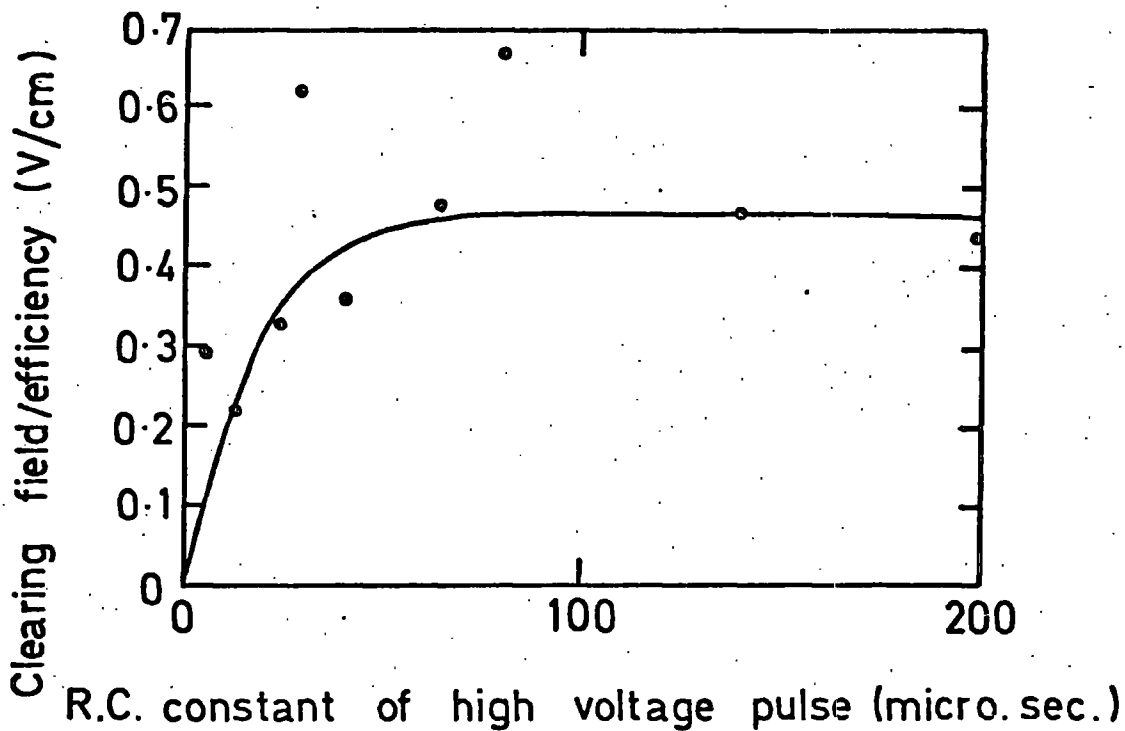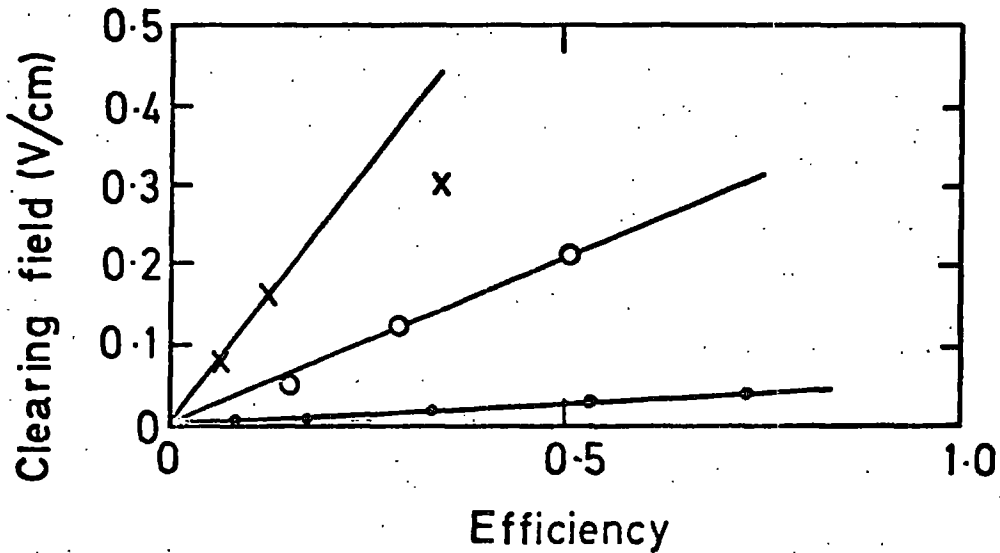
x   26·8 micro.sec.R.C. high voltage pulse.
o   40·0 micro.sec.R.C. high voltage pulse.
•   0·4 micro.sec.R.C. high voltage pulse.

(Different sets of points are not necessarily for the
same repetition rate)

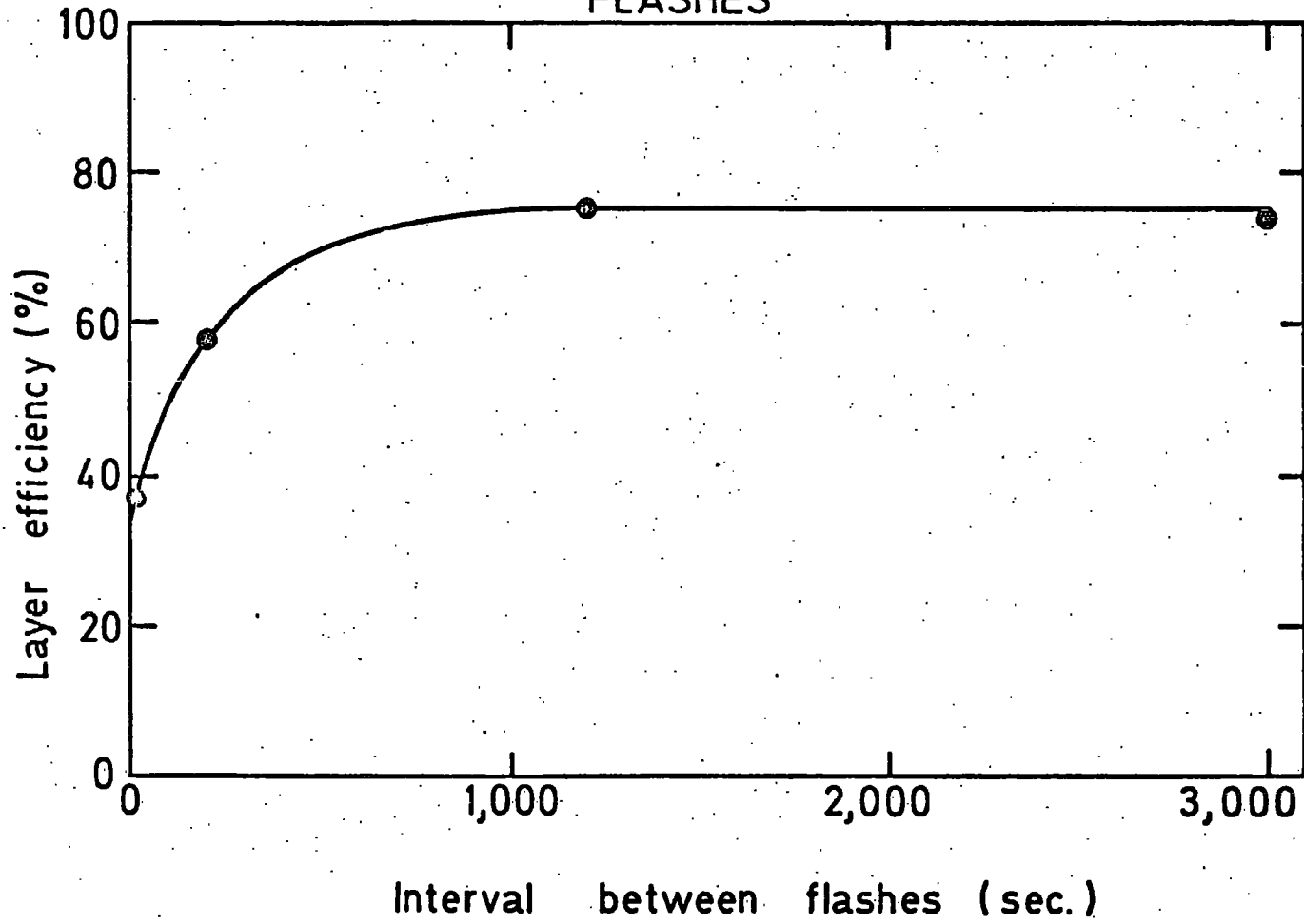FIGURE 16   EFFICIENCY AS A FUNCTION OF INTERVAL BETWEEN FLASHES

Figure (14) shows clearing field/efficiency as a function of high voltage pulse length. It can be seen that the curve is flat beyond about 80 microsec.; this is because all the positive ions have been swept out of the gas, which is in agreement with the data of Pack and Phelps.

Figure (15) shows clearing field as a function of efficiency for 3 different high voltage pulse lengths. Straight lines are obtained for each pulse length. For the rates at which the clearing field effect becomes appreciable, $\exp(-t/\tau)$ tends to zero, and the constant of proportionality in the above equation can be found for a particular pulse length.

Figure (16) shows the interval between flashes as a function of layer efficiency, the efficiency falling fast for intervals of less than about 10 minutes. From the theoretically obtained curves of efficiency as a function of delay, for different drift velocities, shown in figure (17), it can be seen that the drift velocity must fall to approximately 10^3 cm/sec. for it to have no appreciable effect on the efficiency. This corresponds to an induced field of 10^{-3} V/cm. If the induced field does not fall to approximately this value before the next event, then there will be a loss of efficiency. This marks the threshold beyond which rate effects will become apparent, as was shown in figure (16). The degree to which the induced field affects the efficiency will depend also on the delay in applying the high voltage pulse.

3.2.3 The Long Term Clearing Field

The long term clearing field appears to be of an entirely different nature to that of the short term field, however, as with

FIGURE 17
EFFICIENCY AS A FUNCTION OF DELAY FOR DRIFT VELOCITIES OPPOSING THE APPLIED FIELD.

Delay (micro.sec.)
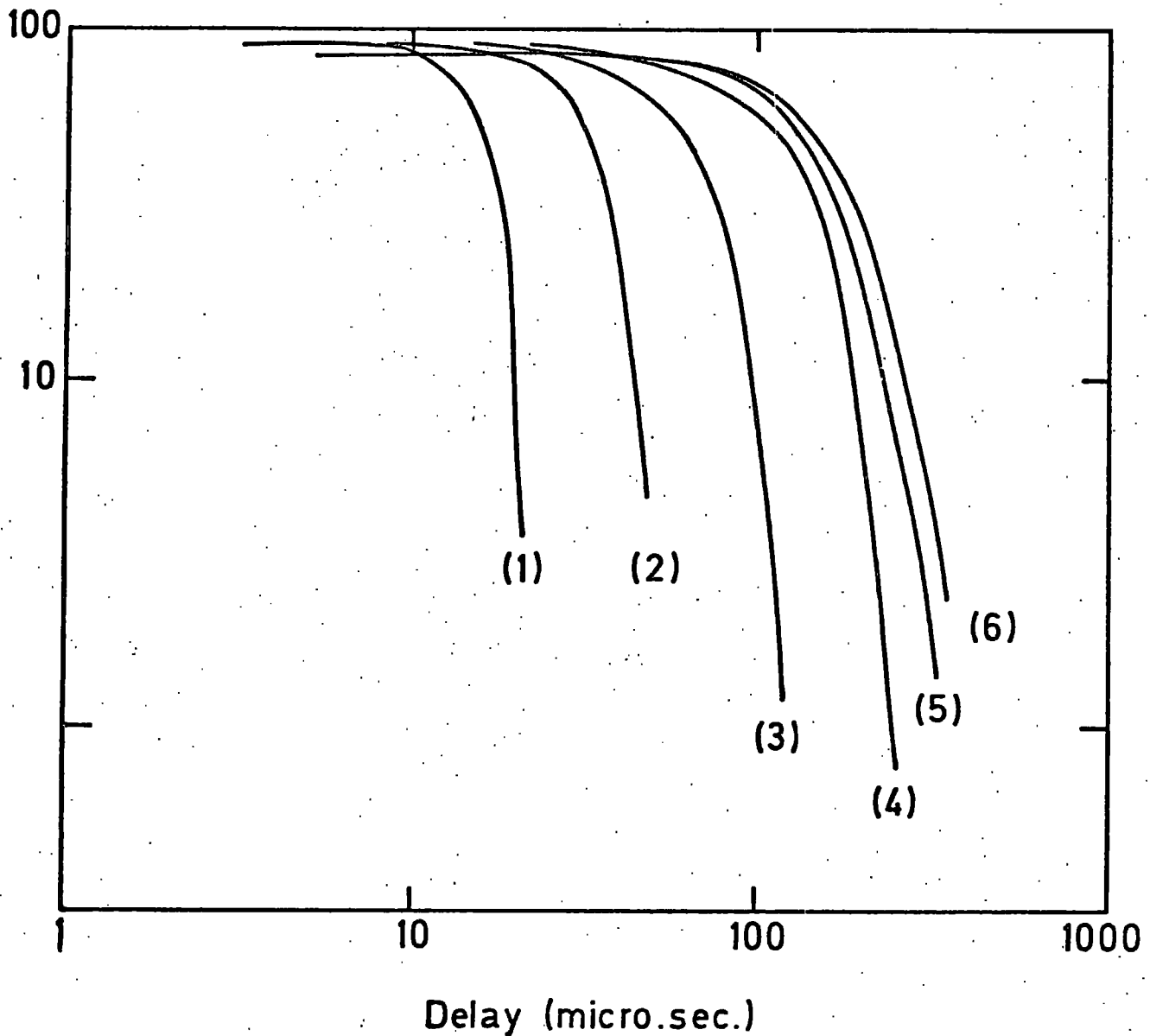
(1) $V = 10^5$ cm./sec.

(2) $V = 5 \times 10^4$ cm./sec.

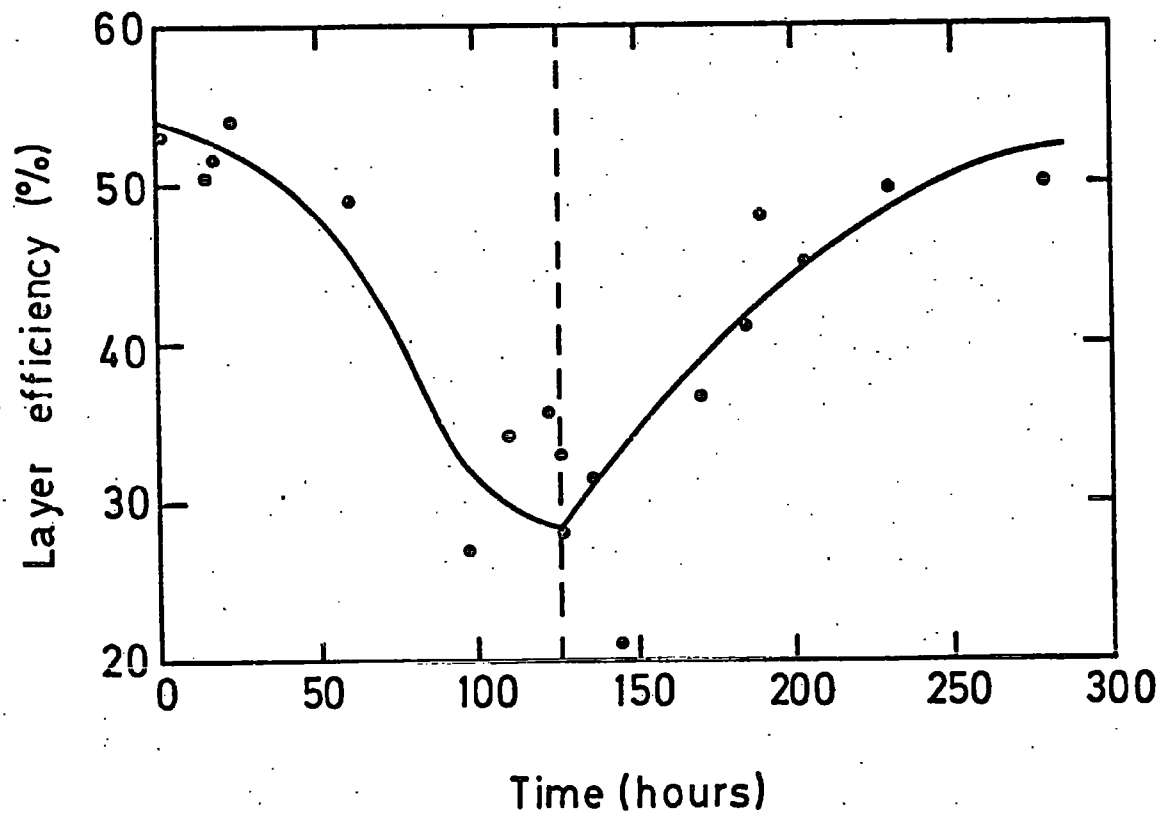(3) $V = 2.5 \times 10^4$ cm./sec.

(4) $V = 10^4$ cm./sec.

(5) $V = 4 \times 10^3$ cm./sec.

(6) $V = 0$ cm./sec.

FIGURE 18   CLEARING FIELD EFFECT DURING AND AFTER HIGH EFFICIENCY RUN.

Termination of high efficiency run.

the short term field, the effect only occurs if the tube flashes.
Holroyd demonstrated this by using a triggering system which only
covered one side of a broad array of flash tubes. The system was
operated at a high rate of 1 flash per tube per minute, for several
days. The tubes in the array, which lay within the volume covered by
the trigger system, flashed much more frequently than those outside
the trigger system. Those covered by the trigger system were found to
have an efficiency of 35%, while those outside, had an efficiency of
44%, showing that the long term clearing field is also due to the
actual discharge.

It can be seen from figure (18), that the field is only
produced by running at high rates for a number of days, and that the
recovery times are equally long.

Unlike the short term field, the long term field is affected
by the pulse height, becoming predominant about 6 KV/cm. in the case
of Holroyd's tubes. This is shown in figure (19). The effect may
exist below 6 KV/cm., and may possibly be observed if sufficient time
is allowed for the effect to build up.

Two possible explanations for the long term field have
been offered:

1) Polarisation in the glass. It may be that the minimum
energy needed to cause polarisation requires fields greater than
6 KV/cm., which would explain why the fields become apparent only
above this field value. Little information is available at the present
on the polarisation properties of glass.

2) Trapping of electrons in the glass. Most glass surfaces,
unless kept under stringent conditions, will aquire a thin layer of
water on their surfaces. Energetic electrons may penetrate this layer

FIGURE 19   efficiency as a function of applied field
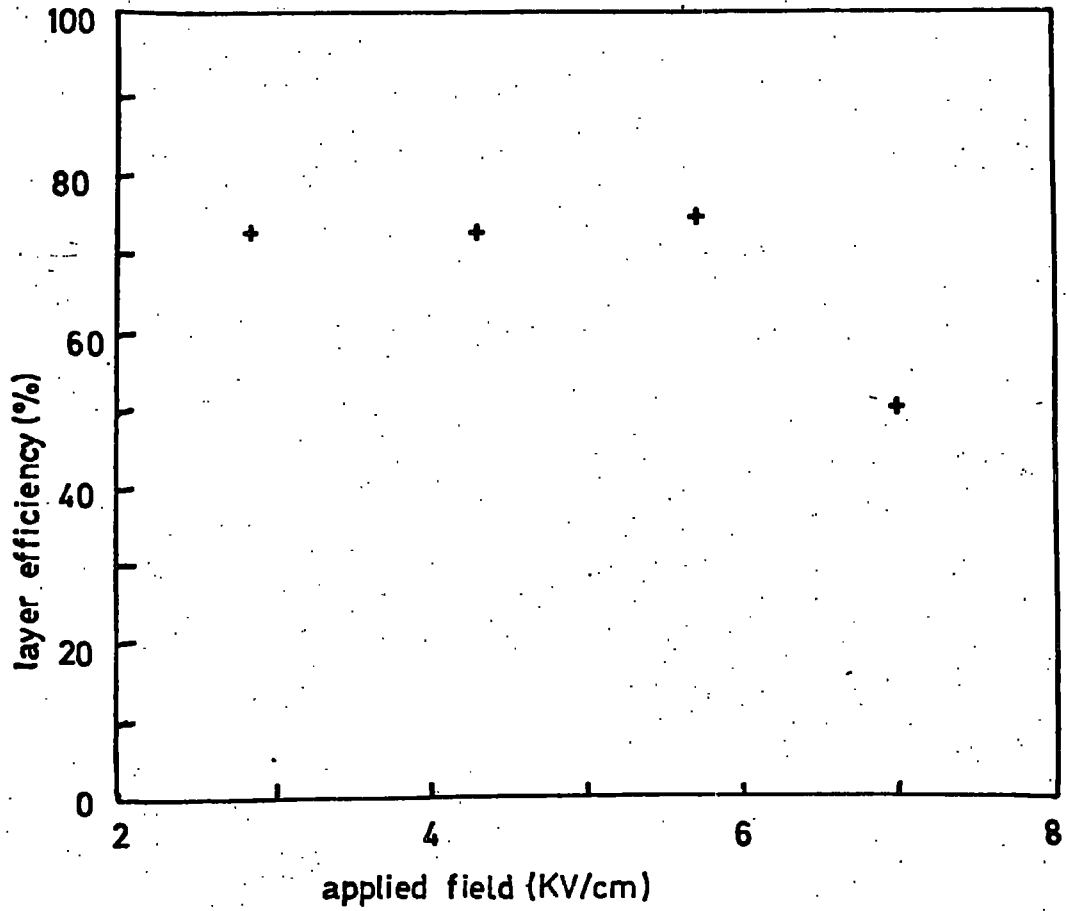
and become trapped in the glass. Because of the greater resistance
of the glass than of the water layer, they will move much more
slowly, and require longer times to recombine with the positive ions.
This process will occur only when the electrons aquire enough energy
to penetrate the water layer, which would account for the dependence
on applied field.

However, when tubes which exhibit the long term clearing
field effect, are operated with a high voltage pulse of the opposite
polarity, the effect of the clearing field disappears immediately.
Presumably it is cancelled out by the short term field of the following
discharge. This seems to indicate that the long and the short term
fields are of the same polarity, which would not be the case if the
long term field were due to polarisation, which would produce a field
of the opposite polarity to that caused by charge separation.

3.3 Removal of Clearing Fields

The degree to which the short term clearing fields affect
the efficiency of the tubes depends on the number of positive ions
deposited on the walls of the tube, the rate at which the two charge
components can recombine, and the delay in applying the high voltage
pulse.

The number of positive ions swept to the wall can be
reduced by making the high voltage pulse length as short as possible,
without impairing the discharge.

Holroyd (4) has investigated ways of increasing the rate
of recombination of charge, by increasing the surface conduction of
the inner surface of the glass tube, either by the addition of water

vapour to the gas, or by coating the surface with stannic oxide.

Clearing field effects would become negligible for most applications, if the resistance of the glass could be reduced to about $10^7\Omega$. If the resistance is reduced further, the glass would screen the gas from the applied field, requiring higher fields to be applied if the efficiency is to be maintained. It may be for this reason that some of Holroyd's stannic oxide coated tubes, which had a resistance of $10^4\Omega$, did not flash at all. The tubes which were observed to flash, did so spuriously, probably because of irregularities in the oxide surface producing localised high fields, resulting in field emission. The results of the tests with coated tubes were inconclusive.

The addition of small quantities of water vapour (0.04 mm. Hg pressure), caused an increase in efficiency at high rates. This may be due to induced fields, too small to affect the efficiency noticably, changing the attachment coefficient. Also it may be that at high rates the surface characteristics of the glass may be modified, absorbing large quantities of water vapour.

The characteristics of the tubes containing water vapour improved with age, as more water was absorbed by the glass, lowering its resistance.

Tubes which contained liquid water showed a high rate of spurious flashing, which was probably caused by high fields developing across the gas-water boundary giving rise to field emission.

All tubes containing water vapour suffered a loss of light output. This is because the water molecules have a high attachment coefficient, mopping up the electrons produced in the discharge. The effect of the addition of water vapour on the digitisation pulse is

unknown, but since the operation requires a coupling between the gas plasma, and the probe, any reduction in the density of the plasma is likely to reduce the probe output.

No definite conclusions can be drawn from these tests, since the concentration of water vapour was not accurately controlled, and the water used had an unknown quantity of oxygen dissolved in it.

. Bipolar ringing pulses, obtained by the use of an inductive load in the R.C. circuit, was found to be a simple way of reducing the clearing fields. The electrons are still swept to the wall, mostly during the first half period of the pulse, but the positive ions just oscillate about their mean positions, and drift back to the electrons after the removal of the high voltage pulse.

Using bipolar pulses at rates of 1/10 sec./tube, the efficiency-delay curves obtained coincided with the theoretical curves of Lloyd, which assumed only diffusion. This indicates that no clearing fields were built up.

Problems may be encountered using a ringing pulse with high pressure tubes, which require a fast rise time to be efficient. Also it may prove difficult to apply such ringing pulses to large arrays, because of their large capacitance. These problems may possibly be overcome by using two separate pulses of opposite polarity, separated by a few hundred nsec.

The effect of using alternately applied pulses of opposite polarity may prove effective, and is at present being investigated at Durham.

The early observations by Crouch (2), indicated that contamination of the outer surface was also important, conditions of

high humidity completely removing all traces of induced clearing

fields. This is supported by experimental results presented in the

next chapter, and is the subject of present investigations at Durham.

3.4 Conclusions

The mechanisms of the short term fields are reasonably

well understood. Although an acceptable solution has yet to be found,

it is possible to work at reasonable rates (50/sec.) without too

severe a reduction in efficiency, using low resistance "Jena 16B"

glass. This has been born$_f^e$ out by tests with an array in the Daresbury

positron beam (9).

No satisfactory explanation, or solution has been found

for the long term clearing field, although the problem is not as

severe as the short term effect, since it requires running at high

rates for long periods.

During investigations into the mechanism by which the

induced fields decay, it was found that large variations in efficiency

occured if the contamination of the outer surface of the tube was

varied. This supports the observations of Crouch, and represents a

possible means of reducing the clearing fields. The results of these

experiments are presented in the following chapter.

References

1 Note on the Detailed Characteristics of Flash Tubes.

  D.R. Pickersgill, Internal Report, 1968,

  University of Durham.

2 Case-Wits-Irvine Conversi hodoscope efficiency and high

  voltage pulsing system. M.F. Crouch. Internal Report,

  Case Western Reserve University, 1968.

3 An investigation of the pulse rate effect on the efficiency

  of neon flash tubes. H. Ferguson, B.C. Rastin.

  Nucl. Inst. Meth. 96 (1971), 405-408.

4 F.W. Holroyd, Ph.D. Thesis, 1971, University of Durham.

5 A.V. Phelps, J.L. Pack. Phys. Rev. 121 (1961)

6 R.J. Stubbs, University of Durham, Private communication.

7 Effect of glass resistance on the internal clearing field

  in neon flash tubes. Int. Conf. on Inst. for High

  Energy Physics, Frascati, 1973, 221-223.

8 A digitized neon flash tube chamber for γ ray detection.

  J.E. Chaney et al. Nucl. Inst. Meth. 125 (1975) 189-196.

9 A modified γ ray detector. J.M. Breare et al. 1975

 Internal Report NI-75-4 University of Durham.

CHAPTER 4

EXPERIMENTAL INVESTIGATION OF DECAY OF CLEARING FIELDS

In the previous chapter the nature of the induced clearing field was discussed in the light of present knowledge. It, was assumed that the fields decayed exponentially due to the movement of electrons over the glass surface. Volume conduction will also be involved in the decay of the fields. In an attempt to clarify the extent to which each process is involved the following experiments were carried out.

Investigation of the decay of the clearing fields is complicated at room temperature by contamination of the surfaces of the tubes, mainly by water vapour. For this reason it was decided to make the observations at elevated temperatures where the effects due to surface contamination will be less. Also, by making observations at different temperatures, the variation of τ, the decay constant, with temperature, may be found and compared with the variation of surface and volume resistance with temperature. This will give an indication of the extent to which each process is involved in the decay of the clearing fields.

From the values of τ obtained at high temperatures (40°C to 100°C) one is able to extrapolate to a value of τ at room
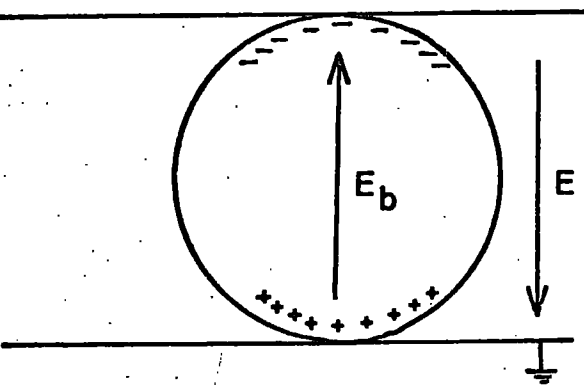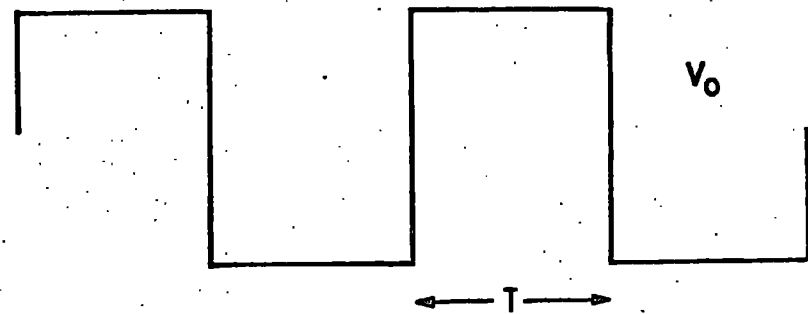
E – applied field

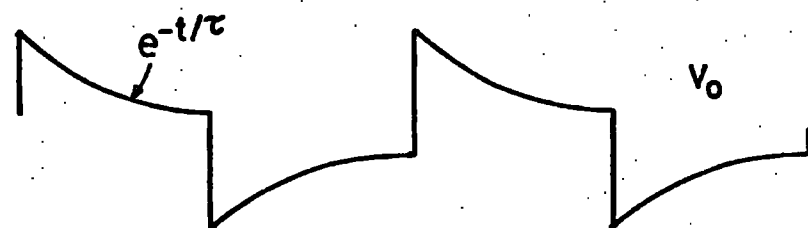E_b – backing off field

resultant internal field = $E - E_b$

FIGURE 20 backing off of applied field

V_o

external applied field

$e^{-t/\tau}$

V_o

internal applied field

V_e

effective square wave field

$V_o > V_e$

FIGURE 21   applied, attenuated and effective fields

temperature, which is free from the effects of surface contamination.

Comparing this value with the experimental value of τ at room

temperature, an estimate of the effect of surface contamination can

be made.

4.1 Measurement of Decay Time (τ) of Internal Clearing Fields

The internal clearing fields result from charge separation

during the application of the high voltage pulse. These charges are

swept to the walls of the tube, to which they adhere, producing an

electric field which backs off the applied field, as shown in figure

(20).

The effective field inside the tube (E_F) is given by:

$$E_F = E - E_B$$

where E = applied field

E_B = backing off field

Within a few hundred nsec. the effective field has fallen

to such a low value that it can no longer maintain the discharge,

which then ceases. The charges remaining on the glass will then move

round the walls under the influence of the electric field, with a

time constant (τ) which depends on the resistance of the glass, and

the capacitance of the flash tube.

By applying an external clearing field of variable frequency

and magnitude, and observing the effect on the efficiency of the

tubes, it is possible to obtain a value for τ.

-42-

4.1.1 Determination of τ

Figure (21) shows the externally applied square wave field, and the resultant field inside the tube. The resultant field is attenuated due to the intrinsic capacity of the tube, and assuming an exponential decay, the flash tube behaves like a "high pass" circuit, the effective field decaying with time constant τ.

For very high frequencies (T $\ll \tau$), the field is changing faster than the charges can move to counteract it, and the effect of the attenuation will be negligible, resulting in an almost perfect square wave.

The detecting efficiency (η) is dependent on the field strength across the inside of the tube ($E-E_B$), at the time of traversal of the ionising particle. The higher the field, the greater the number of primary electrons swept to the walls before the application of the high voltage pulse.

For a square wave field, which is attenuated (ie. $\tau \approx$ T), the detecting efficiency will be increased, since the field is reduced. Measuring η for a large number of events, such that they are randomly distributed over the whole cycle, will give a larger value of η than if the field were unattenuated. Increasing the size of the half period (T), the efficiency will increase, until eventually the applied field is effectively D.C. and the internal efficiency is 100%. In this case the field is completely backed off.

Considering the attenuated waveform shown in figure (21), it is possible to postulate a square wave field of the same half period (T) and of magnitude V_E, which if applied internally across the tube, would give the same efficiency as the attenuated waveform.

The value of V_E can be found by applying a high frequency

square wave ($T \ll \tau$), which is not attenuated. Knowing the values of V_0 and V_E and assuming a relationship between V_0, V_E and τ can be found, then it should be possible to calculate the value of τ. Therefore the proceedure to find τ is:

1) Apply a square wave of magnitude V_0 for various T, and measure the efficiency.

2) Apply high frequency calibration square wave ($T \ll \tau$) and find the value of V_E.

3) Knowing V_E, calculate τ from the mathematical relationship between the attenuated square wave and the equivalent square wave.

4.1.2 Relationship Between Attenuated and Equivalent Square Wave Fields

The following relationship was derived by Chaney (I) and was used by him to obtain values of τ for tubes heated to 100°C.

Assume for simplicity that the induced fields decay exponentially; this can be written as:

$$V = V_0 e^{-t/\tau}$$

where V_0 = applied voltage at time $t = 0$

For the attenuated and equivalent square wave fields to give the same efficiency over a large number of events we need:

$$\int_0^T P_I \, dt = \int_0^T P_E \, dt$$

$$\int_0^T P_I \, dt = P_E \, T$$

where $P_I(t)$ = probability of detecting one event at a given time t in the attenuated square wave field.

and P_E = probability of detecting one event in equivalent square wave field — a constant.

now $P_I(t) \propto V_I(t)$

where V_I = electron drift velocity in the attenuated internal field

and $P_E \propto V_E$, a constant

therefore $\int_0^T V_I \, dt = V_E \, T$

and $V = K\left(\dfrac{X}{P}\right)^{\frac{1}{2}} = AV^{\frac{1}{2}}$

where V = voltage

X = field strength

P = pressure of gas

K = electron mobility

A = a constant

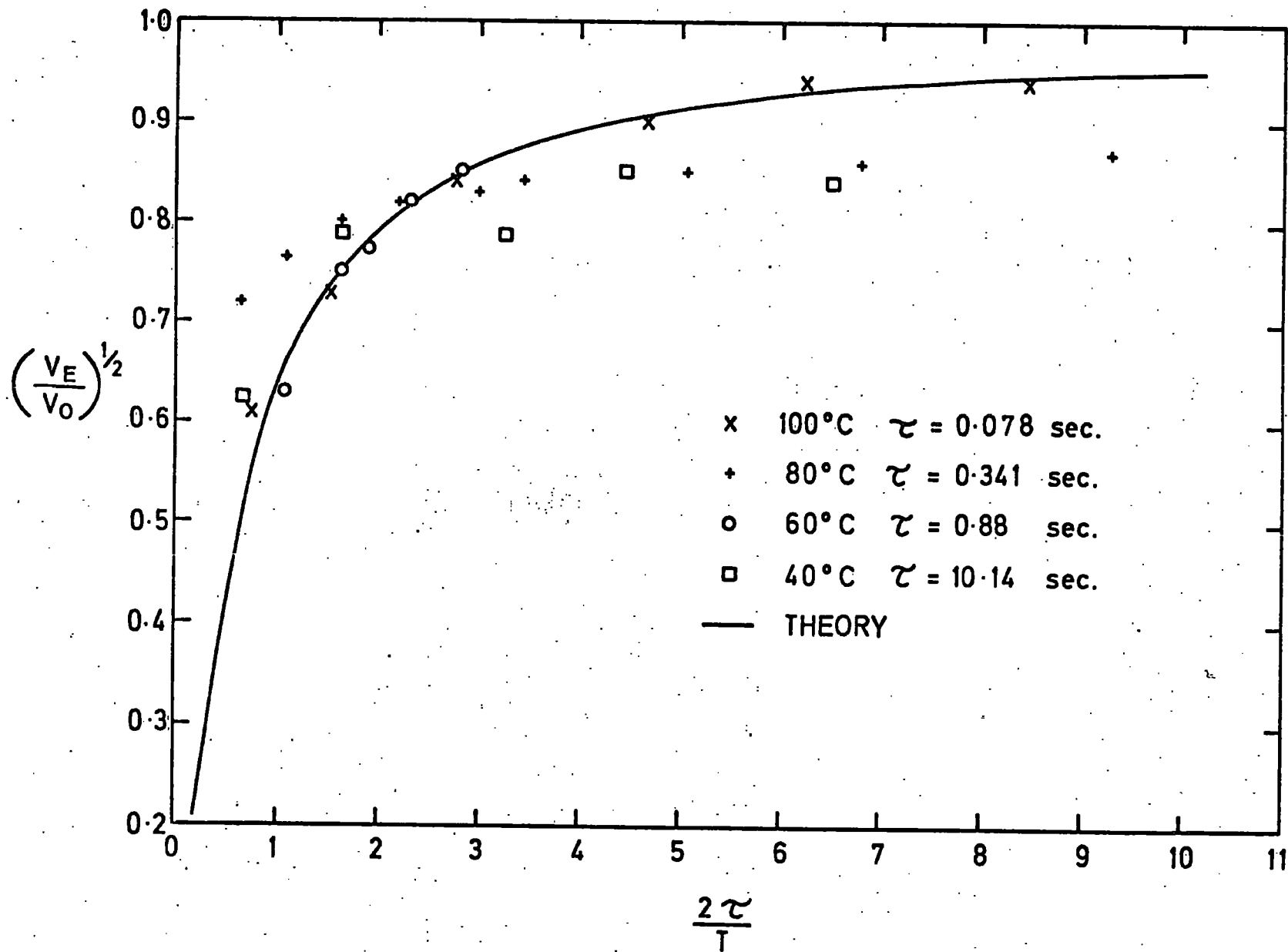therefore $\int_0^T V^{\frac{1}{2}} \, dt = V_E^{\frac{1}{2}} \, T$

FIGURE 22

Substituting $V = V_o \, e^{-t/\tau}$

we get $\int_0^T (V_o \, e^{-t/\tau})^{\frac{1}{2}} \, dt = V_E^{\frac{1}{2}} \, T$

giving $V_E^{\frac{1}{2}} = \dfrac{2V_o^{\frac{1}{2}}\tau}{T} (1-e^{-T/2\tau})$

Knowing V_o, V_E and T it is possible to calculate τ.

For simplicity the above relationship is rearranged to give a universal curve of $(V_E/V_o)^{\frac{1}{2}}$ as a function of $2\tau/T$. This curve is shown in figure (22). Values of T are obtained from plots of efficiency as a function of applied clearing field frequency, and values of V_E are obtained from plots of efficiency as a function of the magnitude of the clearing field. A fit can then be made to the curve by iteration.

4.2 Apparatus

All results given in this chapter were obtained using 1.8 cm diameter tubes, 50 cm long, with 1 mm thick walls. The tubes were made from S95 soda glass, and filled with 70% Ne, 30% He. Thin black polythene sleeving was used to prevent photons from one discharging tube causing adjacent tubes to ignite.

The tubes were arranged in 3 layers of 6 tubes per layer, the layers being separated by the electrodes in the standard manner. Cosmic rays were used as a source of ionising particles, giving an event rate of approximately 9/sec. This could be varied by inhibiting the logic for a known amount of time after each event.

T₁ , T₂ , T₃ = thermometer   flash tubes   perspex window

X T_1 X T_2 X T_3

inner wall
heater element
metal foil
outer wall
empire tape electrical insulation
} thermal insulation

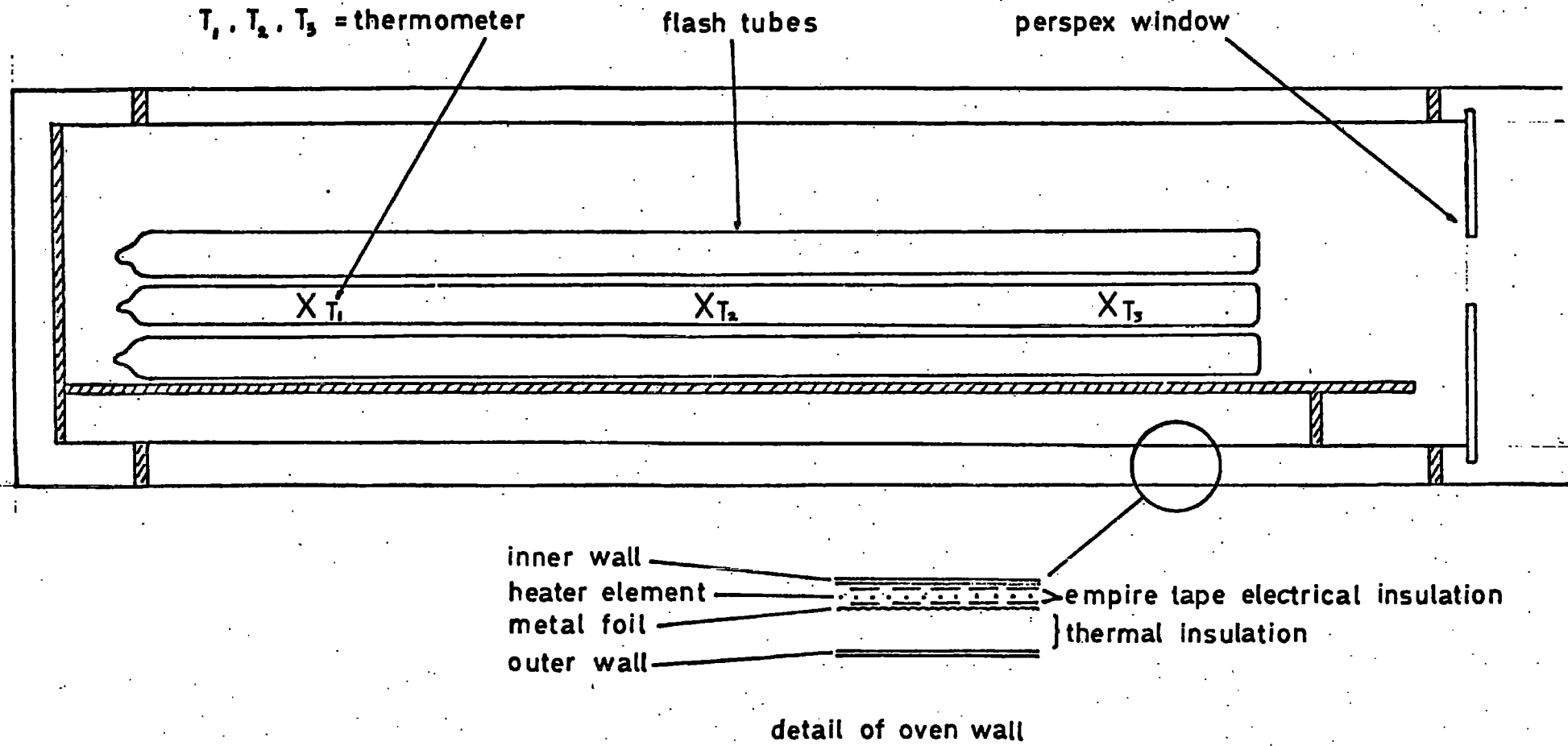detail of oven wall

FIGURE 23   the oven (side elevation)
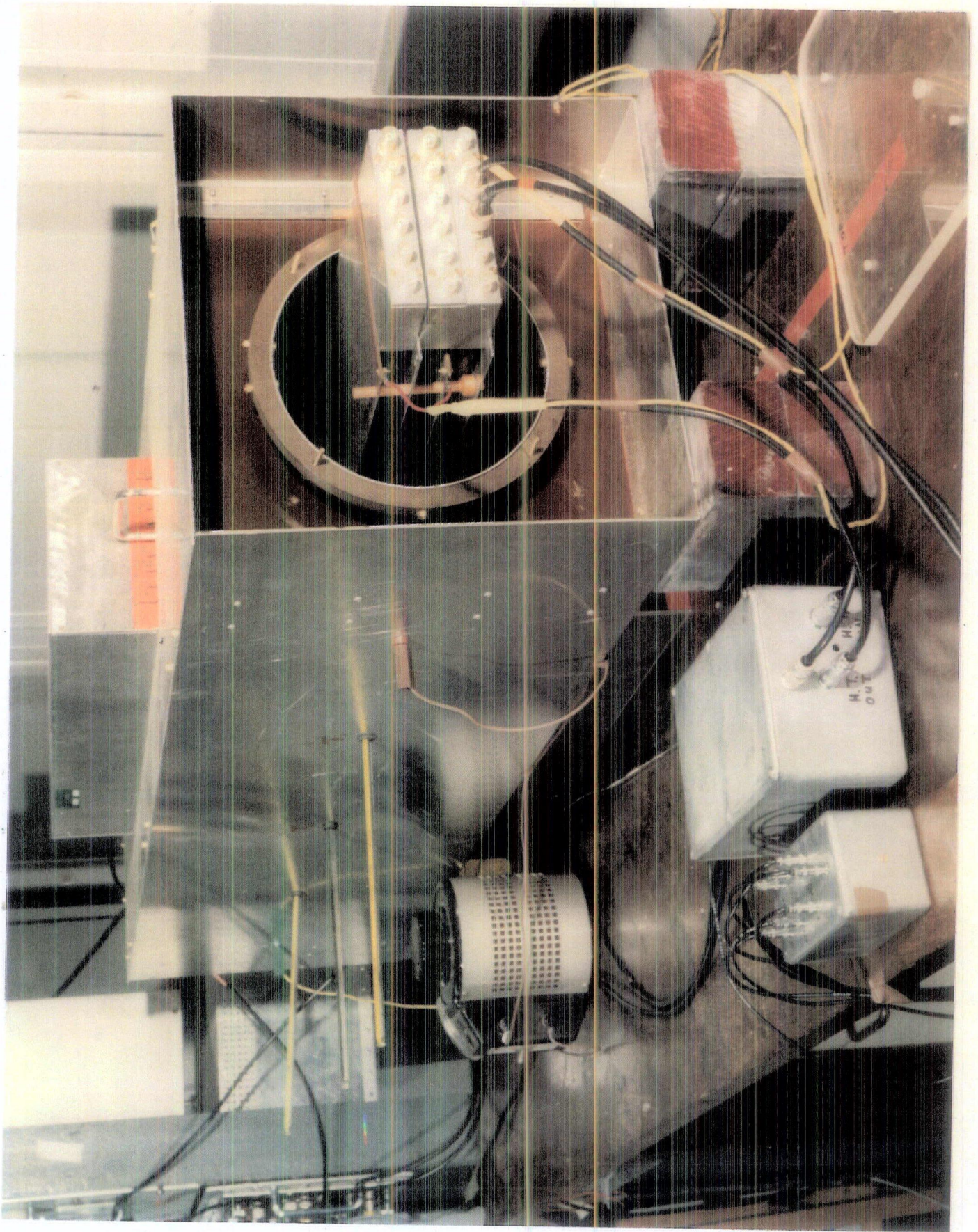
FIGURE 24   oven containing digitised flash tube array

FIGURE 25   the logic

1000 pF

3.3 KΩ

1 KΩ

0·1 μF
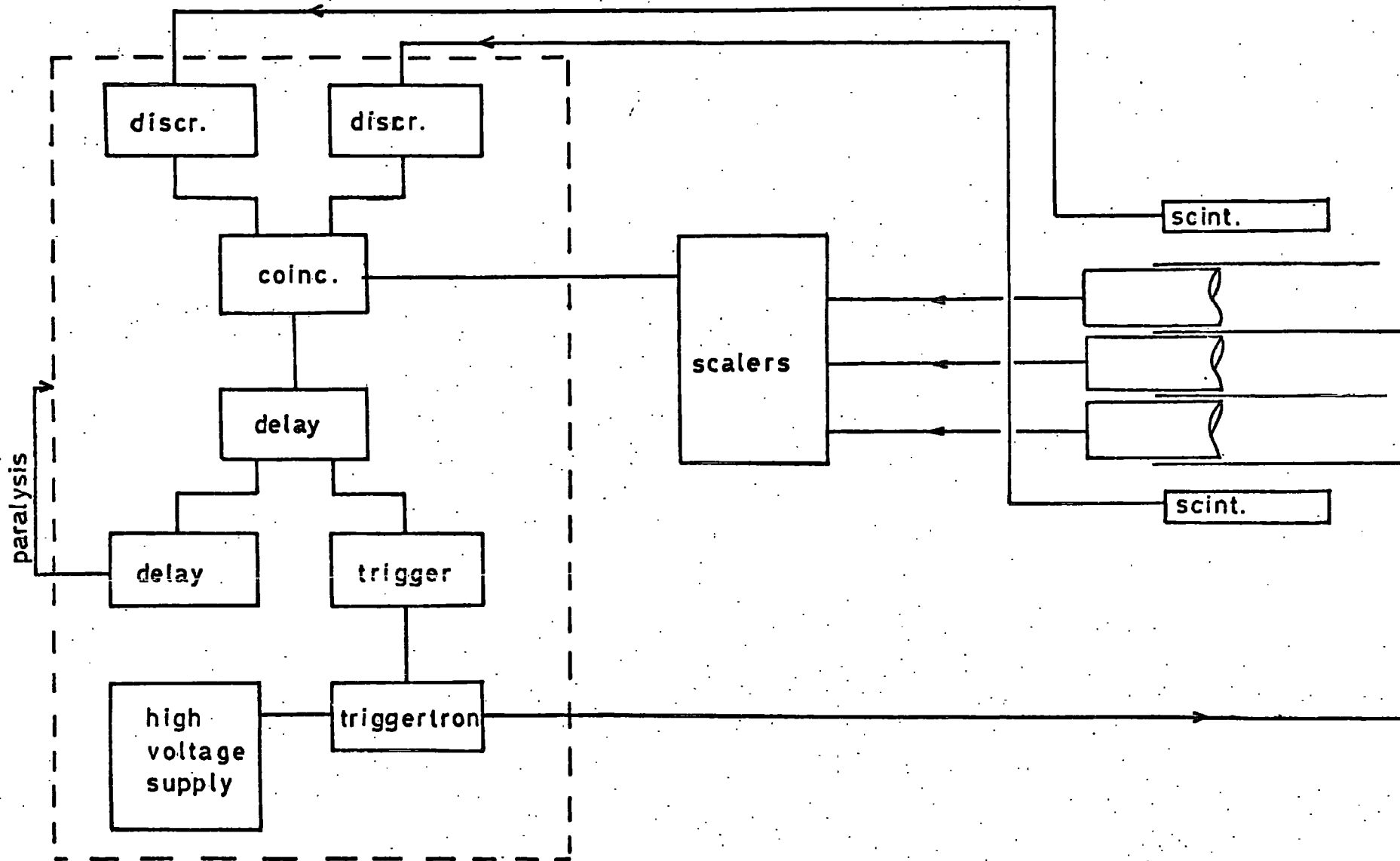
clearing field

spark gap   1 MΩ

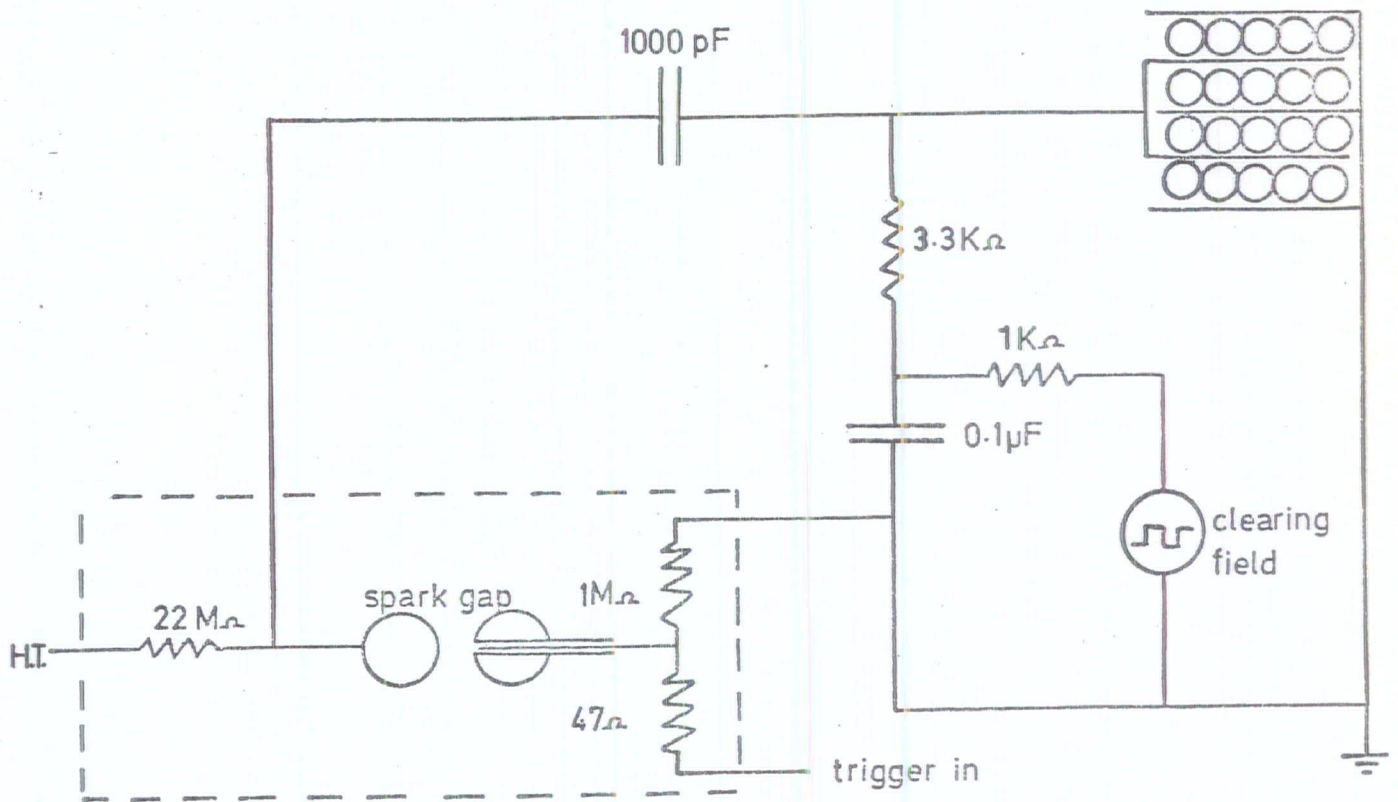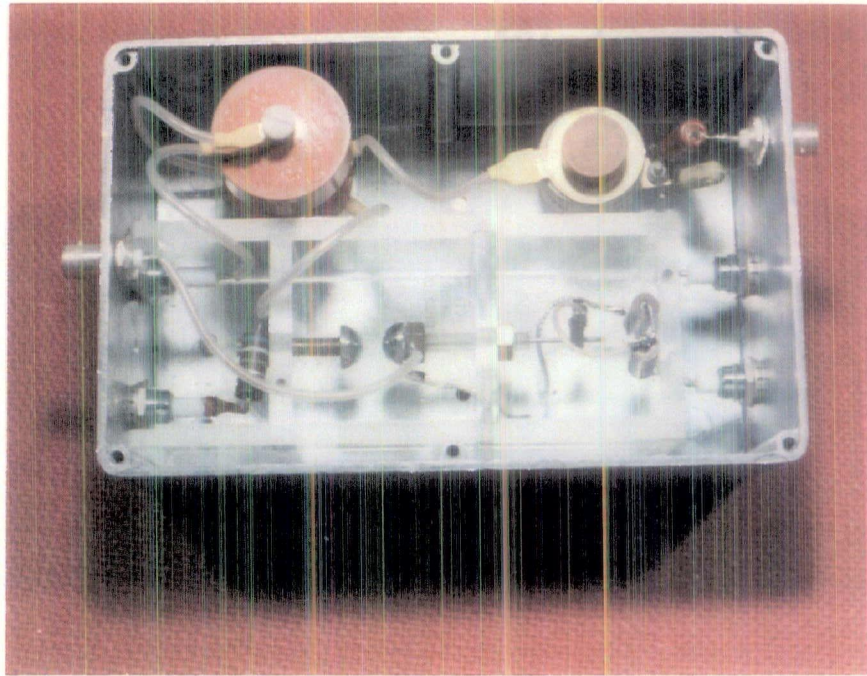H.T.   22 MΩ

47 Ω

trigger in

FIGURE 26   high voltage pulsing circuit

4.2.1 The Oven

To investigate the variation of τ with temperature, the tubes had to be maintained at a constant temperature for long periods of time, with a minimum temperature variation over the tubes' length.

To fulfill these criteria an electrically heated oven was constructed, and is shown in figures (23) and (24). Using this oven, temperature ranges between $20^{\circ}C$ and $110^{\circ}C$ were obtainable, with a variation of less than $2^{\circ}C$ over the length of the tube.

The tubes were observed through a perspex window at one end of the oven; all results were recorded in this manner. Although facilities existed for digitised output, difficulty was experienced due to electrical pickup in the scalars.

4.2.2 Logic and Pulsing Systems

Cosmic rays were used as a source of ionising particles, the passage of a cosmic ray being detected by plastic scintillators, with an active area of 4 cm. x 4 cm., placed above and below the flash tube array. The logic used to trigger the array is shown in figure (25). The inherent delay of the apparatus was approximately 250 nsec. This delay was increased by means of a GG200 gate generator to obtain times of 1.0, 2.5 and 4.0 microsec. between the passage of the ionising particle and the application of the high voltage pulse.

A high voltage pulse of up to 15 KV was obtained by discharging a 1000pF capacitor across a 3.3 KΩ resistor. This produced an exponentially decaying pulse, with a decay constant of 3.3 microsec., and a rise time of approximately 50 nsec. The switching action was provided by a standard triggered air spark gap, as shown in figure (26). The whole of the pulse generating system was enclosed in a
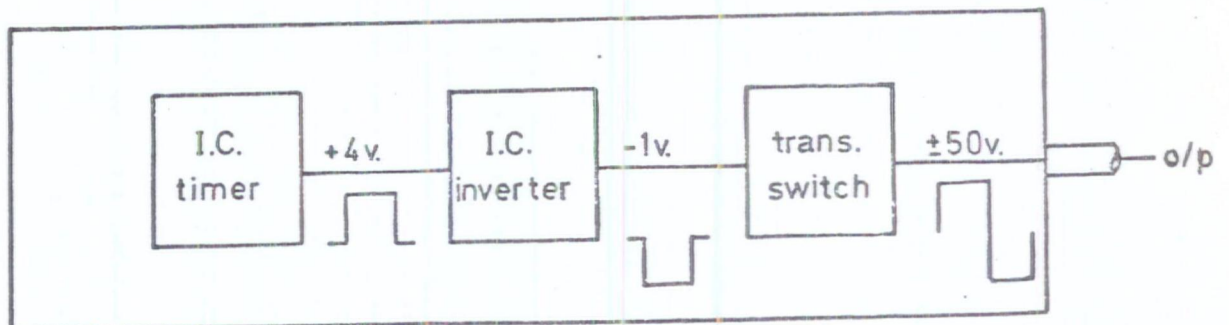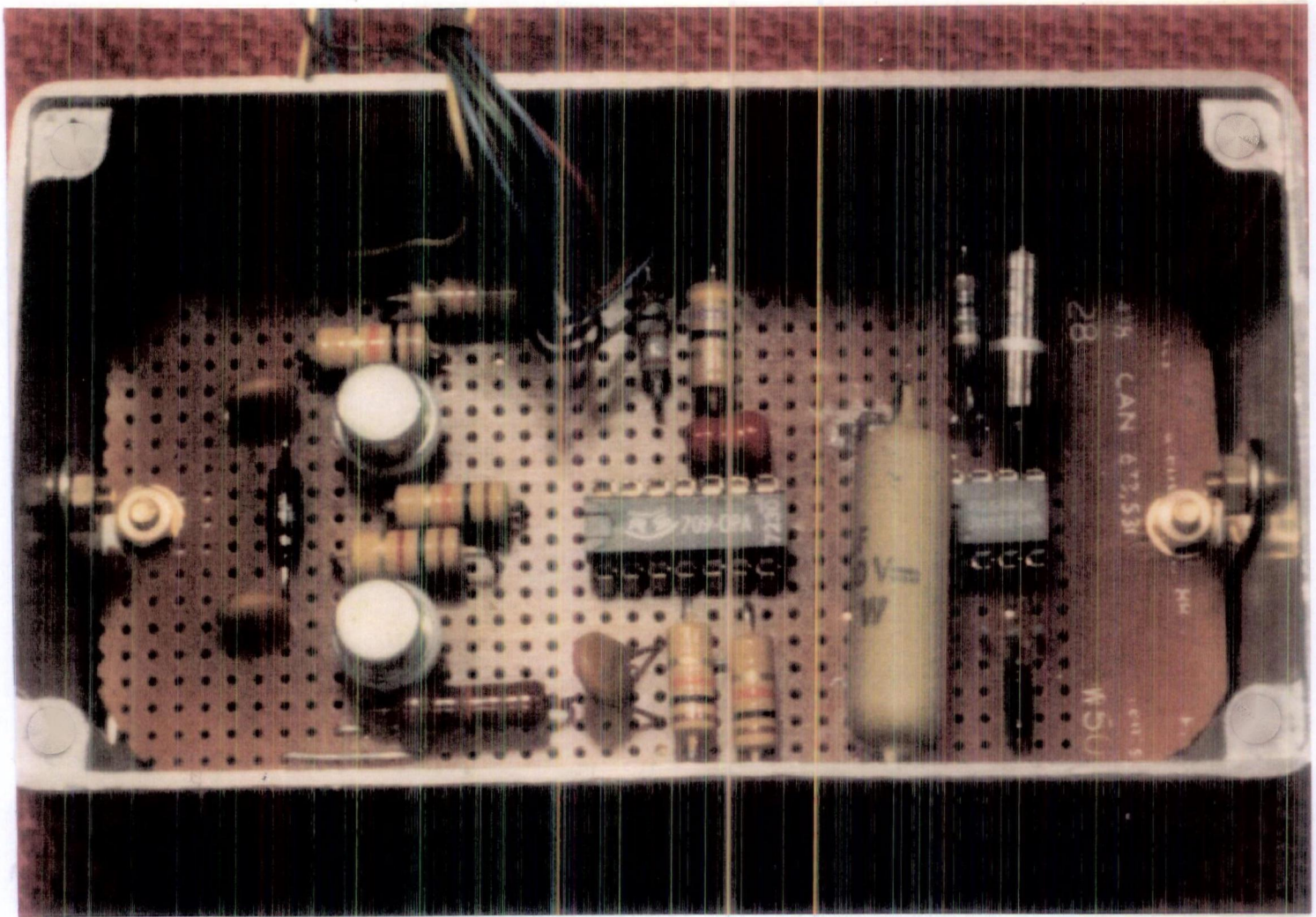
FIGURE 27   generation of square wave clearing field

metal box to reduce electrical interference.

4.2.3 Generation of Square Wave Clearing Field

For the purpose of this experiment it was necessary to generate a square wave field of variable magnitude (0 V to 50 V), variable frequency (0 to 100 Hz), with a fast rise time.

This was achieved using the circuit shown in figure (**27**). An integrated circuit timer provided a positive going pulse of period 10 microsec. to 1 hour, and magnitude of 4 V. This was inverted by a 709 operational amplifier, to make it drive two switching transistors, giving a square wave of up to $\pm$ 50 V.

Difficulty was experienced due to electrical pickup flipping the polarity of the pulse. This was overcome by screening the circuit in a metal box, using a filtered mains power supply, and use of a "low pass" filter on the output to the high voltage plates, isolating it from the high frequency ringing of the high voltage pulse.

4.3 Variation of τ with Temperature

Using the apparatus described above, graphs of efficiency as a function of applied clearing field voltage and frequency were obtained for a range of temperatures between $20^{\circ}C$ and $100^{\circ}C$. These are shown in figures (**28**) to (**35**).

Using the method described in section 4.1, values of τ were obtained for each temperature. The fit obtained using these values of τ, to the graph of $(V_E/V_0)^{\frac{1}{2}}$ as a function of $2\tau/T$ is shown in figure (**22**).

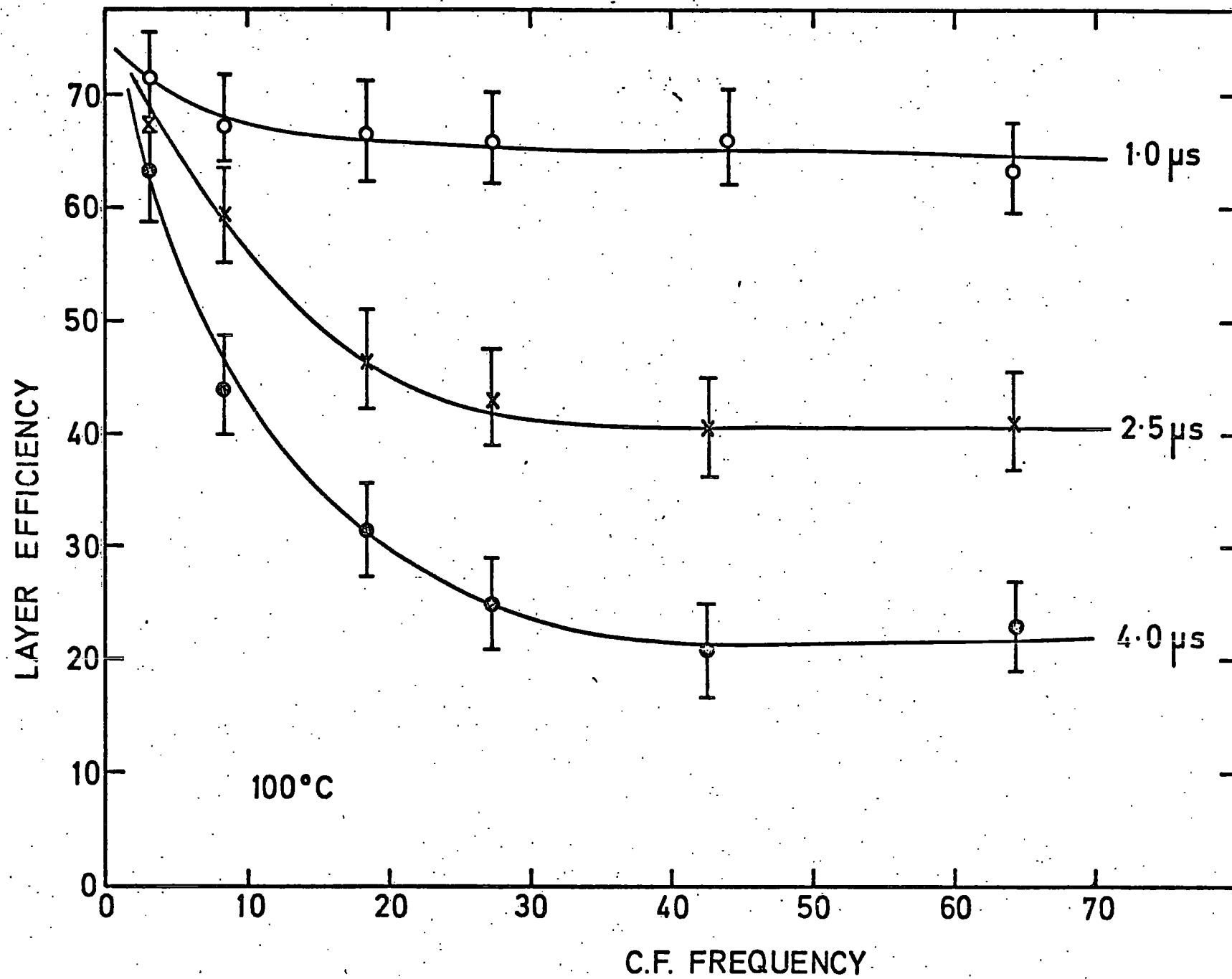Assuming a value of 5 pF for the capacitance of the flash tubes (**2**), and using the relationship

FIGURE 28
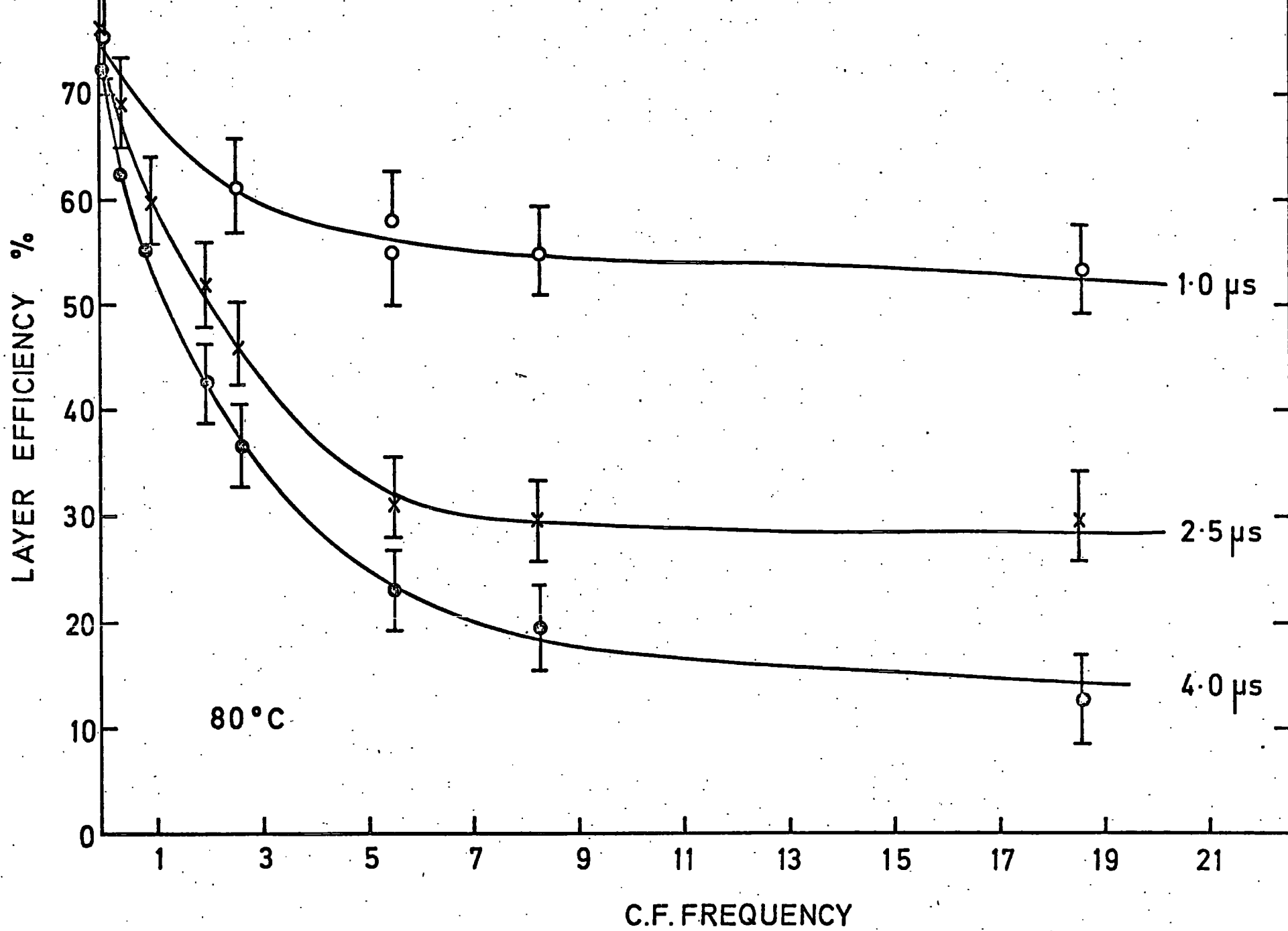
FIGURE 29
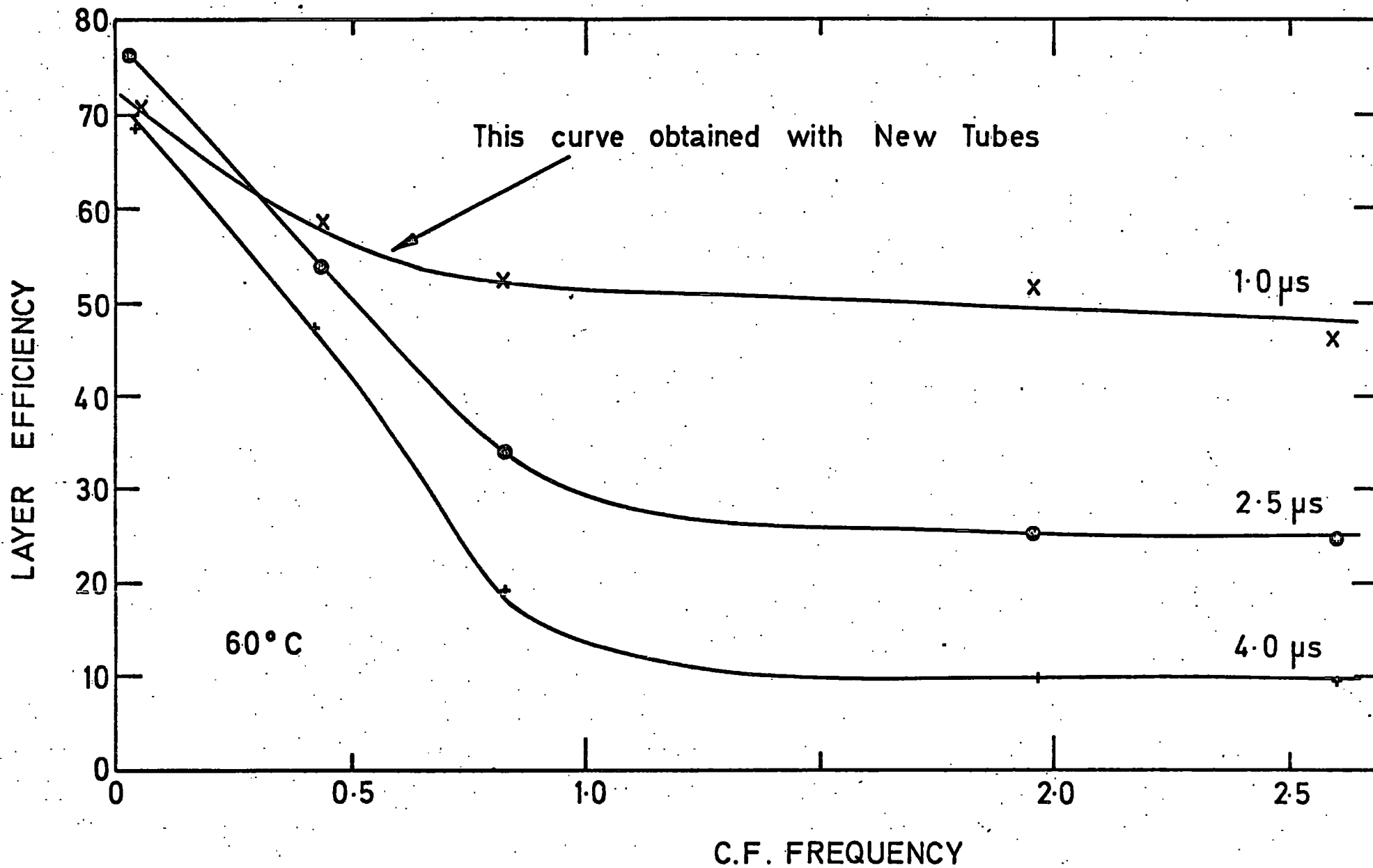
FIGURE 30
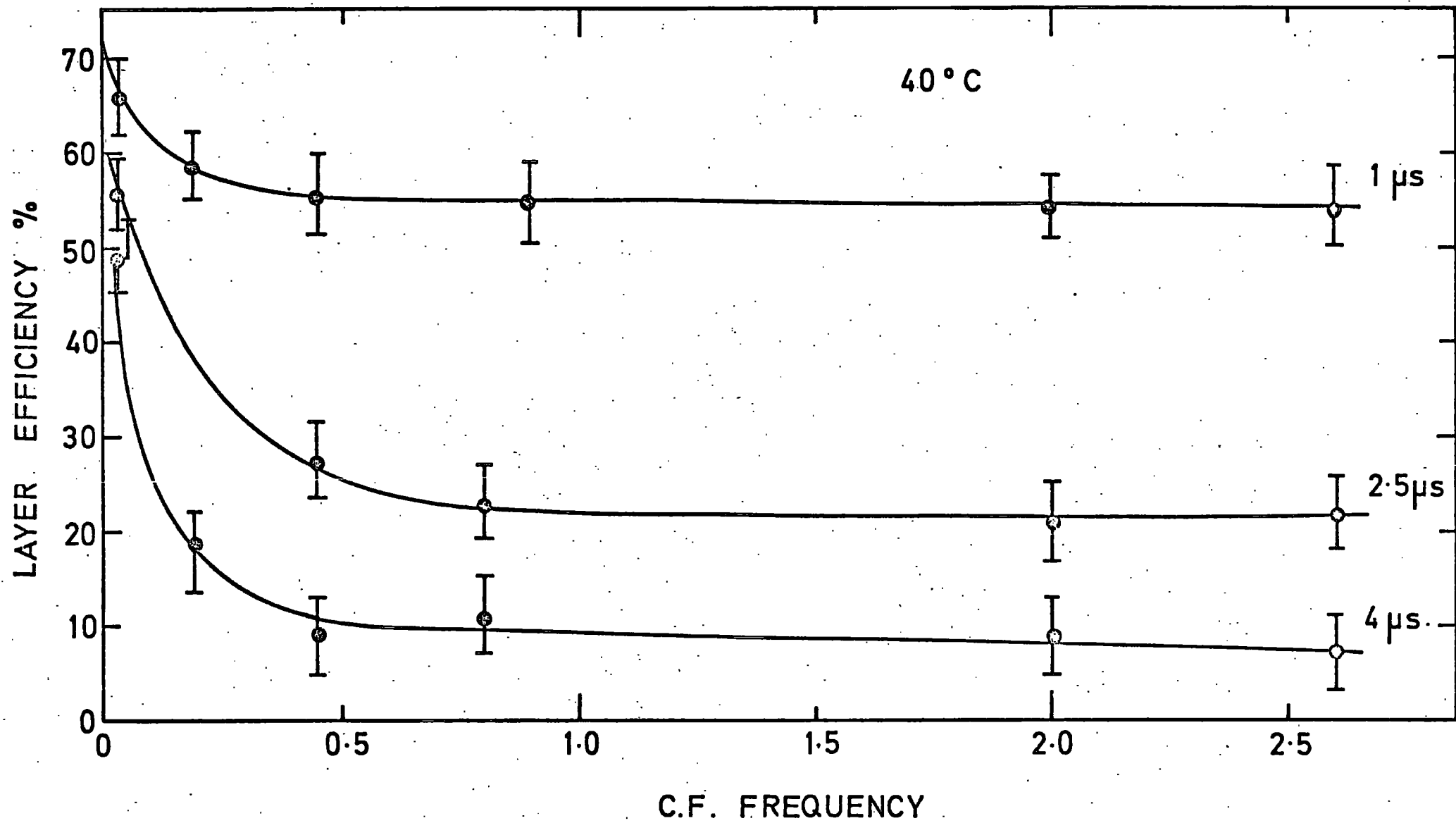
FIGURE 31
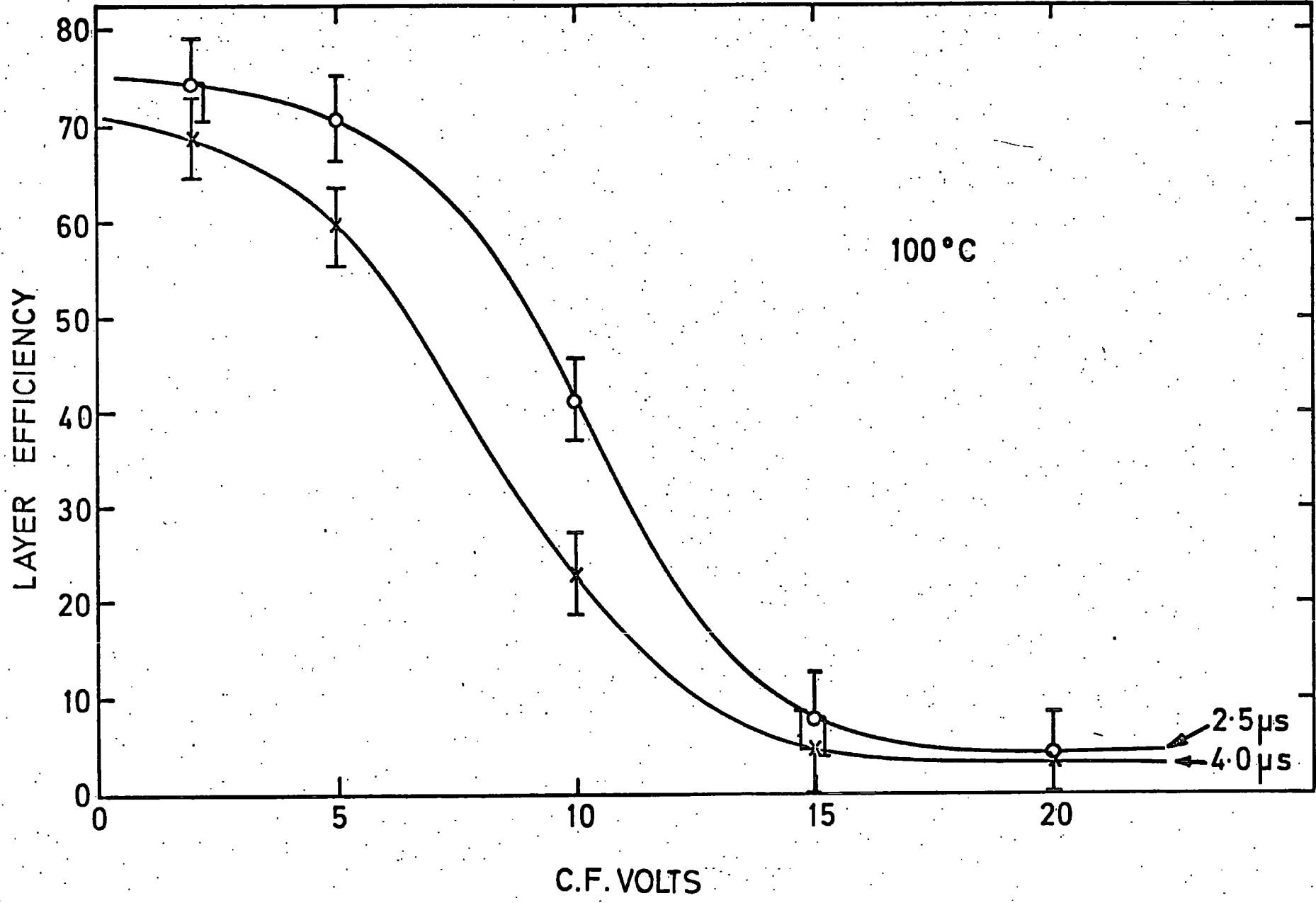
FIGURE 32
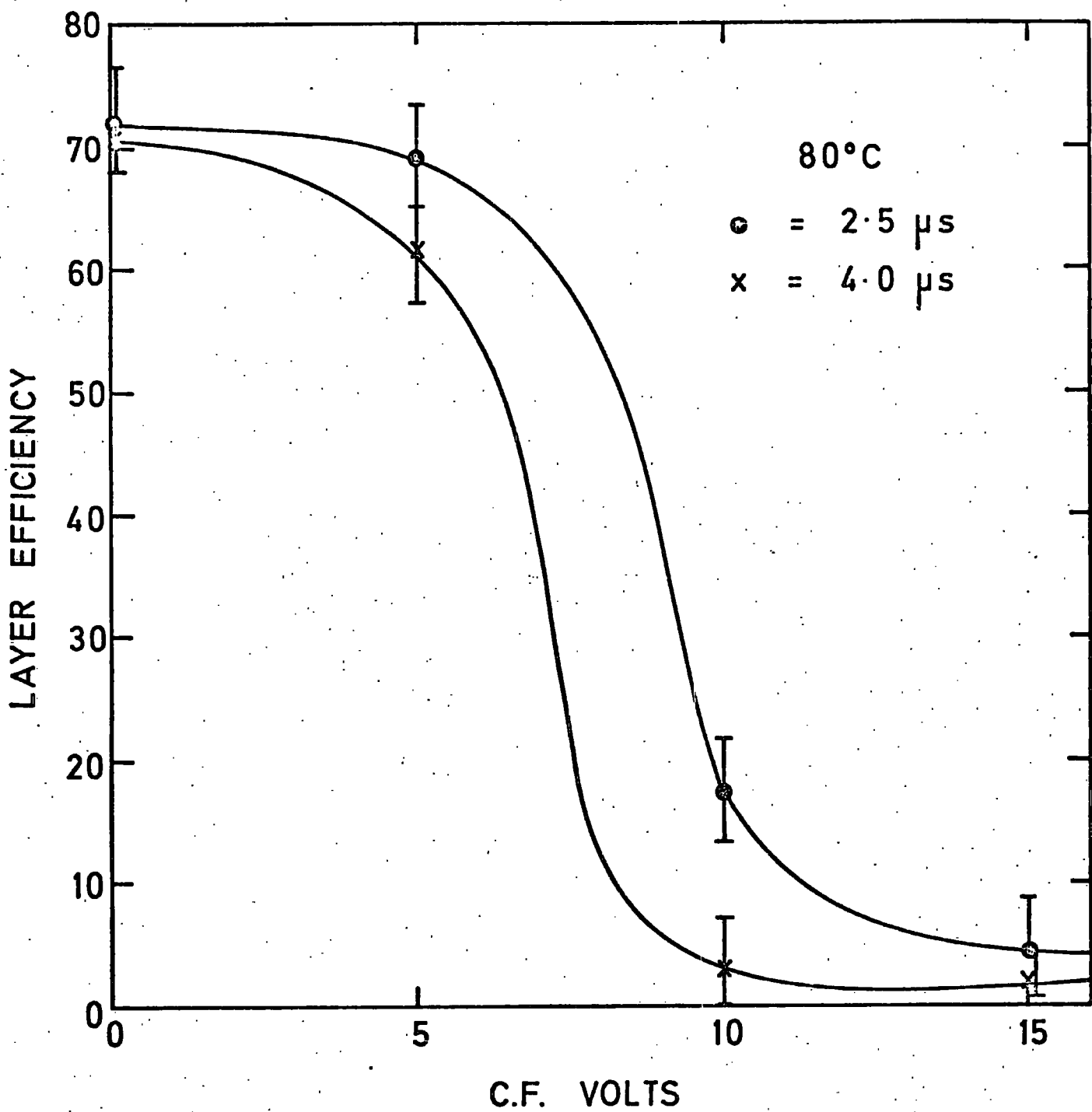
FIGURE 33
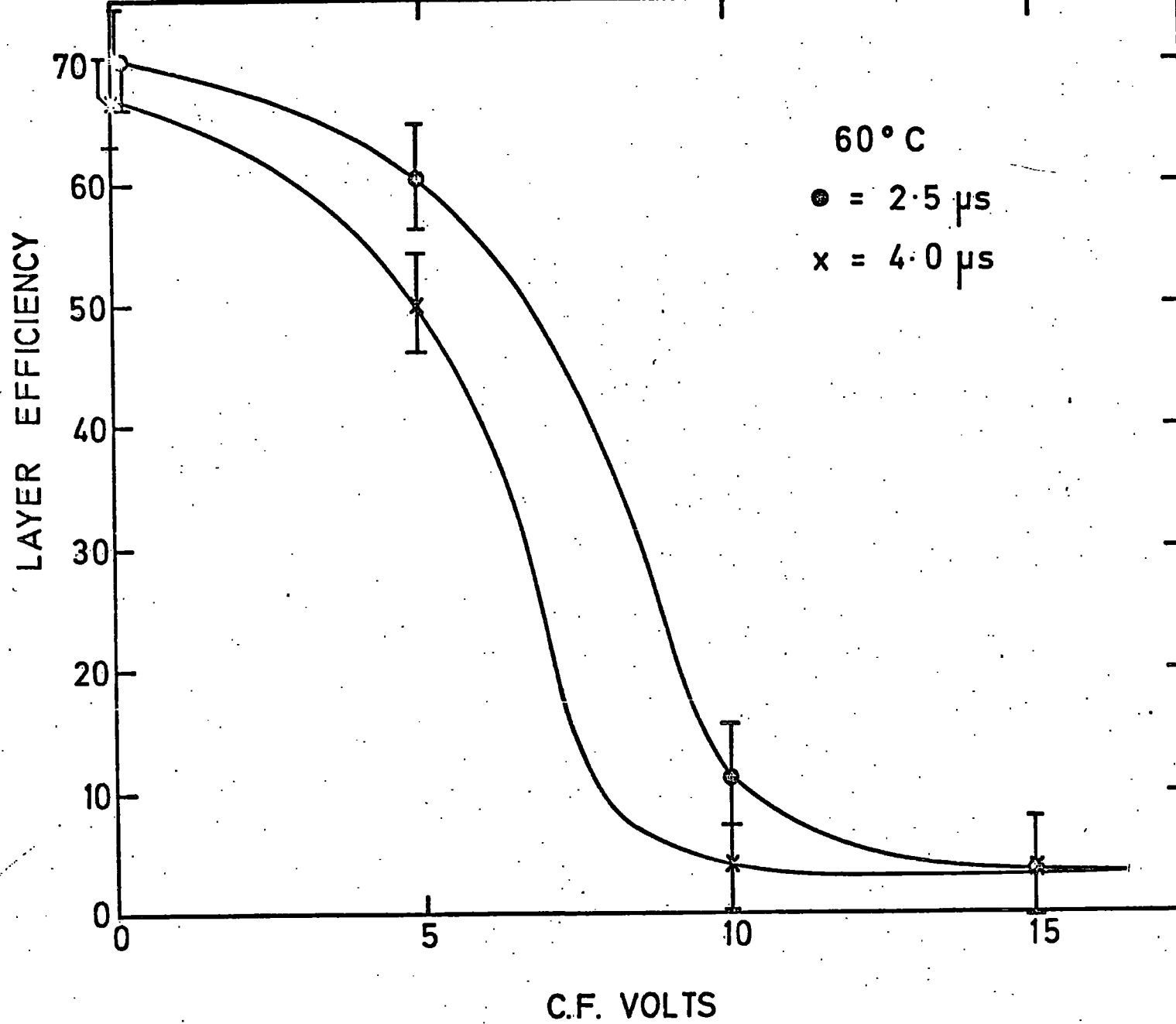
FIGURE 34
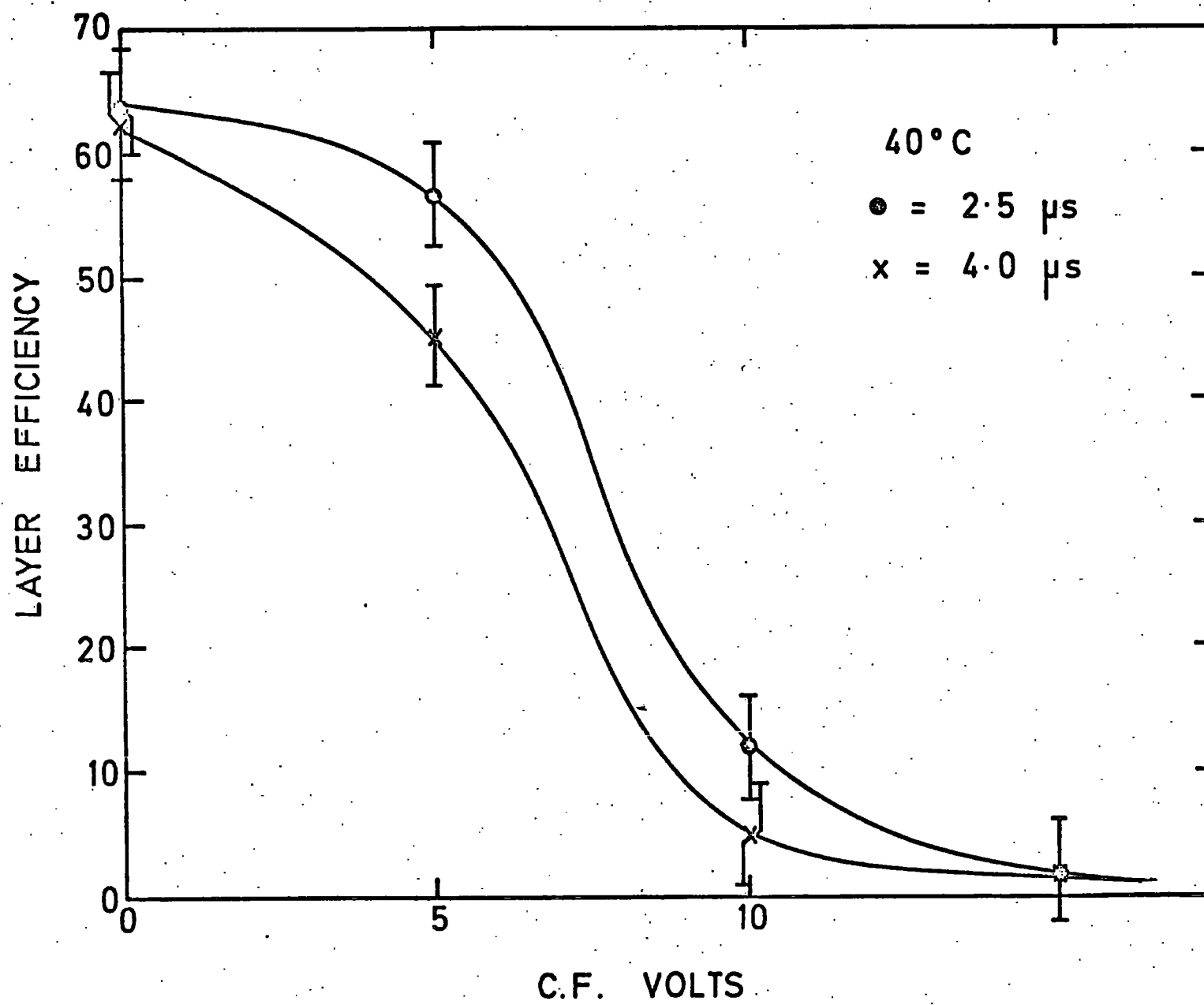
FIGURE 35

Table 1

Temperature ($^{\circ}$C)	τ (sec.)	R(Ω)
20	0.18	3.6×10^{10}
40	10.41	2.08×10^{12}
60	0.88	1.76×10^{11}
80	0.34	6.8×10^{10}
100	0.075	1.56×10^{10}

Table 2

Surface Treatment*	τ (sec.)	R(Ω)
1	Not obtainable	Not obtainable
2	0.013	2.7×10^{9}
3	3	0.15	3.1×10^{9}

* See page 48 for definition.

$$\tau = RC$$

values of R, the resistivity of the glass may be found. These are shown in table (1), with their corresponding values of temperature and τ.

Figure (36) shows volume resistance as a function of 1/T, obtained by direct measurement by Breare for S95 soda glass (3). It can be seen that for temperatures of 40°C and above, a good agreement is achieved. The slight discrepancy is possibly due either to the use of an incorrect value for the capacitance of these particular tubes, or to the fact that it is possible to obtain discrepancies of up to 2% in the resistance of different samples of S95 soda glass (4).

The values obtained for τ at 20°C showed a much greater spread than for those above 40°C, and were up to 2 orders of magnitude below the value obtained by Breare.

4.4 Variation of τ with Surface Contamination

To investigate this effect, the outer surfaces of the tubes were subjected to varying degrees of contamination. It is difficult to measure, or control the exact amount of contamination of the tubes during experimental observations. Even in the sealed environment of the oven, the effect of water vapour condensing onto the previously "clean" surfaces of the tubes, can be seen as the efficiency steadily rises over periods of a few hours.

The tubes were contaminated in the following way;

1) Heated to 100°C for 36 hours, in a sealed oven containing silica gel to remove water vapour from the air.

2) Placed in a steam filled enclosure for 4 hours, then
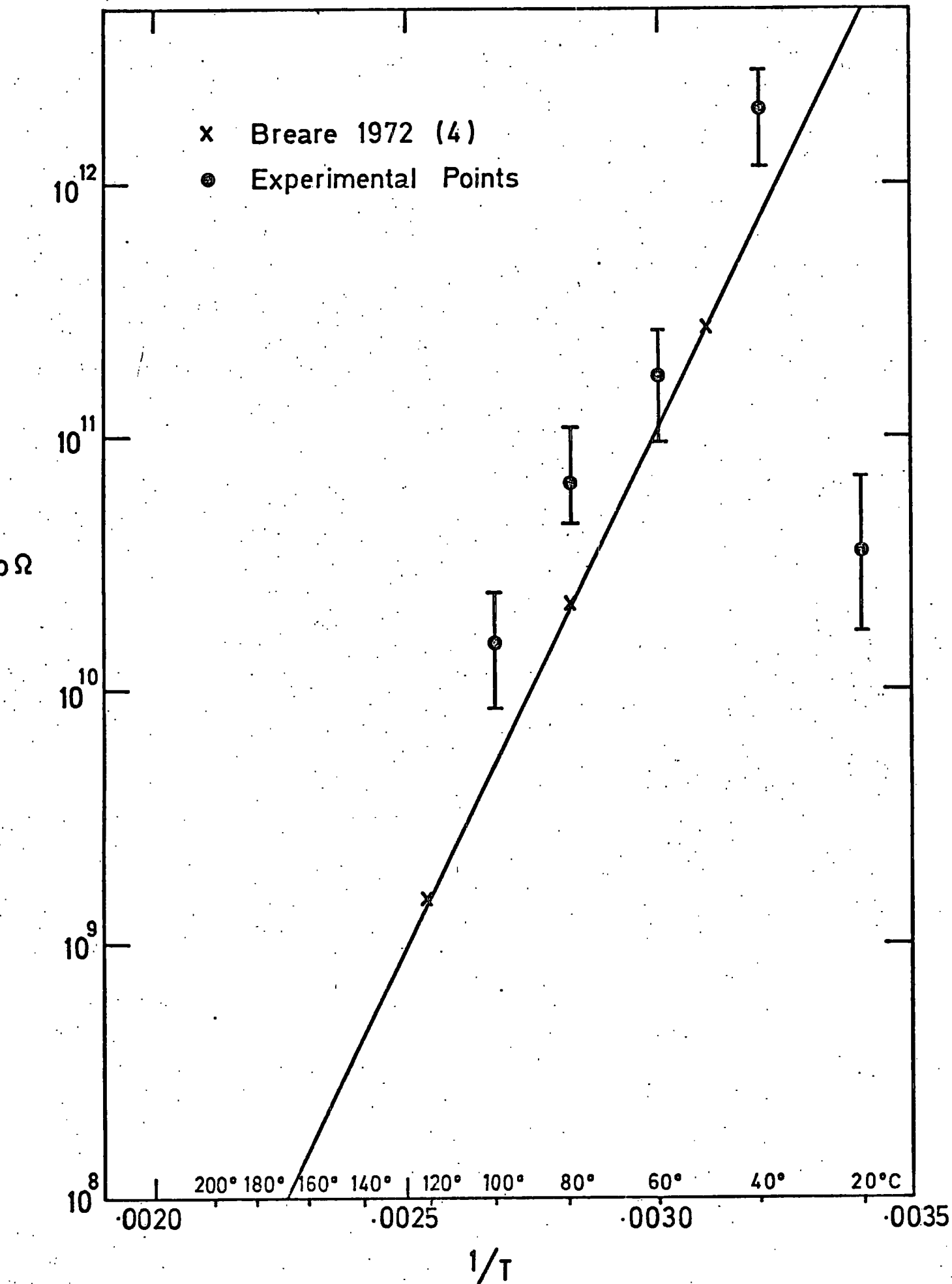
FIGURE 36

left in a damp atmosphere for 12 hours, such that water was constantly condensing onto the surfaces.

3) Heated to 90°C for 8 hours to remove the excess water vapour from the previous treatment.

The results of these 3 surface treatments are shown in table (2). If process 1 removed all the water vapour, then at 20°C, τ should be approximately 25 sec. and the charges should back off the applied field at a frequency of about 0.15 c/sec. However it was not possible to obtain a relationship between applied clearing field frequency, and the efficiency, the experimental points appearing to be randomly distributed between efficiencies of 20% and 40% for frequencies between 0.04 and 10 Hz. No explanation for this failure has yet been found.

Process 2 produced very low values of τ and R, which is consistent with the fact that the surfaces contained large amounts of water vapour.

Process 3 produced a value of R an order of magnitude higher, as expected, since a large proportion of the water had been driven off.

4.5 Discussion of Results

It can be seen from figure (36) that for temperatures of 40°C and above, the values of R, obtained from τ, follow closely the volume resistance curves obtained by Breare. It should not be concluded from this that the fields decay by conduction through the volume of the glass, since for clean glass, the volume resistance and surface resistance are almost equal. Also, very little electron

conduction takes place in the volume of the glass, conduction consisting mostly of a drift of the sodium ions through the glass structure (5). Therefore it seems reasonable to conclude that the fields decay by movement of charge over the glass surface.

Since the charges are deposited on the inner surface of the flash tube, it would be expected that only the conductivity of this surface is of importance. Also, since the flash tube is sealed, the amount of contaminants available to be deposited on the inner surface is fixed, and it would be expected, therefore, that the values of τ obtained after heating the tubes, and allowing them to cool, would be always approximately the same.

However, it has been shown that the value of τ depends on the degree of contamination of the outer surface, as was indicated by the results of Crouch (6). Since τ was determined by observation of the efficiency, which in turn is influenced by the magnitude of the clearing field, the results indicate the presence of an additional field, opposing that due to the charges deposited on the inner walls. This additional field, whose magnitude is dependent on the resistivity of the outer surface, must be due to charges residing on the outer surface of the flash tube.

4.6 Suggestions for Further Investigation

Investigation of the effects of outer surface contamination would be greatly simplified if a way could be found of controling the amount of contamination on the surface. The use of water vapour requires a careful control of local atmospheric conditions and is therefore impractical. A conducting substance in a solution of varying concentration painted on the outer surface is one possibility.

If this conducting layer were opaque, it would also serve as a means of screening the tubes from the effects of an adjacent tube discharging.

With a surface resistance of 10^7 to $10^8 \Omega$, very little variation of τ with temperature should be found, assuming that the conducting layer is unaffected by temperature.

The dependence of efficiency on pulse length, magnitude and repetition rate should also change, as will the sensitive and recovery times. It is expected that the tubes will have characteristics similar to those predicted by Lloyd, who considered diffusion as the only means by which the primary electrons could be lost from the gas.

It will also be necessary to investigate the degree to which the conducting layer screens the gas from the applied high voltage field, and a lower limit found for the surface resistance, beyond which efficient operation of the tubes would require an impractically high voltage.

Assuming that the results of these tests show that decreasing the outer surface resistance of the tubes, has no detrimental effects on the tubes' characteristics, it should then be possible to operate flash tubes at the high rates found in accelerator experiments, without the loss of efficiency caused by internal clearing fields.

References

1   J.E. Chaney, Ph.D. Thesis, 1974, University of Durham.

2   F.W. Holroyd, Ph.D. Thesis, 1971, University of Durham.

3   The effect of glass resistance on the internal clearing
        fields in neon flash tubes. Proc. Int. Conf. on Inst.
        for High Energy Physics, Frascati 1973, 221-223.

4   W. El Disouki, Durham University, Private communication.

5   P. Sutton, Prog. Dielectrics. 2 (1960) 112-164.

6   Case-Wits-Irvine Conversi hodoscope efficiency and high
        voltage pulsing system. M.F. Crouch, Internal Report,
        Case Western Reserve University, 1968.

CHAPTER 5

PROBLEMS ARISING FROM THE OPERATION OF A FLASH TUBE
CHAMBER IN THE DARESBURY LABORATORY e^+ TEST BEAM

The problems discussed in this chapter are those which arose whilst investigating the performance of a flash tube chamber in the Daresbury Laboratory e^+ test beam. The purpose of these investigations was to determine the feasibility of using flash tubes as a detector for high energy gamma rays. The use of high energy positrons to simulate photon induced showers of the same energy is justified by theoretical (1) and experimental (2) results which show only small differences between photon and electron induced showers.

The research is being conducted by workers at Durham (3, 4) who have found that the degree of spatial and energy resolution obtainable with the flash tube chamber, make it highly competitive with other forms of gamma ray detector.

5.1 Detection of Gamma Rays.

A photon may be detected by recording the interaction products produced when it passes through an absorbing medium. These interaction products will consist principally of electrons, positrons and secondary photons, produced by the photoelectric effect, Compton

effect and pair production, depending on the energy of the incident photon. These three interactions, and the energy range in which they predominate are shown below.

Photoelectric	$\gamma + A \rightarrow A^+ + e^-$	0.01 MeV to 0.5 MeV
Compton	$\gamma + e^- \rightarrow \gamma' + e^-$	0.1 MeV to 10.0 MeV
Pair Production	$\gamma + A \rightarrow A + e^+ + e^-$	1.02 MeV and higher

To determine the energy of a photon it is required that the photon and its interaction products are totally absorbed within the sensitive volume of the detector. For energies below 1 MeV, semiconductor Si and Ge detectors are used (5, 6). Photons of energy between 1 MeV and 100 MeV are detected using inorganic crystal scintillators (7, 8). However, beyond these energies the interaction products of photons are no longer physically contained within the sensitive volume of the detector, which therefore ceases to provide a measure of the total energy of the incident photon. To record the energy of photons above 100 MeV requires much greater amounts of absorbing material than can practically be provided by the above mentioned detectors.

Above a certain energy, the interaction products of the initial photon may be sufficiently energetic to produce further interactions, developing into a shower. This multiplication process continues until the energy of the final interaction products falls below a certain threshold level, beyond which no further multiplication can occur, and the shower ceases.

Beyond 10 MeV pair production is the dominant interaction process, and it has been shown that the total number of electrons
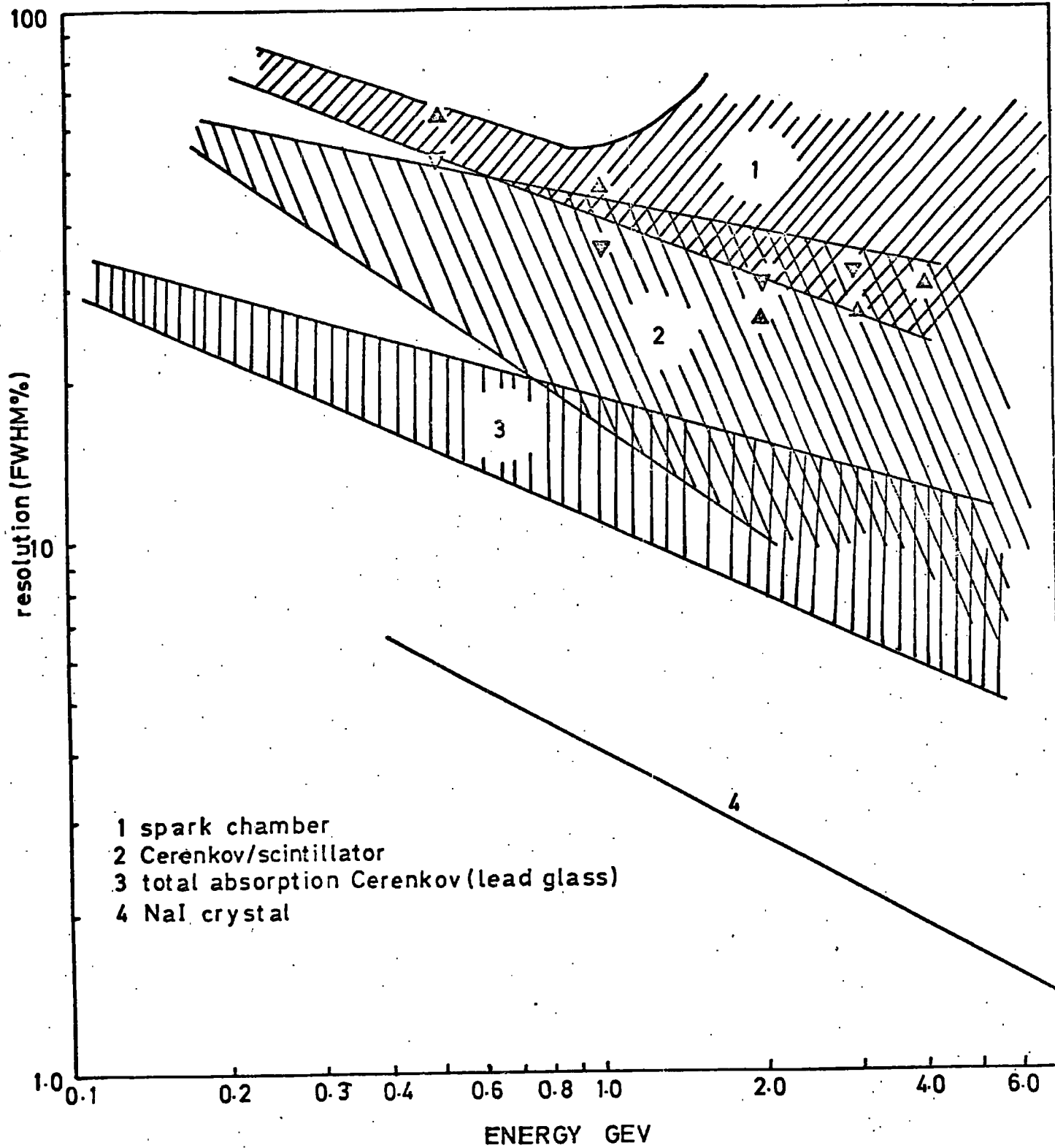
FIGURE 37   energy resolution of gamma ray detectors

produced in a photon induced shower is proportional to the energy of the initial photon (1, 9, 10). Most gamma ray detectors beyond the energy range of the inorganic crystal scintillator make use of this relationship, by being sensitive to the number of electrons produced in the shower. These detectors have two common forms:

1) Composite constructions of electron sensitive detectors sandwiched between layers of absorbing material. The shower is then sampled in depth, and the outputs of the individual detectors are summed to give a measure of the energy of the incident photon.

The electron sensitive detecting elements may consist of strips of plastic scintillator (11, 12, 13, 14), or a Cerenkov type material such as lucite (11, 15). Alternatively, spark chambers may be used as the detecting elements. Detectors of this form have an additional advantage, not only do they give a measure of the energy of the incident photon, but study of the shower shape will provide some spatial information about the original photon. It is into this category that the composite flash tube detector falls.

2) Homogeneous devices, such as the lead glass Cerenkov counter (16, 17, 18, 19), which in effect continuously samples the shower developed in a block of PbF_2, by means of a photomultiplier tube attached to one end of the lead glass block. A crude degree of spatial resolution is achieved by constructing a matrix of such blocks, each with its own photomultiplier tube.

Figure (37) shows a comparison of the energy resolution (FWHM) of the above mentioned devices, as a function of the incident

photon energy. Also shown are the latest values of energy resolution obtained using the composite flash tube chamber (4), which is seen to lie between the best resolving composite spark chamber, and the poorest resolving Cerenkov/scintillator devices.

As a device which offers some degree of spatial resolution, as well as energy resolution, the composite flash tube detector, although in an early stage of development, is generally superior to the composite spark chamber type of detector.

5.2 A Gamma Ray Detector Utilising Flash Tubes

The following is a brief description of the prototype of a gamma ray detector currently being developed at Durham.

The detector was of the total absorption type, consisting of 8 flash tube modules, to sample the shower, interspaced with sheets of lead. Each module consisted of 2 orthogonal planes of 8 tubes per plane, providing X, Y coordinates of the shower position. The two planes of each module were separated by a common high voltage electrode, and contained between two earth electrodes. A space was provided between each module for the insertion of up to 2 radiation lengths of lead.

A total of 128 tubes were employed in the chamber. The tubes were constructed of S95 soda glass, 1.6 cm. internal diameter, 50 cm. long, with 0.1 cm. thick walls, and were filled with 70% Ne, 30% He + 1% CH_4 at 600 torr pressure. With the application of a 30 V/cm. alternating clearing field, the tubes were found to have sensitive and recovery times of 1.0 microsec. and 7 msec. respectively. The tubes were sleeved in thin PVC tubing to prevent photons from one discharging tube causing adjacent tubes to flash.
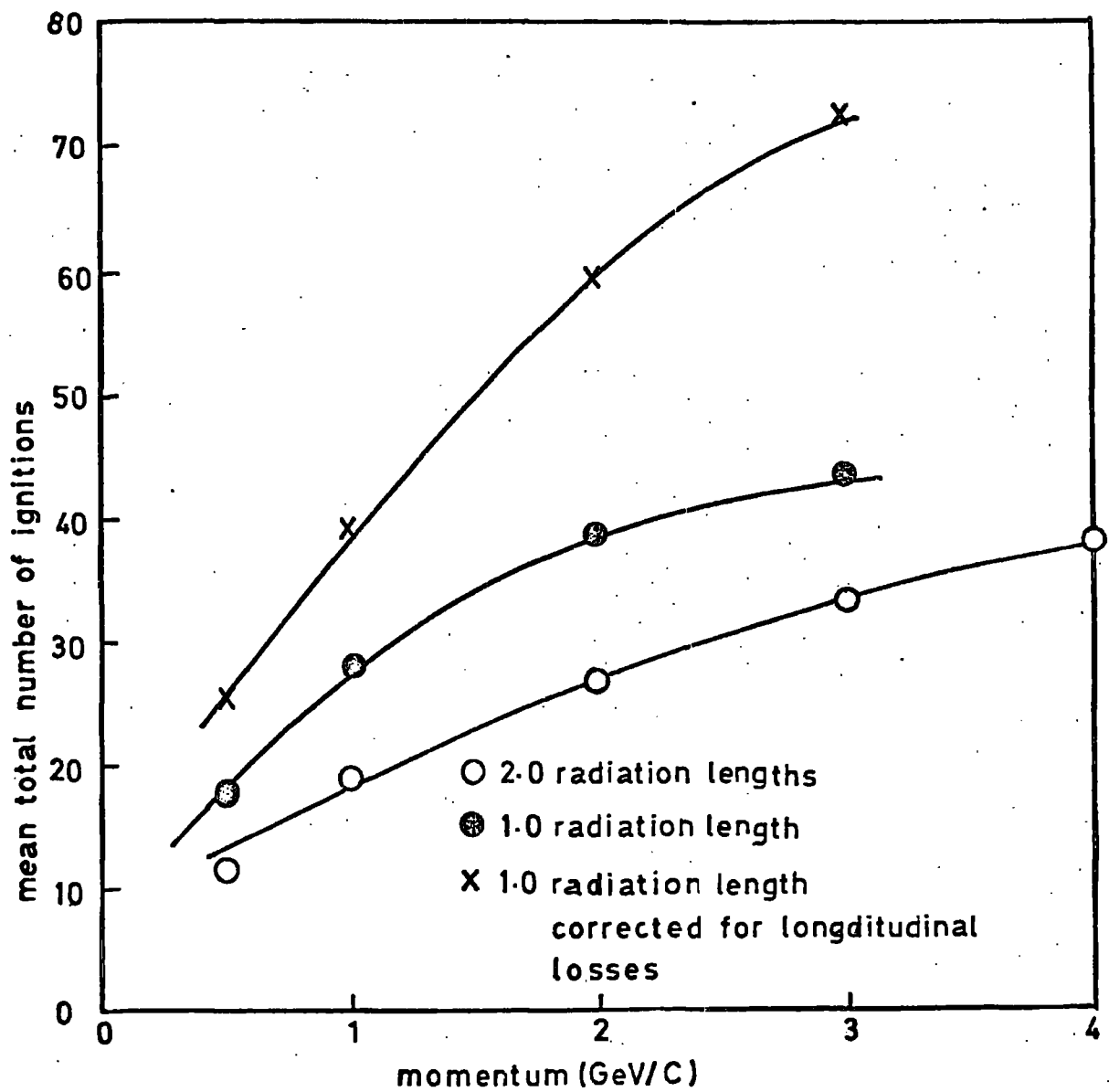
FIGURE 38   Mean total number of tubes igniting versus positron energy

The ends of the tubes were seated in an aluminium base block, which held the digitisation probes, consisting of a 6BA brass screw and a 2.2 KΩ resistor, against the face of the tubes. The outputs of the digitisation probes were fed directly into eight 16 bit CAMAC pattern units, where they were stored, until being read by a PDP 11 computer. The data was output in the form of paper tape.

The readout was very susceptible to electrical pickup from the high voltage pulsing system, and required that the chamber and pulsing system be completely enclosed in an aluminium case.

An event was recorded by a coincidence between suitably placed scintillation counters. This in turn was used to fire a triggertron spark gap (20) by means of which a high voltage pulse was applied to the electrodes. This pulse was formed by discharging a 6,000 pF capacitor across a 330Ω resistor, producing a field of 6 KV/cm., with a decay time of 2.0 microsec.

5.3 Problems Associated with the Energy Resolution of the Chamber

The energy of the incident photon is characterised by the number of flash tube ignitions, however, this does not give a direct measure of the energy, and it will vary from one detector to another, according to the geometry of the detector. Therefore it is necessary for all detectors used in shower sampling to be callibrated in a beam of known energy.

Figure (38) shows the mean total of tubes igniting as a function of the incident positron energy. It can be seen that above 1 GeV the curve departs from the linear relationship one expects from theory. There are two main factors contributing to this:
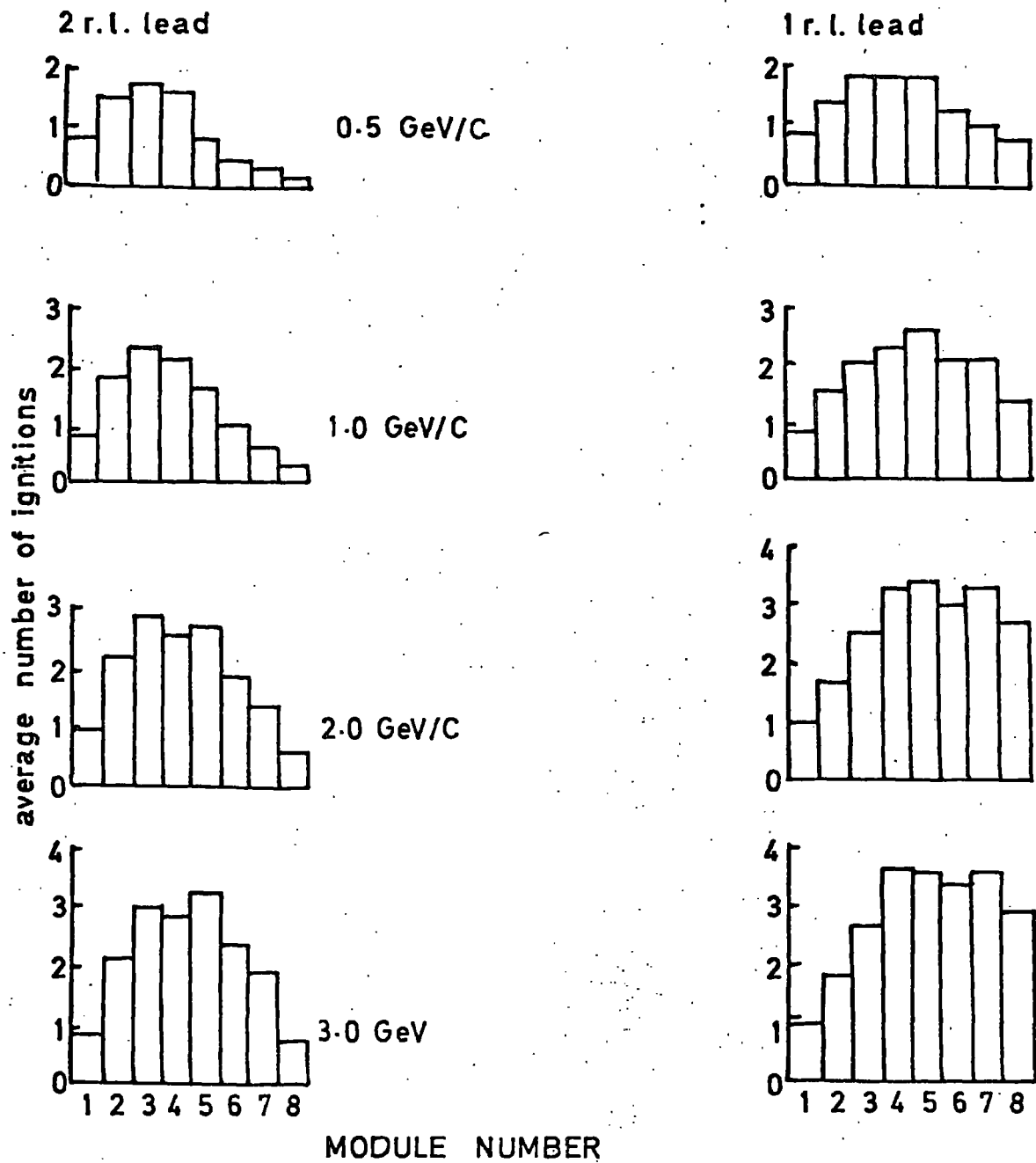
FIGURE 39   the average number of ignitions for each module at different momenta
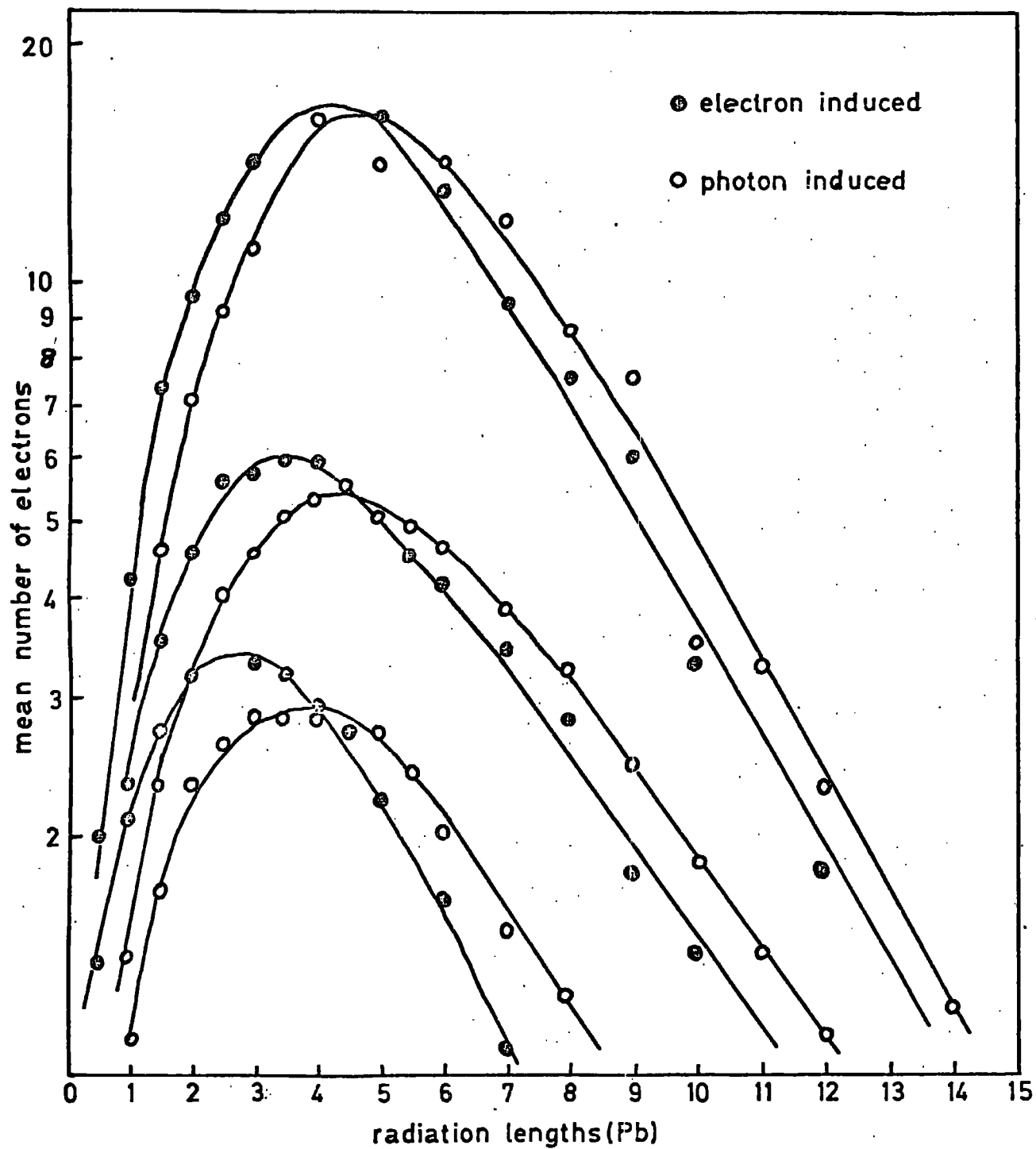
FIGURE 40   mean number of elecrons produced as a function of target depth and primary energy

1) The shower is not contained inside the detector, but leaks out of the sides and rear of the chamber. Leakage from the rear of the chamber is particularly high in cases of high incident particle energy and small quantities of absorber. This is illustrated by figure (39) where with only one radiation length of lead between the modules, a significant proportion of the shower escapes from the rear of the chamber at high energies. Corrections for this loss can be made by integrating the two radiation length curve over 14 radiation lengths, producing a curve which is more linear, and in better agreement with the Monte Carlo predictions for the number of electrons produced.

2) As the energy of the incident positron increases, so does the density of the shower it produces; this is illustrated in figure (40). With the large diameter tubes used in the prototype module a poor sensitivity to individual electrons is to be expected. This is illustrated in table 1, which compares the predicted number of electrons in a shower with the number of tubes which flashed.

The electron sensitivity may be improved by increasing the distance between the absorbers. This would necessitate a longer chamber, but would also help to reduce the leakage from the sides and rear of the chamber. Further increase in electron sensitivity may be achieved by using smaller diameter tubes with thinner walls. However, a practical limit is soon reached, since smaller diameter tubes require higher gas pressures, which, if the tube is to be sufficiently robust, requires that the wall thickness be increased, eventually becoming comparable to the internal diameter of the tube. This results in large insensitive volumes and a reduction in the layer efficiency

of the module.

Further improvement in resolution may be obtained by sampling the shower in several different projections. This is achieved by increasing the number of sampling planes after each layer of absorber, thus making the total number of detected electrons less susceptible to fluctuations in the spatial structure of the shower. Figure (38) shows a third resolution curve, which was obtained by using only one layer of flash tubes after each layer of absorber. It can be seen that the use of two orthogonal layers gives a 30% increase in energy resolution.

Since, from figure (41), the mean number of electrons at any target thickness is small, large fluctuations in the number of detected electrons can be expected, resulting in poor resolution. This situation can be improved by sampling the shower more frequently, ie. by decreasing the absorber thickness and increasing the number of detecting modules.

The resolutions achieved using the prototype chamber are shown in figure (42). The energy resolution is defined as the full width of the frequency distributions of the total number of tube ignitions, at half maximum. From this definition, and from theoretical considerations, the resolution should improve as $1/\sqrt{E}$. It can be seen that up to about 1 GeV, this relationship holds, resolutions of 36% and 46% being achieved for 1.0 and 2.0 radiation lengths of lead respectively at 1 GeV. Beyond 1 GeV, errors are introduced by shower leakage from the sensitive volume of the detector, and the insensitivity of the tubes to individual electrons.
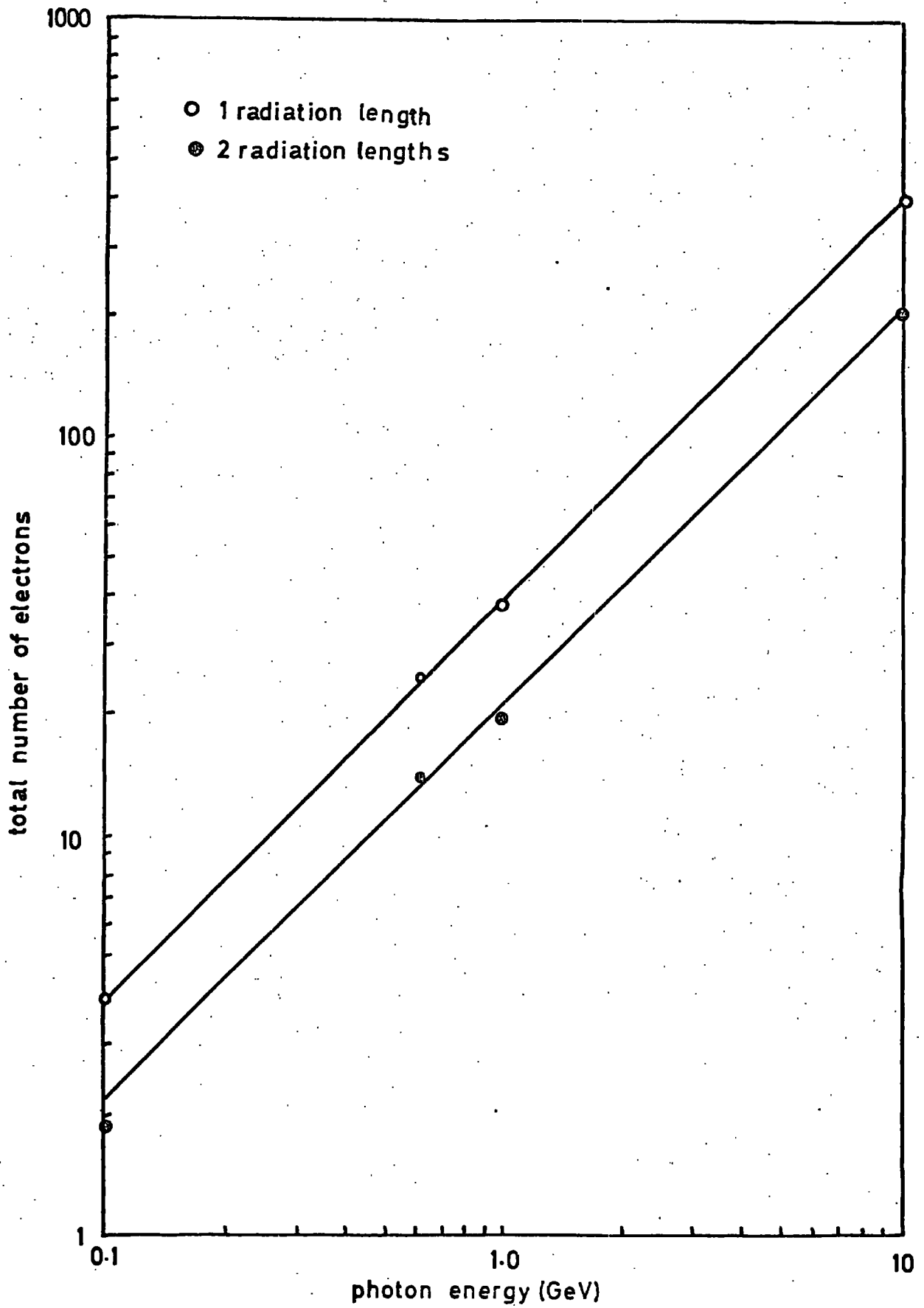
FIGURE 41   total number of electrons expected by sampling
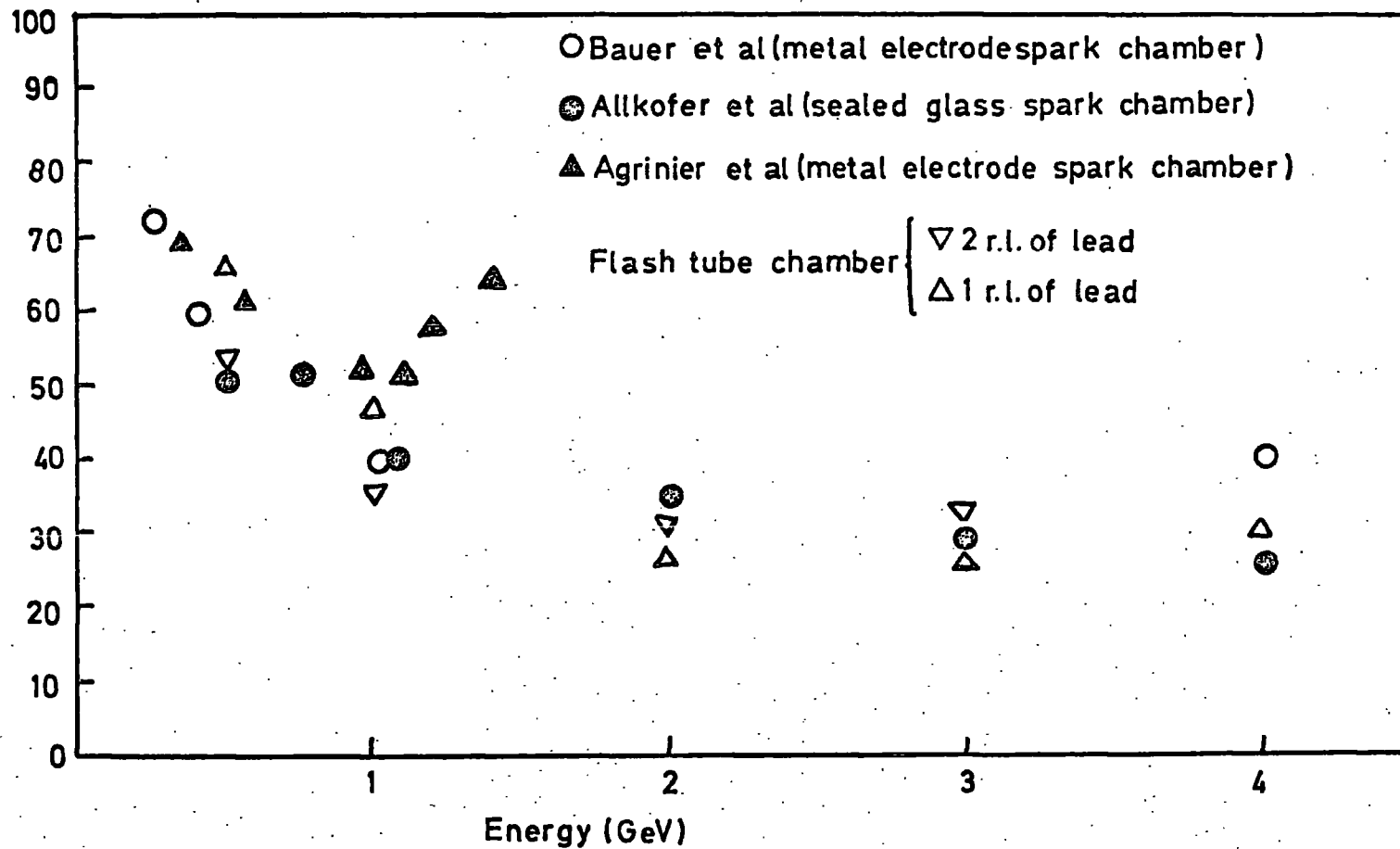at 1 and 2 radiation length intervals as a function
of primary photon energy

FIGURE 42   A comparison of resolution with spark chamber devices

5.4 Problems Associated with the Spatial Resolution of the Chamber

The spatial resolution of a gamma ray detector is a difficult quantity to measure, since it depends very much on the methods used to analyse the data. In the case of the flash tube detector, the method used was to determine the centre of gravity of the shower in each detecting module, and fit a straight line to the points obtained (21). However, electrons produced at large lateral and longitudinal distances are subject to greater fluctuations than those produced near the core of the shower, and must be weighted such that their contribution leads to small errors in the determination of the shower axis.

The lateral weighting factor was obtained by assuming that the distribution of shower particles in a particular module may be represented by a function of Gaussian form, from which a weighting factor for each of the shower defining tubes could be obtained.

The longitudinal weighting factor was obtained by determining the standard deviation (σ) of the distribution of fluctuations of the calculated shower centres for each module, about the real centre. The real centre is defined by the tube which ignites in the first module (indicating the point of entry of the incident positron) and the fact that the incident beam was parallel to better than $\pm 0.4^{\circ}$. This provided a weighting factor ($1/\sigma$) for each module, which was then used in the least squares fit of the shower centres of each module.

From analysing the data in the above manner, and expressing the resolution as the width of the distribution which contains 76% of the data. The apex and angular deviations obtained are shown in table II. This gives a spatial resolution of between 1.0 and 3.0 cm., and

TABLE I

Comparison of predicted number of electrons in a shower, with the number of tubes which flash.

Energy (GeV)	Target Thickness (Radiation lengths)	Expected No. of Electrons	Number of F.T. Ignitions	Sensitivity (%)
0.5	1.0	16.7	9.7	58.1
0.5	2.0	10.0	6.4	63.9
1.0	1.0	31.4	13.4	42.8
1.0	2.0	20.2	9.8	48.7

TABLE II

Percentage of data lying between given limits obtained at a range of energies using a weighted iterative fit.

Energy (GeV)	% of Data Lying Between Fixed Limits			
	Apex Deviation (cm)		Angle (degree)	
	±0.5	±1.5	±1.5	±2.5
2 radiation lengths of lead target				
0.5	44.4	73.4	35.7	44.1
1.0	49.8	77.6	31.6	55.0
2.0	54.2	78.0	36.8	62.2
3.0	55.7	76.6	43.0	63.6
1 radiation length of lead target				
0.5	58.3	79.7	40.1	54.3
1.0	48.0	85.2	37.7	69.4
2.0	63.6	84.5	49.9	82.1
3.0	61.2	82.3	50.5	75.8

an angular resolution of approximately 5%. However, since the location

of the incident particle is known from the first module, to ±a tube

diameter, (0.8 cm.), which lies inside the resolution range, it is

expected that the spatial resolution is better than 1.6 cm.

Figure (42) compares the above results with those obtained

by other workers, using comparable devices such as spark chambers as

the detecting elements. It can be seen that the spatial resolution

is comparable to that obtained using the best spark chambers of the

current limited type (22). It is clear from the above results that

great improvement in spatial resolution will result from using

smaller diameter tubes.

5.5 An Improved Gamma Ray Detector

Having defined the criteria necessary for good energy and

spatial resolutions, an improved detector was constructed (4). The

improvements to the chamber design can be summarised as:-

1) Increasing the number of modules, thereby increasing the

sampling frequency, and enabling the amount of target material between

the modules to be reduced, without increasing the likelihood of the

shower escaping from the chamber.

2) Increasing the overall chamber dimensions, thus reducing

lateral and longitudinal shower leakage.

3) Decreasing the tube diameter and wall thickness, thereby

increasing the sensitivity to individual electrons.

The basic design features of the detector were changed very little. The number of modules was increased to 12, each module containing 2 orthogonal planes of 32 tubes, making a total of 768 tubes. The tubes were made from low resistance Jena 16B glass, 50 cm. long, 8.2 mm. internal diameter, with 0.5 mm. thick walls. The tubes were filled with 70% Ne, 30% He + 2% CH_4 at 2.3 atmospheres pressure. The mean internal efficiency of the tubes was 98%, the recovery and sensitive times, 0.6 ms. and 1.4 microsec. respectively. This should allow repetition rates of 1 KHz, however, the upper limit is likely to be dictated by the induced clearing fields.

The data aquisition programme was improved by interfacing the PDP 11 with the Daresbury Laboratory IBM 370, allowing data to be stored directly onto disc, and later transfered to magnetic tape for analysis. The increased number of tubes meant that the data could not be directly fed into the PDP 11. The outputs from the digitisation probes was used to set latches. The states of these latches after each event was read into 3 CAMAC input registers and the latches reset. The data was then processed by the on-line computer. An improved high voltage pulsing system, using a ceramic thyratron was developed, which enabled the chamber to be pulsed at a higher repetition rate.

The initial programme of work was to repeat the previous investigations, and to compare the performances of the two detectors. These results are summarised in tables III and IV.

From these two tables it can be seen that the chamber is capable of giving an average energy resolution of 44% FWHM and a spatial resolution of about 8 mm. over the energy range 0.5 GeV to 2.5 GeV. The improvement in the spatial resolution is in agreement

with that expected by reducing the diameter of the tubes. However the energy resolution shows little improvement; this is unexpected, since the increased sampling of the shower, the improved individual electron sensitivity, and the reduced shower leakage, should all help improve the energy resolution.

One explanation for this poor energy resolution is that the tubes at the centre of the modules, which are heavily weighted in the shower analysis, had a low efficiency. This occurred because the high voltage pulse, used during the determination of the tubes' efficiency, contained a fast rising 20 KV spike. This spike (initially thought to be due to electrical interference on the oscilloscope) caused normally efficient tubes to flash spuriously. These tubes were replaced by apparently normal tubes, which when operated under the correct high voltage conditions (no spike) were found to be inefficient.

One simple way of determining the spread of the efficiency of the tubes is to scan the beam several times across the chamber.

Another effect influencing the performance of the detector has come to light during further investigation of the efficiency of the tubes. It has been found (23) that the strength of the digitisation signal is critically dependent upon the distance of the flash tube wall from the high voltage electrode. This effect is at present under investigation, but preliminary results have shown that increasing the separation between the tube wall and the high voltage electrode by 0.6 mm. reduced the digitisation pulse from 40 V to about 2 V.

Although a measure of the distribution of tube diameters has yet to be made, it is known that variations of 0.6 mm. are not uncommon. Consequently the digitisation pulses obtained from many

TABLE III

SPATIAL RESOLUTION OF CHAMBER

Energy of Positron (GeV)	X Direction	Y Direction
0.6 Radiation Lengths of Lead Between each Module		
0.5	4	4
1.0	3	3
1.5	4	4
2.0	3	3
2.5	3	3
3.0	4	4
3.5	6	4
1.2 Radiation Lengths of Lead Between each Module		
0.5	11	14
1.0	11	11
1.5	11	11
2.0	9	9
2.5	9	11
3.0	8	8
1.8 Radiation Lengths of Lead Between each Module		
1.0	16	16
2.0	9	55
3.0	14	7

TABLE IV

ENERGY RESOLUTION OF CHAMBER

Energy of Positron (GeV)	Resolution
0.6 Radiation Lengths of Lead Between each Module	
0.5	43
1.0	46
1.5	42
2.0	46
2.5	40
3.0	44
1.2 Radiation Lengths of Lead Between each Module	
0.5	68
1.0	47
1.5	38
2.0	39
2.5	42
3.0	35
1.8 Radiation Lengths of Lead Between each Module	
1.0	55
2.0	35
3.0	28

tubes will not be of a sufficient magnitude to set the integrated circuit latches, resulting in a loss of efficiency.

Ways of modifying the detector to allow for the variation in tube diameter, ensuring a constant separation between the high voltage plate and the tube wall, are being sought. However, closer tolerances should be specified for tubes used in future detectors. This is not an unreasonable request if it is ensured that all tubing used comes from the same production batch.

Although the chamber was operated at a number of different rates, in view of the problems discussed above, the results should not be considered as conclusive. It was found that at an event rate of 50 per second, the efficiency dropped by between 10% and 14%, which may be a result of induced internal clearing fields. This will be investigated during future tests.

5.6 Conclusions

Tests carried out with the prototype chamber have shown that a detector consisting of flash tube detecting elements, interspersed with lead absorber, offers a degree of spatial and energy resolution comparable to that achieved with the best current limited spark chamber-lead absorber type of detector. The performance of the detector depends principally on its ability to contain the electron shower, and on the individual electron sensitivity of the flash tubes.

An improved detector was built, satisfying more fully the above criteria. The performance of this detector fell short of that expected, due to errors in determining the efficiency of the tubes, and to an unforeseen effect arising in the digitisation system. The

problems are now understood and are being rectified. Future tests will

provide a more reliable measure of the detector's performance.

References

1   H. Messel, D. Crawford. Electron photon shower distribution
        functions. Pergamon Press, 1970.

2   W.K. M^{C}Farlane et al. Nucl. Inst. Meth. 91 (1971) 85.

3   A digitised neon flash tube chamber for γ ray detection.
        J.E. Chaney et al. Nucl. Inst. Meth. 125 (1975) 189.

4   A modified γ ray detector. J.M. Breare et al. Internal
        Report NI-75-4 Durham University.

5   M^{C}Kay, K.G. Phys. Rev. 84 (1951) 829.

6   Friedland et al. Nucleonics 18 (1960) 2

7   G.F.G. Garlick Proc. Nucl. Phys. 2 (1952) 51.

8   K. Siegbahn. Alpha-Beta and Gamma-ray Spectroscopy,
        New York, Interscience Publishers Inc. 1965

9   U. Volkel, Internal Report, DESY 65/6 1965.

10   U. Volkel, Internal Report, DESY 67/16 1967.

11   C.A. Heusch, Int. Conf. Electron and Photon Interactions at
        High Energies. Hamburg,1965, 408.

12   D. Muller. Phys. Rev. 5 (1972) 2677.

13   A. Zichichi. Proc. Int. Conf. Inst. for High Energy Physics.
        Frascati, 1973, 565.

14   Pugh et al. Rev. Sci. Inst. 25 (1954) 1124.

15   W.K. M^{C}Farlane et al. Nucl. Inst. Meth. 91 (1971) 85.

16   Blumenfeld et al. Nucl. Inst. Meth. 97 (1971) 427.

17   Y. Hemmi. Nucl. Inst. Meth. 56 (1967) 213.

18   Lewis et al. Proc. Int. Conf. Electron and Photon Interactions
        at High Energies. Hamburg, 1965, 424.

19   Daresbury Laboratory, Annual Report 1973 106.

20   Sletten et al. IEEE Monograph, $\underline{193}$ (1965)   54.

21   J.E. Chaney, Ph.D. Thesis,1974, University of Durham.

22   O.C. Allkoffer, Internal Report, 1973, University of Kiel.

23   Dr. B. Nandi, University of Durham, Private communication.

CHAPTER 6

CONCLUSIONS.

The flash tube, which was among the first of the current generation of detectors to be developed, has played a significant role in the field of cosmic ray physics. The flash tube has many commendable features. It is simple and robust, allowing large sensitive volumes to be obtained without undue cost. Because of its elemental construction a flash tube array has a high multitrack efficiency, and also allows the geometry of a detector to be readily modified to adapt to the changing requirements of an experiment. A simple method of digitising the outputs has been developed, which does not require any amplifiers or sophisticated electronics to interface it with the conventional computerised data aquisition systems currently in use.

However, the flash tube had three characteristics which hitherto has prevented its use on accelerator counter experiments, namely, long sensitive and recovery times, and a loss of detecting efficiency with high event rates.

Short sensitive and recovery times are required by accelerator experiments, because of the high background radiation and the need to operate at high rates. The recovery and sensitive times

have been reduced to a millisecond or less, and a few microseconds respectively, by the application of an alternating clearing field, and the addition of small quantities of methane to the gas mixture. These times are well within the requirements of most accelerator counter experiments.

The drop in efficiency at high rates has been shown to be due to internal clearing fields, caused by charges, resulting from the discharge, adhering to the inside walls of the tube. The use of low resistance Jena 16B glass increases the rate of decay of these fields, allowing an event rate of up to 50 Hz, without undue loss of efficiency. Experiment has shown that the effects of these internal fields can be further reduced by decreasing the surface resistance of the outer wall of the tube.

A prototype gamma ray detector has been built, using a composite construction of flash tube detection elements, sandwiched between lead absorbers. Although this detector was of a relatively crude design, it was found to have a performance comparable to similar detectors using current limited spark chambers as the detecting elements. An energy resolution of 36% FWHM and an angular resolution of about 4° being obtained.

From the criteria for good resolution, obtained with the prototype detector, an improved detector was constructed, using smaller tubes and having a larger number of detecting elements. The performance of this improved detector fell short of expectations. This was due to faults in the high voltage pulsing system, affecting efficiency measurements, and a hitherto unsuspected effect arising in the digitisation system. These problems are now understood and further tests should give a true indication of the detector's performance.

ACKNOWLEDGEMENTS